Contrasting genomic and phenotypic outcomes of hybridization between pairs of mimetic butterfly taxa across a suture zone

Jérémy Gauthier, Donna Lisa De-silva, Zachariah Gompert, Annabel Whibley, Céline Houssin, Yann Le Poul, Melanie Mcclure, Claire Lemaitre, Fabrice Legeai, James Mallet, et al.

Manuscript published in Molecular Ecology as:
Gauthier J, de Silva DL, Gompert Z, Whibley, A, Houssin C, Le Poul Y, McClure M, Lemaitre C, Legeai F, Mallet J, Elias M. 2020 Contrasting genomic and phenotypic outcomes of hybridization between pairs of mimetic butterfly taxa across a suture zone. Molecular Ecology. 29: 1328-1343. https://doi.org/10.1111/mec.15403

Contrasting genomic and phenotypic outcomes of hybridization between pairs of mimetic butterfly taxa across a suture zone

Jérémy Gauthier[1,2], Donna Lisa de Silva[3], Zachariah Gompert[4], Annabel Whibley[5], Céline Houssin[3], Yann Le Poul[3,6], Melanie McClure[3], Claire Lemaitre[1], Fabrice Legeai[1], James Mallet[7] and Marianne Elias[3]

[1] Univ Rennes, Inria, CNRS, IRISA, F-35000 Rennes, France

[2] Geneva Natural History Museum, 1208 Geneva, Switzerland

[3] Institut de Systématique, Évolution, Biodiversité, CNRS, MNHN, EPHE, Sorbonne Université, Université des Antilles, Paris, France

[4] Department of Biology, Utah State University, Logan, UT 84322-5305, USA

[5] School of Biological Sciences, University of Auckland, Auckland, New Zealand

[6] Ludwig-Maximilians Universität München, Fakultat für Biologie, Biozentrum, Grosshaderner Strasse 2, 82152 Planegg-Martinsried, Germany

[7] Department of Organismic and Evolutionary Biology, Harvard University, Cambridge, MA 02138, USA

Corresponding Author:

Jérémy Gauthier

Geneva Natural History Museum, 1208 Geneva, Switzerland

mr.gauthier.jeremy@gmail.com

Abstract.

Hybrid zones, whereby divergent lineages come into contact and eventually hybridize, can provide insights on the mechanisms involved in population differentiation and reproductive isolation, and ultimately speciation. Suture zones offer the opportunity to compare these processes across multiple species. In this paper we use reduced-complexity genomic data to compare the genetic and phenotypic structure and hybridization patterns of two mimetic butterfly species, *Ithomia salapia* and *Oleria onega* (Nymphalidae: Ithomiini), each consisting of a pair of lineages differentiated for their wing colour pattern and that come into contact in the Andean foothills of Peru. Despite similarities in their life history, we highlight major differences, both at the genomic and phenotypic level, between the two species. These differences include the presence of hybrids, variations in wing phenotype, and genomic patterns of introgression and differentiation. In *I. salapia*, the two lineages appear to hybridize only rarely, whereas in *O. onega* the hybrids are not only more common, but also genetically and phenotypically more variable. We also detected loci statistically associated with wing colour pattern variation, but in both species these loci were not over-represented among the candidate barrier loci, suggesting that traits other than wing colour pattern may be important for reproductive isolation. Our results contrast with the genomic patterns observed between hybridizing lineages in the mimetic *Heliconius* butterflies, and call for a broader investigation into the genomics of speciation in Ithomiini - the largest radiation of mimetic butterflies.

Keywords. Hybridization, Ithomiini, introgression, differentiation, admixture mapping, mimicry

Introduction

Speciation is the ultimate process responsible for the considerable biological diversity observed on Earth. Hybrid zones, whereby divergent lineages come into contact and potentially hybridize, can provide insights into the mechanisms involved in population differentiation and reproductive isolation, and ultimately speciation (Barton & Hewitt, 1989; Ravinet et al., 2017; Safran & Nosil, 2012). When hybrid zones span an environmental transition, populations across the hybrid zone diverge not only because of genetic drift but also due to local adaptation to different environments. Over time, drift and selection can lead to the emergence of barriers to gene flow that increase reproductive isolation, resulting in heterogeneous patterns of differentiation and introgression across the genome (Barton & Bengtsson, 1986; Ravinet et al., 2017; Safran & Nosil, 2012). Genomic regions with low rates of introgression are more likely to be associated with divergent selection and reproductive isolation (Gompert & Buerkle, 2009; *Heliconius* Genome Consortium, 2012; Mallet, 2005; Mallet & Barton, 1989; Jay et al., 2018). Assessing the genetic structure of hybrid zones can therefore shed light on the evolutionary processes at play during the early stages of speciation by revealing the number and distribution of loci presenting deviant patterns of differentiation and introgression compared to the genome-wide average (Bierne, Welch, Loire, Bonhomme, & David, 2011). Additionally, while genetic mapping of adaptive traits has classically relied on controlled crosses, which cannot be performed in many organisms, hybrid zones enable the application of admixture mapping approaches that take advantage of natural mixing and recombination to investigate the genetic basis underlying adaptive phenotypic variation (Buerkle & Lexer, 2008; Gompert & Buerkle, 2013; Pallares, Harr, Turner, & Tautz, 2014).

Many studies have focused on hybrid zones to unravel the processes generating local adaptation (e.g. Jones et al., 2012; Larson, Andrés, Bogdanowicz, & Harrison, 2013; Soria-Carrasco et al., 2014) and reproductive isolation (e.g. Christe et al., 2016; Teeter et al., 2008)

and have revealed different patterns (Barton & Hewitt, 1985, 1989; Gompert & Buerkle, 2009; Kronforst et al., 2013; Rieseberg, Whitton, & Gardner, 1999; Teeter et al., 2010; Via & Hawthorne, 2002). These differences may stem from differences in the organisms studied, but may also stem from differences in the environmental conditions faced by populations of these organisms, such that comparative interpretations are rather limited. To investigate the repeatability of genetic and phenotypic differentiation, reproductive isolation and introgression patterns across incipient species diverging under similar environmental conditions are needed. Suture zones are areas where multiple recently diverged pairs of taxa come into contact and hybridize (Remington, 1968), and typically span a sharp environmental gradient or a dispersal barrier (Dasmahapatra, Lamas, Simpson, & Mallet, 2010; Endler, 1977; Moritz et al., 2009). With replicated pairs of divergent and hybridizing lineages, suture zones offer an exceptional opportunity to compare levels and patterns of hybridization and reproductive isolation in relation to genomic and phenotypic divergence in a common environmental setting (Moritz et al., 2009; Nosil, Funk, & Ortiz-Barrientos, 2009; Rissler & Smith, 2010).

Müllerian mimicry in butterflies, in which multiple defended species locally converge on warning wing colour patterns and form mimicry 'rings' (Bates, 1862; Muller, 1879), provides an excellent system to unravel the mechanisms underlying adaptation and speciation. Two large neotropical mimetic butterfly tribes, Heliconiini and Ithomiini (Nymphalidae, 77 and 393 species, respectively) are particularly well suited. Heliconiine and ithomiine species typically comprise multiple geographical subspecies that differ in colour patterns (Brown, Sheppard, & Turner, 1974). Because warning colour patterns in mimetic butterflies are under strong positive frequency-dependent selection locally (Kapan, 2001; Mallet & Barton, 1989), divergent mimetic subspecies are often separated by narrow hybrid zones maintained by migration-selection balance (Mallet & Barton, 1989). Mimicry generates postzygotic

reproductive isolation via higher predation on intermediate-patterned, non-mimetic hybrids (Merrill et al., 2012) and prezygotic reproductive isolation if there is also assortative mating for colour pattern among subspecies (Jiggins, Naisbit, Coe, & Mallet, 2001; McClure et al., 2019; Merrill et al., 2011; 2012). Mimicry is therefore a strong ecological driver of speciation, and is believed to have triggered the diversification of large radiations of heliconiine and ithomiine butterflies (Jiggins et al., 2001; Kozak et al., 2015). Studies of genetic differentiation and the basis of colour pattern variation in mimetic butterflies have almost exclusively focused on heliconiine butterflies (particularly the genus *Heliconius*), where a few major-effect genes (dubbed the mimicry 'toolkit', (Joron et al., 2006)) have been found to control wing pattern variation (Martin et al., 2012; Mazo-Vargas et al., 2017; Nadeau et al., 2016; Reed et al., 2011; Westerman et al., 2018) and to be highly differentiated across hybrid zones, while the rest of the genome seems highly permeable (Nadeau et al., 2014). By contrast, because of practical limitations (difficulties in maintaining captive populations and making controlled crosses), much less is known about population genetics of Ithomiini species (but see Dasmahapatra, Lamas, Simpson, & Mallet, 2010; McClure & Elias, 2016; McClure et al., 2019), let alone of the genetics of wing pattern variation. Yet, Ithomiini numerically dominate forest communities of day-flying Lepidoptera and are believed to be some of the main drivers of both Müllerian and Batesian mimicry (whereby palatable species mimic unpalatable aposematic species) among Lepidoptera in the Neotropics (Bates, 1862; Beccaloni, 1997; Muller, 1879). Because of the ecological importance of Ithomiini, shedding light on how populations are structured across hybrid zones and elucidating the genetic basis of wing pattern variation would significantly advance our understanding of adaptation and speciation in mimetic butterflies.

The foothills of the Andes in the region of Tarapoto are transitional between lowland rainforest and mid-elevation mountain forest. This area is a major suture zone for a range of organisms (Roberts et al., 2006; Smith et al., 2014; Weir, 2006) including heliconiine and ithomiine mimetic butterflies (Dasmahapatra, Lamas, Simpson, & Mallet, 2010; Nadeau et al., 2014; Whinnett et al., 2005) that harbour divergent wing colour patterns across the suture zone. Here we take advantage of the Tarapoto suture zone to assess the patterns of genomic and phenotypic divergence and infer the extent of reproductive isolation across the hybrid zone for two widespread ithomiine species, *Ithomia salapia* and *Oleria onega*, that each harbour divergent wing colour patterns across the Tarapoto suture zone. The two species have broadly similar life histories (e.g., forest habitats, mimicry, Solanaceae hostplants) and although they are somewhat differently distributed throughout the Neotropics, in the area of Tarapoto their populations have similar distributions. In this area, *I. salapia* comprises two subspecies: *I. salapia aquinia*, on the Amazonian side, which has a transparent yellow colour pattern surrounded by an orange and black line with small white dots; and *I. salapia derasa*, on the Andean side above about 500m alt., has a similar yellow pattern but surrounded by a thick black line with large white dots (Figure 1). In addition to being found on the Amazonian side of the Escalera mountains, *I. salapia aquinia* is also found on the other side of the mountains, in the lowlands of the Río Mayo valley near Tarapoto.

On the Andean side (including in the lowlands of the Río Mayo) *O. onega* ssp. nov. 2 has translucent white wings with black patterning that splits the apical part of the forewing into two white 'windows', while in the Amazonian subspecies *O. onega janarilla* the forewing black patterning nearly splits the apical part of the forewing into four windows (Figure 1).

Thus, whereas *I. salapia* has a strictly altitude-based distribution of populations, *O. onega* has populations that differ geographically East-West, independently of altitude. For

each species, the two subspecies belong to distinct mimicry rings, which they numerically dominate. Therefore, *I. salapia* and *O. onega* likely play a major role in divergence and maintenance of their respective mimicry rings. Individuals with intermediate patterns are sometimes found in the contact zone, suggesting that occasional interlineage hybrids are produced.

In this paper we carry out population genomic analyses and quantify wing colour pattern variation in samples from Andean, Amazonian and intermediate populations of *I. salapia* and *O. onega* to address the following questions: (1) what are the overall patterns of differentiation, admixture and introgression between subspecies for each taxon pair? (2) To what extent does introgression vary across the genome, and are genetic regions associated with colour pattern among those that exhibit higher differentiation and reduced introgression? (3) How repeatable are the patterns of differentiation, introgression and genotype-phenotype association across the two taxon pairs?

Material and Methods

Sampling

Sampling was performed in five study sites in the region of Tarapoto in Peru (Figure 1a; details in Supplementary Table 1: gives each site, GPS coordinates and the number of each sex of *I. salapia* and *O. onega* sampled, before and after filtering). One hundred and twelve (112) *I. salapia* specimens were sampled from five localities, and 149 *O. onega* specimens were sampled in five localities.

Genotyping by sequencing (GBS)

DNA was extracted from ¼ of thorax of each individual using the Qiagen DNeasy blood and tissue kit, following the manufacturer protocol. We generated reduced genomic complexity libraries for each specimen using a GBS (genotyping by sequencing) approach (Gompert et al., 2012; Parchman et al., 2012). Briefly, genomic DNA was digested with the restriction endonucleases EcoRI and MseI and resulting fragments were ligated to double-stranded adaptor oligonucleotides. These adaptors consisted of the Illumina sequencing priming sites followed barcodes that allow for the identification of sequences for each individual. These barcodes allowed us to multiplex all individuals into one library. Sequencing of the library was completed by the National Center for Genome Research (Santa Fe, NM, USA) on an Illumina HiSeq platform; 100 base single-end sequencing reads were generated.

SNP calling

First, sequencing primers were removed, sequences were demultiplexed and associated with each individual based on internal barcode sequences. SNP-calling was performed on samples from each species separately using `DiscoSnp-RAD`, a *de novo* reference-free and assembly-free method (Gauthier et al., 2017; Uricaru et al., 2015). SNPs are identified from particular arrangements in the De Bruijn graph built using a k-mer size of 31 and a minimal coverage of 2 for each allele (Gauthier et al., 2017; Uricaru et al., 2015). Individuals with more than 90% missing genotypes were excluded (Supplementary Table 1) resulting in a final dataset consisting of 105 samples for *I. salapia* and 142 for *O. onega*. SNPs scored in at least 80% of the samples (i.e. sites with < 20% missing data) and with a minor allele frequency above 0.01 were retained using `vcftools` (Danecek et al., 2011) resulting in a dataset of 17,779 SNPs for *I. salapia* and 15,894 SNPs for *O. onega*.

Population structure analyses

Population genetic structure was investigated using a subset of SNPs, where only one SNP per GBS locus was considered so as to minimize the effects of linkage disequilibrium that would occur within loci, as often recommended (Falush, Stephens, & Pritchard, 2003). A total of 8,219 SNP for *I. salapia* and 5,133 SNP for *O. onega* were retained. To investigate genetic structure, we used principal component analysis implemented for genetic data in the `adegenet` R package (Jombart & Ahmed, 2011). We used Bayesian admixture analysis implemented in `Structure` (Pritchard, Stephens, & Donnelly, 2000) to estimate admixture proportions, that is, the proportion of each individual's genome inherited from each of *K* hypothetical source populations. We ran analyses with *K* from 1 to 6 with 3 independent Markov chains each, using 200,000 steps and including 10,000 burn-in steps. We checked the results obtained in each run to verify convergence of the chains to a stable posterior distribution. The most likely number of clusters was identified using Evanno's method (Evanno, Regnaut, & Goudet, 2005) implemented in `Structure Harvester` (Earl & vonHoldt, 2012).

Genome-wide introgression and estimates of differentiation

To investigate introgression among each population pair and to search for loci potentially associated with reproductive isolation, we used a genomic cline approach using `bgc` (Gompert & Buerkle, 2012). Loci acting as barriers to gene flow and linked regions should exhibit reduced introgression into the foreign genomic background. Locus-specific introgression is characterized by the probability ϕ of being inherited from a given parental population (here, the Amazonian lineage; the probability of being inherited from the Andean lineage is therefore $1 - \phi$). These probabilities are compared to the genome-wide average

probability, which corresponds to the hybrid index. Introgression patterns can be summarized by two locus-specific genomic cline parameters: α, the genomic center parameter, and β, the genomic cline rate parameter. The genomic cline center parameter α specifies an increase (positive values of α) or decrease (negative values of α) in the probability of ancestry of the focal population (here, the Amazonian lineage). Positive or negative α values denote an asymmetry in the direction of introgression with hybrids having increased or decreased ancestry from one or the other ancestral lineage, respectively. The genomic cline rate parameter β specifies the cline steepness, with an increase (positive values of β) or decrease (negative values of β) in the rate of transition from low to high probability of ancestry (Gompert & Buerkle, 2011). Positive or negative β values are associated with a high or low level of gene flow, respectively. We estimated the posterior probability distribution of hybrid indices and cline parameters with `bgc`. MCMC of 50,000 steps including 10,000 burn-in steps for *I. salapia* samples and 100,000 with 30,000 burn-in steps for *O. onega* samples were used to reach mixing, and convergence was verified graphically by plotting log-likelihood distributions. For a given SNP, outlier introgression from the genome-wide average was identified as credible when the 95% credible intervals of the cline parameters α and β excluded zero. These SNPs deviating from global pattern should reflect unusual patterns of evolution acting on these loci. We used the admixture model implemented in `entropy` (version 1.2) to estimate admixture proportions and intertaxon ancestry (Gompert et al. 2014). This model explicitly estimates the proportion of each individuals' genome where the two allele copies are derived from different source populations (i.e., the proportion of the genome with intertaxon ancestry). `entropy` also incorporates uncertainty in genotypes due to limited sequence coverage and sequencing errors. We fit the model using Markov chain Monte Carlo (MCMC). We ran the MCMC algorithm three times with 15,000 iterations following a 5,000

iteration burnin, and with a thinning interval of 5. We assumed the number of source populations (*K*) was two.

Genome-wide weighted and per-SNP genetic differentiation F_{ST} were estimated using Weir and Cockerham's method (Weir & Cockerham, 1984) implemented in `vcftools` (Danecek et al., 2011). To do so, only samples from parental lineages, that is, samples from the initial localities distant from the hybrid zone, were kept. To identify outlier SNPs with elevated genetic differentiation, the threshold was fixed to the 95th percentile of F_{ST} distribution obtained by random sampling with replacement of 100,000 values.

Wing pattern analyses

Photographs of dorsal and ventral sides of detached wings of 90 and 94 of the genotyped specimens of *I. salapia* and *O. onega*, respectively, were taken with a Nikon D90 digital camera and a 105 mm lens on a white background with a piece of millimeter paper for scale. For each specimen, dorsal and ventral patterns of fore- and hindwings were quantified using Colour Pattern Modeling (CPM, (Le Poul et al., 2014) as follows: wings were first extracted from their background, resulting in eight images per specimen (2 wings [forewing and hindwing] x 2 lateral sides [left/right] x 2 vertical sides [ventral/dorsal]); for each image, wing pattern was described by semi-automatically categorizing wings into a finite number of colours (yellow, black, orange and white for *I. salapia*; white, black and orange for *O. onega*). Damaged wings were discarded, and when left and right wings were available only one randomly chosen side was used in subsequent analyses. Homologous wings were then aligned according to both shape and pattern (Le Poul et al., 2014), and a binary principal components analysis based on one-hot encoding of colours (i. e., where each colour is encoded by a string

of bits among which only one takes the value 1) was performed on the colour of homologous pixels shared by all wings. Principal component (PC) scores were used as a quantitative measure of colour pattern in subsequent analyses.

Admixture association mapping

To identify SNPs associated with variation in wing patterns, we performed association mapping using the Genome-wide Efficient Mixed Model Association tool (`GEMMA`) (Zhou & Stephens, 2012, 2014). We used the multivariate linear mixed model (mvLMM) to test marker associations with multiple phenotypes and to estimate genetic correlations among complex phenotypes. To do so, we retained all wing pattern PCs that explained more than 1% of the variation in each species as variables. This included 14 variables accounting for 57.1% of the variation in wing pattern for *I. salapia* and 18 variables explaining 54.9% of the variation for *O. onega*. Both the variation linked to sex and the confounding effect of population structure (Freedman et al., 2004; Price et al., 2006) were integrated into the models by implementing a relatedness matrix between individuals generated using `GEMMA` (Zhou & Stephens, 2012) and the first population structure PC (obtained using `adegenet` R package (Jombart & Ahmed, 2011)) as a covariate. Analyses were carried out using the option -lmm 1 to perform a Wald test evaluating the probability of the null hypothesis that the marker effect sizes for all phenotypes were zero. For the identification of SNPs significantly associated with wing pattern, the threshold was fixed to a p-value adjusted using (i) a classical Bonferroni correction, which divides the significance threshold by the number of multiple comparisons, that is, the number of molecular markers multiplied by the number of variables, and (ii) using the false discovery rate (FDR) method (Benjamini & Hochberg 1995). We considered SNPs identified by both of these correction methods as significantly associated with wing pattern.

To test whether outlier SNPs by the three approaches, i.e. differentiation genome-scan, introgression pattern and admixture mapping, are distributed randomly or if there is enrichment in shared outlier SNPs, we used two methods: a Pearson's Chi-squared test to compare shared outlier to a random distribution and a bootstrap of 1,000 random samplings among SNPs to estimate confidence interval of such shared SNPs.

Similarities with other Lepidoptera genomes

Loci containing SNPs identified as outliers in the genetic differentiation or the differential introgression approaches were screened by BLAST against all annotated butterfly reference genomes in LepBase v4 (Challis, Kumar, Dasmahapatra, Jiggins, & Blaxter, 2016) to investigate the gene content of homologous genomic regions. This was performed using the BLASTn tool available on the LepBase platform (Priyam et al., 2019). Best hits, their location in reference genomes and genes were then investigated manually.

Results

Our reduced complexity genotype by sequencing approach coupled with Illumina sequencing produced 77.8 million reads distributed relatively evenly between samples with a mean of 340,940 reads per individual (sd: 157,991) for *I. salapia* samples and a mean of 270,602 reads per individual (sd: 103,734) for *O. onega*. From this sequencing data, SNP calling and filtering steps resulted in final datasets of 17,779 SNPs from 6,972 loci for *I. salapia* samples and 15,894 SNPs from 4,524 loci for *O. onega* samples.

Population genetic structure

For *I. salapia* we considered two parental lineages, an Amazonian lineage corresponding to subspecies *aquinia* sampled from two sites, Km-26 Yurimaguas-Tarapoto (1) and San Miguel de Achinamiza (2), and an Andean lineage corresponding to subspecies *derasa* and sampled from one site Puente Aguas Verdes (5). Between these sites a zone that is geographically and altitudinally intermediate and where those lineages are in contact was sampled at two sites (sites Km-42 Tarapoto-Yurimaguas (i3) and La Florida (i4), hybrid zone) (Figure 1a). The genetic structure, identified by multivariate analyses on genetic data (Figure 2a) as well as `Structure` (Figure 2b), highlight that the samples likely segregate in 3, best clustering, or 2 groups (Evanno's method: higher ΔK of 5037.42 for K=3 and 718.12 for K=2). These results shows that the two parental lineages are distinct and show a low level of admixture. They have a weighted genome-wide differentiation F_{ST} of 0.177 between the two. In the intermediate populations, we did not find putative F1 hybrids (i.e. individuals with hybrid index close to 0.5 and high intertaxon ancestry). Rather, four individuals (subpopulation 3.1, Figure 2b) were genetically similar to individuals from the parental Amazonian *aquinia* lineage, and the 28 other samples had equal levels of admixture with the majority of their genetic content associated with the Andean *derasa* population (Figure 2b). Hybrid indices estimated for these individuals is also indicative of this (Figure 2c).

The distribution of *O. onega* hybrids in the study area is somewhat similar to that observed in *I. salapia*. The genetic structure, identified by multivariate analyses on genetic data (Figure 2a) as well as `Structure` (Figure 2b), highlight the samples likely segregate in 2, best clustering, or 3 groups (Evanno's method: highest ΔK of 9887.07 for K=2 and 7.76 for K=3). This species also consists of two parental lineages corresponding to an Amazonian subspecies, *O. onega janarilla*, collected from two sites, Km-26 Yurimaguas-Tarapoto (1) and San Miguel de Achinamiza (2) and an Andean subspecies, *O. onega* ssp. nov. 2 (Gallusser, 2002; Dasmahapatra, Lamas, Simpson, & Mallet, 2010), sampled at Puente

342 Serranoyacu (5). In addition to these sites, a geographically and altitudinally intermediate
343 zone was also sampled (sites Shapaja-Chazuta (o3) and a site spanning Quebrada Yanayacu to
344 Laguna del Mundo Perdido (o4), hybrid zone) (Figure 1b). The two parental lineages are
345 genetically divergent with a weighted genome-wide differentiation F_{ST} of 0.372, more than
346 twice as high as between *I. salapia* parental lineages. The samples from the hybrid zone
347 comprise a mix of individuals with low and intermediate levels of admixture. Most
348 individuals have a low level of admixture (39 out of 46 had $q < 0.2$), and are genetically
349 closest to the Amazonian parental lineage. The stronger link with the Amazonian lineage
350 suggests a directionality in hybridization different from that of the *I. salapia* hybrid zone.
351 Three individuals show hybrid indices that suggest almost equal contributions from each
352 parental lineage (Figure 2a,b,c). One of these has a high level of intertaxon ancestry, which
353 suggests it is an F1 hybrid. The two other individuals have lower heterozygosity, which is
354 consistent with recent backcrossing. In conclusion, both species show some evidence of gene
355 flow and introgression, but both also exhibit strongly bimodal phenotypes (sensu Jiggins &
356 Mallet, 2000) in the region of the hybrid zone, suggesting strong reproductive isolation in
357 both species. However, *O. onega* displays somewhat more evidence of ongoing hybridization
358 and gene flow than *I. salapia*.

359

360 *Genomic patterns of introgression and differentiation*

361 Introgression varied across the genome for each taxon pair, with distinct patterns of
362 introgression for the two studied species, *I. salapia* and *O. onega*, as demonstrated by the
363 distributions of the genomic cline center (α) and rate parameters (β) (Figure 3). In each
364 species the center parameter (α) is highly variable, with point estimates (posterior median)
365 ranging from -3.067 to 2.864 for *I. salapia* and from -5.785 to 5.907 for *O. onega*. With
366 respect to α, many loci show introgression patterns that differ credibly from the genome-wide

average. Loci with positive center parameter α are more likely to be inherited from the Amazonian parental lineage than the rest of the genome. Conversely, loci with negative α are more likely to be inherited from the Andean lineage. For *I. salapia*, 2125 SNPs (11.95 % of all SNPs) have a center parameter α that differ from the genome-wide average, consistent with different levels of introgression than the average of the rest of the genome. Among the SNPs with credible evidence of differential introgression, most of them (1637 out of 2125, i. e., 77%) have excess ancestry from the Amazonian populations whereas the genome-wide average is more closely associated with the Andean population (Figure 2b,c). In *O. onega*, where intermediate populations are genetically closer to the Amazonian lineage, 2146 SNPs (13.50 % of all SNPs) have a center parameter α that significantly deviates from the genome-wide average. The distribution is reversed compared to *I. salapia*, however, with most of those SNPs (1406 out of 2146, i. e., 66%) having a lower probability of being inherited from the Amazonian parental lineage. This is expected, as there is more statistical power to detect differential introgression of alleles of the less common (i.e., minor) ancestry type.

Regarding the genomic cline rate parameter (β), the profiles for the two species are markedly different. In *I. salapia* species, β hardly shows any variation, ranging from -0.681 to 0.738, whereas the variation observed in *O. onega* is higher by tenfold, ranging from -7.710 to 8.440. Such a large variation in *O. onega* is probably due to the heterogeneity of the hybridization profiles observed in the hybrid zone (Figure 2b). While in *I. salapia* no SNPs are different from the genome-wide expectation, in *O. onega*, 1274 SNPs have a genomic cline rate (β) credibly different from the genome-wide pattern, with 447 and 827 SNPs having higher and lower values, respectively. These 447 SNPs with steeper introgression patterns than the genome-wide average are characteristic of SNPs putatively associated with barrier loci (i.e., in LD with barrier loci).

391 This difference observed between *I. salapia* and *O. onega* can be explained, at least in part, by
392 the fact that there is hardly any variation among hybrids in *I. salapia* in our sampling. Perhaps
393 an even larger sample than at present would show additional variation. In any case, the
394 absence of variation in the *I. salapia* hybrids is a result in itself but limits the capacity to
395 detect variation in patterns of introgression.

396 Genetic differentiation (F_{ST}) between parental lineages was heterogeneous across the genome,
397 ranging from ~0 to 1.000 with a weighted mean value of 0.177 for *I. salapia* and from ~0 to
398 1.000 with a weighted mean value of 0.372 for *O. onega*. The genome scan also identifies
399 outlier SNPs that deviate from the genome-wide distribution and have unusually high levels
400 of differentiation. In *I. salapia*, the 95th percentile threshold corresponds to an F_{ST} value of
401 0.415, and was exceeded by 890 SNPs. In *O. onega*, the 95th percentile threshold corresponds
402 to an F_{ST} value of 0.686, and was exceeded by 795 SNPs.

403

404 *Phenotypic variation*

405 For both species, the first principal component on colour pattern separates Andean from
406 Amazonian lineages (Fig. 4). However, the two species differ in where along this axis
407 specimens from intermediate populations fall. For *I. salapia*, most specimens in the hybrid
408 zone cluster with the Andean *I. salapia derasa*, while only four (with a predominantly
409 Amazonian genetic background) cluster with Amazonian *I. salapia aquinia* (Figure 4). No
410 individual in this sample has a markedly intermediate color pattern along this first principal
411 component. By contrast, most *O. onega* from the hybrid zone have an intermediate position
412 along the first principal component. For both species, the second axis highlights variation
413 associated with sex and as a result males and females are segregated along this axis. While
414 sexual dimorphism is moderate and of the same magnitude in both lineages of *O. onega*, it is
415 more pronounced in the Andean lineage *I. salapia derasa* and virtually absent in the

Amazonian lineage *I. salapia aquinia*. Sex was therefore included as a factor in our phenotype-genotype analyses, along with genetic structure.

Phenotype-genotype relationship and association mapping

Despite the low variability among hybrid individuals from the hybrid zone, especially for *I. salapia*, we attempted to associate genetic variation in specific SNPs to wing pattern variation. All principal components (PCs) explaining at least 1% of total phenotypic variation were included in association mapping (i.e. 14 variables for *I. salapia*, jointly explaining 57.1% of the variance, and 18 for *O. onega*, jointly explaining 54.9% of the variance). Association mapping using `GEMMA` revealed several PCs for which a large phenotypic variation is explained, specifically more than 80% phenotypic variation explained (pve) for 7/14 PCs for *I. salapia* and for 4/18 PCs for *O. onega*. When combining all PCs that were retained (i.e., all those that explained at least 1% of the phenotypic variation), 59.3% of the phenotypic variation is explained for *I. salapia* and 26.3% for *O. onega* (Supplementary Figure 2). The PCs explaining most genetic variation are also those harbouring the largest proportions of wing pattern variation. Specifically, 84.3% of the wing pattern variation is explained for *I. salapia* and 65.3% for *O. onega*. The multivariate linear mixed model of `GEMMA` performs tests to evaluate the probability that SNPs are associated with phenotypic variation and outputs the corresponding p-value resulting from a Wald test. Retaining significant SNPs concurrently in Bonferroni p-value correction and FDR approach, 88 SNPs (0.49% of all SNPs) were significantly associated with wing patterns in *I. salapia* and 109 SNPs (0.69% of all SNPs) in *O. onega* (Figure 5).

We then focused on the differentiation and introgression patterns of SNPs associated with wing pattern. A very small number of SNPs, 17 for *I. salapia* and 4 for *O. onega*, combine

strong association with wing pattern and high levels of differentiation, but in *I. salapia* the SNP with the strongest association with wing pattern is also an outlier in genome scan for differentiation (Figure 5).

With all of these approaches combined, we observe both differences and similarities between *I. salapia* and *O. onega* in the number of SNPs similarly identified as outliers by multiple approaches. The proportion of SNPs combining both high differentiation levels (F_{ST}) and differential introgression (α), and which are characteristic of loci potentially involved in adaptation in hybrid samples, are of the same order in *I. salapia* and in *O. onega* (1.81%, 321/17,779, for *I. salapia*, and 1.59%, 253/15,894, for *O. onega*, Figure 6), and higher than expected at random (Pearson's Chi-squared test, p-value = 1.32e-114 and 95% CI = [103, 135] for *I. salapia* and Pearson's Chi-squared test, p-value = 2.99e-54 and 95% CI = [92, 123] for *O. onega*). SNPs previously identified as potentially involved in adaptation and adaptive introgression, combining high differentiation levels (F_{ST}) and differential introgression (α), do not have a specific enrichment in SNPs significantly associated with wing pattern. In *I. salapia* and *O. onega* the numbers of SNPs that fit this description are low, respectively only two and one SNPs, and do not differ from a random distribution (Pearson's Chi-squared test, p-value = 0.74 and 95% CI = [0, 4] for *I. salapia* and Pearson's Chi-squared test, p-value = 0.57 and 95% CI = [0, 4] for *O. onega*). The main difference between the two species consists in the SNPs with differential positive genomic cline rate values (β) and potentially involved in reproductive isolation. None of the SNPs in *I. salapia* have positive β while a non-trivial proportion do in *O. onega*, i.e. 447 SNPs or 2.81%. Among these SNPs only a small fraction is also significantly associated with wing pattern variation (5) and not enriched compared to a random distribution (Pearson's Chi-squared test, p-value = 0.26 and 95% CI = [1, 6]). Moreover, among the SNPs involved in both, high differentiation level and positive β (71)

and potentially involved in reproductive isolation, none of them is associated with wing pattern variations (Figure 6).

Similarities with other Lepidoptera genomes

We used BLASTn to investigate the potential functional roles of the loci carrying the SNPs highlighted by the approaches listed above. We identified homologous regions in the *D. plexippus* genome for loci containing SNPs significantly associated with wing patterns (12/67 loci for *I. salapia* and 21/99 for *O. onega*; Supplementary Table 3). None of the genes known to control colour pattern variation in Lepidoptera and identified in the *D. plexippus* genome, i.e. *optix*, *cortex*, *WntA*, *ebony* and *aristaless*, were identified.

On the other side the BLASTn of loci with SNPs potentially involved in adaptation and adaptive introgression or reproductive isolation highlighted candidate genomic region and gene in the genome of *D. plexippus* (37/277 loci for *I. salapia* and 66/218 for *O. onega* potentially involved in adaptation and adaptive introgression and 73/389 loci potentially involved in reproductive isolation for *O. onega*; Supplementary Table 2). We here report the list of scaffold containing these loci of interest which are potential candidates for genes involved in local adaptation and reproductive isolation, and on which further functional analyses could be performed to investigate underlying biological functions (Supplementary Table 2).

Discussion

The comparison of genome-wide patterns of genetic differentiation, introgression and genotype-phenotype associations in two species, *I. salapia* and *O. onega*, that face similar environmental transitions revealed some surprisingly large phenotypic and genomic

differences. Below, we discuss potential reasons for the differences observed in light of biological and ecological information.

Genomic and phenotypic differentiation patterns across the Tarapoto suture zone: similarities and differences

Both *I. salapia* and *O. onega* are distributed across an important environmental gradient in the region of Tarapoto in Peru, and both species consist of an Andean and Amazonian lineage. Our analysis of wing pattern variation confirms that Amazonian and Andean lineages of both species are phenotypically different (as is seen by the human eye) and also reveals a subtle sexual dimorphism not readily discernible.

Phenotypic differentiation between populations of each species is associated with strong overall genomic differentiation, especially in *O. onega*. These findings are consistent with those obtained by Dasmahapatra, Lamas, Simpson, & Mallet (2010) using four loci, which also revealed inter-lineage differentiation for these taxa, with the strongest genetic differentiation occurring in *O. onega*.

However, the genomic and phenotypic population structure of hybrid populations differ between *I. salapia* and *O. onega*. Firstly, while all but four of the *I. salapia* individuals sampled in the hybrid zone are genetically closer to the Andean population, most individuals in the *O. onega* hybrid populations we sampled are genetically closer to Amazonian populations. Secondly, one individual in *O. onega* is likely a F1, and two other individuals are recent backcrosses, while no such genetically intermediate individuals were found in our samples of *I. salapia*. Thirdly, the phenotypic structure of hybrid populations mirrors the genomic patterns. Along the first PC individuals in intermediate populations of *I. salapia* are phenotypically closest to the Andean parental lineage (*derasa*), to which they are also closest

genetically. In our sample, intermediate color patterns are not observed in these populations, nor in parental populations. By contrast, individuals in intermediate populations of *O. onega* have intermediate phenotypes between the two lineages, with a tendency to be closer to the Amazonian lineage (*janarilla*), to which they are also closest genetically.

Overall, the patterns detected suggest past gene flow in both species (most individuals have a similar, low hybrid index), with potentially more recent (but rare) gene flow in *O. onega* - although we cannot rule out the fact that we may have missed recent hybrids in *I. salapia*. Genomic differentiation across hybrid zones in Müllerian mimetic butterflies have mostly been documented in the genus *Heliconius*. While *Heliconius* sub-specific lineages sometimes exhibit high genome-wide differentiation across hybrid zones (Martin, Davey, Salazar, & Jiggins, 2019; Van Belleghem et al., 2018), this appears not to be the case in the Tarapoto suture zone. In this region, Nadeau *et al.* (2014) found that in phenotypically differentiated lineages of *H. erato* and *H. melpomene* only loci around pattern gene loci showed genetic differentiation, while the rest of the genome was highly permeable to gene flow, with F_{ST} values ranging from 0.0112 to 0.0280 (see also Martin et al., 2013). This stands in stark contrast to the strong overall differentiation we revealed in ithomiine butterflies from the Tarapoto suture zone (F_{ST} = 0.177 for *I. salapia* and F_{ST} = 0.372 for *O. onega*).

While intermediate populations of *O. onega* show a high extent of genetic heterogeneity, in *I. salapia* all but four individuals from intermediate populations are remarkably similar in their genetic composition. This suggests that intermediate populations of *I. salapia* are hardly exchanging genes with Andean and Amazonian populations, and may be in the process of forming a distinct taxon.

Genomic patterns of introgression

Variation in introgression patterns across the genome can help pinpoint loci involved in adaptation and reproductive isolation (Gompert & Buerkle, 2011; Gompert et al., 2012; Gompert, Mandeville, & Buerkle, 2017). In particular, highly divergent SNPs with deviant genomic cline center parameters (α) or positive genomic cline rate parameter (β) (i. e., exhibiting a steep cline) should be more common in regions of the genome involved in local adaptation or reproductive isolation.

Here, intermediate populations of both *I. salapia* and *O. onega* present SNPs with outlier values in their genomic cline center parameters (α), meaning that these SNPs have an ancestry different from that of the average of the genome. The SNPs exhibiting deviant α should be enriched for genomic regions involved in adaptation or reproductive isolation. Such SNPs (77.0%) are shifted towards Amazonian ancestry in *I. salapia*, whereas the majority of SNPs with deviant α (65.5%) are shifted towards Andean ancestry in *O. onega*. While this may indicate introgression from the parental lineage that is least represented in the genomic background of intermediate populations, in our case such asymmetry may also result from a lower power to detect introgression from the dominant parental background. . Whether some of those SNPs result from adaptive introgression, as has been revealed in *Heliconius* butterflies (*Heliconius* Genome Consortium, 2012; Jay et al., 2018), warrants further study.

Patterns of the parameter cline rate β markedly differ between *I. salapia* and *O. onega*. While in *I. salapia* no SNPs show outlier cline steepness, in *O. onega* many SNPs show narrower or wider clines compared to the genome average. Overall, in *O. onega*, the distribution of genomic cline parameters is wider and more heterogeneous than in *I. salapia*, suggesting less constraints in the hybridization process. Such heterogeneity in *O. onega* allows the identification of loci with specific introgression levels. Highly divergent genomic regions that have low levels of introgression are likely associated with reproductive isolation (Gompert & Buerkle, 2011; Gompert et al., 2012). Low levels of introgression can be the result of several

561 evolutionary processes involving both extrinsic mechanisms, such as divergent selection and
562 environment-dependent selection against hybrids, and intrinsic mechanisms such as an
563 environment-independent reduced hybrid fitness caused by Bateson-Dobzhansky-Muller
564 incompatibilities (Gompert & Buerkle, 2011; Gompert et al., 2012). Correlation of genetic
565 patterns with other evidence (e. g., candidate traits) may shed light on the mechanisms of
566 speciation and reproductive isolation (Ravinet et al., 2017).

567

568 *Genetic bases of colour pattern variation*

569 Our admixture mapping analysis revealed SNPs associated with color pattern in *I. salapia* (88
570 SNPs, representing 0.49% of all SNPs) and *O. onega* (109 SNPs, representing less than
571 0.69% of all SNPs).

572 In nymphalid butterflies, wing pattern variation can be explained by combinations of
573 conserved pattern elements (Martin & Reed, 2014) and tends to be controlled by small
574 numbers of loci (Van Belleghem et al., 2017; Zhang et al., 2017). Previous studies, including
575 studies on mimetic *Heliconius* (Joron et al., 2006; Martin et al., 2012; Nadeau, 2016; Reed et
576 al. 2011; Westerman et al., 2018) and *Papilio* (Timmermans et al., 2014) identified a list of
577 candidate genes such as *WntA*, *optix*, *cortex*, *ebony* and *aristaless*. Some of these have been
578 functionally characterized (Martin & Reed, 2014; Nadeau, 2016; Nadeau et al., 2016). A
579 recent study on *D. plexippus*, the most closely related species to Ithomiini for which a
580 reference genome is available, highlighted the role of *WntA* in vein shape (Mazo-Vargas et
581 al., 2017).

582 None of our candidate loci correspond to genes known to be involved in wing colour pattern
583 in other butterflies. This is likely due to the relatively low-resolution genotype-by-sequencing

584 approach adopted here, such that we may have missed gene regions that were not covered by
585 our loci.

586 Moreover, only a small fraction of loci with SNPs associated with wing pattern (23.9% for *I.*
587 *salapia* and 21.2% for *O. onega*) map to an orthologous region in the *D. plexippus* genome.
588 This deficit is related to the relatively large divergence time between our focal species and *D.*
589 *plexippus* (ca. 42 million years ago, Chazot et al., 2019), which limits our ability to find
590 orthologous regions and more specifically to find regions involved in non-coding regulatory
591 loci. We may therefore have missed loci that contain known genes involved in wing pattern
592 development.

593 Finally, the extremely low level of hybridization observed in *I. salapia* reduces the statistical
594 power of admixture mapping and hampers detection of genomic regions associated with wing
595 pattern variation. The function of most regions identified in our analyses are unknown and
596 represent a starting point for further analyses of these regions, as those regions may contain
597 novel genes in these pathways.

598

599 *Colour pattern and reproductive isolation*

600 Wing colour pattern is known to cause pre- and post-zygotic reproductive isolation in
601 Müllerian mimetic butterflies (e. g., Chamberlain, Hill, Kapan, Gilbert, & Kronforst, 2009;
602 Jiggins, Naisbit, Coe, & Mallet, 2001; Mallet & Barton, 1989; Merrill et al., 2012; Merrill et
603 al., 2011; Naisbit, Jiggins, Linares, Salazar, & Mallet, 2002), including Ithomiini (McClure et
604 al., 2019).

605 In our admixture mapping analysis, we found that only two and one of the significantly
606 differentiated introgression outliers were also associated with wing pattern variation in *I.*
607 *salapia* and *O. onega*, respectively. These figures do not differ from random expectations.

608 These results suggest that wing colour pattern may be moderately involved in reproductive
609 isolation in both species, but since our genomic data do not cover the entire genome, we
610 cannot rule out the fact that we may have missed some important loci involved in wing
611 pattern coloration and with deviant genomic clines.

612 In mimetic butterflies, hybrid individuals with intermediate colour pattern may suffer more
613 predation because they are not recognized as unpalatable (e. g., Merrill et al., 2012), which
614 may in turn select for assortative mating for wing colour pattern through reinforcement (e. g.,
615 Kronforst, Young, & Gilbert, 2007), resulting in reproductive isolation between
616 phenotypically differentiated lineages. Whether individuals with intermediate phenotype
617 suffer increased predation has never been tested in *I. salapia* and *O. onega*, but predation
618 experiments on *Heliconius* species carried out in the same region demonstrated the ability of
619 predators to discriminate fine phenotypic differences (Arias et al., 2016; Chouteau, Arias, &
620 Joron, 2016). Assortative mating seems likely in *I. salapia* and *O. onega* (MM and ME, pers.
621 obs.), and has been documented by genetic and phenotypic characterization of the reared
622 offspring of females collected in hybrid populations of *O. onega* (De Silva, 2010: chapter 5).

623 There are fewer phenotypically intermediate individuals in *I. salapia* than in *O. onega*. This
624 difference might be explained by the mimicry rings to which the two species belong. While
625 the mimicry rings of *I. salapia* lineages are readily discriminated and show little variation
626 within each mimicry ring, the forms *O. onega* belongs to are more variable with overlapping
627 phenotypes (ME pers. obs.; Supplementary Figure 1). Because of the greater variation and
628 overlap of the two *O. onega* mimicry rings in Tarapoto, selection against hybrids with
629 intermediate phenotypes may be reduced compared with that in *I. salapia*, thereby allowing
630 the persistence of greater levels of gene flow between lineages. Whether the absence of
631 intermediate phenotypes in *I. salapia* is due to high mortality of hybrids through predation,

strong assortative mating, hybrid incompatibilities or all of these is currently unknown and deserves further examination.

Other putative adaptive traits

In both species, only a small number of SNPs potentially involved in adaptation or reproductive isolation (i. e., highly differentiated SNPs that show deviant α or significantly positive β) are also associated with wing pattern. This suggests that other traits may play a role in reproductive isolation. Because interactions with local host plants at the larval stage and the ability to fully exploit them often impact fitness in phytophagous insects (Simon et al., 2015), larval hostplant shifts are believed to be an important driver of reproductive isolation. However, in *O. onega* the two lineages utilize the same larval hostplants, *Solanum mite* and related *Solanum* sect. *Pteroidea* species (de-Silva, Vásquez, & Mallet, 2011; Gallusser, 2002). Similarly, *I. salapia derasa* larvae commonly feed on *Witheringia solanacea* (Beccaloni, 1997), a plant also used by *I. salapia aquinia* (JM, MM and ME, unpublished observations). Shifts in hostplant are therefore unlikely to explain divergence between lineages in either of these species, as is the case in another ithomiine genus, *Melinaea*, present in the same region (McClure & Elias, 2016).

The two lineages of *O. onega* have divergent egg-laying behavior: females of the Amazonian population (*janarilla*) lay eggs on the hostplants, while females of the Andean population (ssp. nov. 2) tend to lay eggs off the host plant (Gallusser, 2002). Eggs are typically laid up to 0.5 m away from the nearest host plant individual, on twigs, leaf litter or live non-host plant, which reduces egg predation (de-Silva, Vásquez, & Mallet, 2011). Differences in egg-laying behavior have been shown to cause reduced hybrid fitness in butterflies (McBride & Singer, 2010). This could be the case here, too, if hybrid females lay eggs off the plant, and if first instar larvae are incapable of locating their host plant.

Other putative adaptive traits include adaptations to distinct habitats (higher elevations and cooler temperatures for Andean lineages) and potentially microhabitats where co-mimics are most abundant (e. g., Elias, Gompert, Jiggins, & Willmott, 2008).

Finally, as many butterfly species, Ithomiini probably rely on sexual pheromones during mate choice (Schulz et al., 2004), and differences in sexual pheromones may incur discrimination between lineages. Notably, putative male pheromones have been shown to differ between the two lineages of *O. onega* (Stamm, Mann, McClure, Elias, & Schulz, 2019).

The role of these traits in reproductive isolation remains to be further explored using both experimental and genomic approaches.

Acknowledgements. We thank the Peruvian authorities and Dr Gerardo Lamas (Museo de Historia Natural, Universidad Mayor de San Marcos) for research permits (096-2004-INRENA-IFFS-DCB, 021C⁄C-2005-INRENA-IANP and 236-2012-AG-DGFFS-DGEFFS). We also thank Armando Silva-Vásquez and Fraser Simpson for their precious help in the field. Molecular work was carried out at the Service de Systématique Moléculaire du Muséum National d'Histoire Naturelle (UMS 2700 - OMSI). The support and resources from the Center for High Performance Computing at the University of Utah are gratefully acknowledged. We thank three anonymous reviewers for their useful comments that led us to improve our manuscript.

Data accessibility. Sequence reads are archived at the NCBI SRA in the BioProject PRJNA575968. Scripts describing the whole analytic process have been uploaded to GitHub (https://github.com/JeremyLGauthier/Scripts_Gauthier_et.al_2019_ME).

Author contributions : ME and ZG designed the study. LdS, JM , MM and ME performed sampling. LdS, AW, ZG and ME performed labwork. JG analysed the molecular data, with contributions from ZG, AW, CL and FL. ME, JG, CH and YLP analysed phenotypic data. All authors took part in discussions concerning the analyses and result interpretations. JG wrote the paper, with contributions from all authors.

Funding. This research was funded by a CNRS ATIP grant, two ANR grants (SPECREP ANR-14-CE02-0011 and CLEARWING ANR-16-CE02-0012) and a Human Frontier Science Program (RGP0014/2016) grant awarded to ME. LdS was a postdoc on the ATIP grant and JG and MM were postdocs on the ANR SPECREP grant.

References:

Arias, M., le Poul, Y., Chouteau, M., Boisseau, R., Rosser, N., Théry, M., & Llaurens, V. (2016). Crossing fitness valleys: empirical estimation of a fitness landscape associated with polymorphic mimicry. *Proceedings. Biological Sciences / The Royal Society*, 283(1829).

Barton, N. H., & Bengtsson, B. O. (1986). The barrier to genetic exchange between hybridising populations. *Heredity*, 57(3), 357.

Barton, N. H., & Hewitt, G. M. (1985). Analysis of hybrid zones. *Annual Review of Ecology and Systematics*, *16*(1), 113–148.

Barton, N. H., & Hewitt, G. M. (1989). Adaptation, speciation and hybrid zones. *Nature*, *341*(6242), 497–503.

Bates, H. W. (1862). XXXII. Contributions to an insect fauna of the Amazon valley. Lepidoptera: Heliconidae. *Transactions of the Linnean Society of London*, *23*(3), 495–566.

Beccaloni, G. W. (1997). Ecology, natural history and behaviour of Ithomiine butterflies and their mimics in Ecuador (Lepidoptera: Nymphalidae: Ithomiinae). *Tropical Lepidoptera Research*, *8*(2), 103–124.

Benjamini, Y. & Hochberg, Y. (1995) Controlling the false discovery rate: a practical and powerful approach to multiple testing. *Journal of the Royal Statistical Society Series B*, 57, 289–300.

Bierne, N., Welch, J., Loire, E., Bonhomme, F., & David, P. (2011). The coupling hypothesis: why genome scans may fail to map local adaptation genes. *Molecular Ecology*, *20*(10), 2044–2072.

Brown K. S., Sheppard Philip Macdonald, & Turner John Richard George. (1974). Quaternary refugia in tropical America: evidence from race formation in *Heliconius* butterflies. *Proceedings of the Royal Society B: Biological Sciences*, *187*(1088), 369–378.

Buerkle, C. A., & Lexer, C. (2008). Admixture as the basis for genetic mapping. *Trends in Ecology & Evolution*, *23*(12), 686–694.

Challis, R. J., Kumar, S., Dasmahapatra, K. K., Jiggins, C. D., & Blaxter, M. (2016). Lepbase: the Lepidopteran genome database (p. 056994). doi: 10.1101/056994

Chamberlain, N. L., Hill, R. I., Kapan, D. D., Gilbert, L. E., & Kronforst, M. R. (2009). Polymorphic butterfly reveals the missing link in ecological speciation. *Science*, *326*(5954), 847–850.

Chazot, N., Wahlberg, N., Freitas, A. V. L., Mitter, C., Labandeira, C., Sohn, J.-C., … Heikkilä, M. (2019). Priors and Posteriors in Bayesian Timing of Divergence Analyses: The Age of Butterflies Revisited. *Systematic Biology*, 68(5), 797–813.

Chouteau, M., Arias, M., & Joron, M. (2016). Warning signals are under positive frequency-dependent selection in nature. *Proceedings of the National Academy of Sciences of the United States of America*, *113*(8), 2164–2169.

Christe, C., Stölting, K. N., Bresadola, L., Fussi, B., Heinze, B., Wegmann, D., & Lexer, C. (2016). Selection against recombinant hybrids maintains reproductive isolation in

hybridizing Populus species despite F1 fertility and recurrent gene flow. *Molecular Ecology*, *25*(11), 2482–2498.

Danecek, P., Auton, A., Abecasis, G., Albers, C. A., Banks, E., DePristo, M. A., … 1000 Genomes Project Analysis Group. (2011). The variant call format and VCFtools. *Bioinformatics* , *27*(15), 2156–2158.

Dasmahapatra, K. K., Lamas, G., Simpson, F., & Mallet, J. (2010). The anatomy of a "suture zone" in Amazonian butterflies: a coalescent-based test for vicariant geographic divergence and speciation. *Molecular Ecology*, *19*(19), 4283–4301.

de-Silva, D. L. (2010). Ecology and Evolution in Neotropical Butterflies of the Subtribe Oleriina (Lepidoptera: Nymphalidae: Danainae: Ithomiini). PhD thesis, University of London, 275pp.

de-Silva, D. L., Vásquez, A. S., & Mallet, J. (2011). Selection for enemy-free space: eggs placed away from the host plant increase survival of a neotropical ithomiine butterfly. *Ecological Entomology*, *36*(6), 667–672.

Earl, D. A., & vonHoldt, B. M. (2012). STRUCTURE HARVESTER: a website and program for visualizing STRUCTURE output and implementing the Evanno method. *Conservation Genetics Resources*, *4*(2), 359–361.

Elias, M., Gompert, Z., Jiggins, C., & Willmott, K. (2008). Mutualistic interactions drive ecological niche convergence in a diverse butterfly community. *PLoS Biology*, *6*(12), 2642–2649.

Endler, J. A. (1977). Geographic variation, speciation, and clines. *Monographs in Population Biology*, *10*, 1–246.

Evanno, G., Regnaut, S., & Goudet, J. (2005). Detecting the number of clusters of individuals using the software STRUCTURE: a simulation study. *Molecular Ecology*, *14*(8), 2611–2620.

Falush, D., Stephens, M., & Pritchard, J. K. (2003). Inference of population structure using multilocus genotype data: linked loci and correlated allele frequencies. *Genetics*, *164*(4), 1567–1587.

Freedman, M. L., Reich, D., Penney, K. L., McDonald, G. J., Mignault, A. A., Patterson, N., … Altshuler, D. (2004). Assessing the impact of population stratification on genetic association studies. *Nature Genetics*, *36*(4), 388–393.

Gallusser, S. A. (2002). Biology, behaviour and taxonomy of two *Oleria onega* subspecies (Ithomiinae, Nymphalidae, Lepidoptera) in north-eastern, Peru (Université de Neuchâtel). Retrieved from http://doc.rero.ch/record/2627

Gauthier, J., Mouden, C., Suchan, T., Alvarez, N., Arrigo, N., Riou, C., … Peterlongo, P. (2017). DiscoSnp-RAD: de novo detection of small variants for population genomics (p. 216747). doi: 10.1101/216747

Gompert, Z., & Buerkle, C. A. (2009). A powerful regression-based method for admixture mapping of isolation across the genome of hybrids. *Molecular Ecology*, *18*(6), 1207–1224.

Gompert, Z., & Buerkle, C. A. (2011). Bayesian estimation of genomic clines. *Molecular Ecology*, *20*(10), 2111–2127.

Gompert, Z., & Buerkle, C. A. (2012). bgc: Software for Bayesian estimation of genomic clines. *Molecular Ecology Resources*, *12*(6), 1168–1176.

781 Gompert, Z., & Buerkle, C. A. (2013). Analyses of genetic ancestry enable key insights for
782 molecular ecology. *Molecular Ecology*, *22*(21), 5278–5294.

783 Gompert, Z., Lucas, L. K., Nice, C. C., Fordyce, J. A., Forister, M. L., & Buerkle, C. A.
784 (2012). Genomic regions with a history of divergent selection affect fitness of hybrids
785 between two butterfly species. *Evolution*, *66*(7), 2167–2181.

786 Gompert Z., Lucas L. K., Buerkle C. A., Forister M. L., Fordyce J. A., Nice C. C. (2014).
787 Admixture and the organization of genetic diversity in a butterfly species complex
788 revealed through common and rare genetic variants. *Molecular Ecolology*; *23*(18):4555–
789 4573.

790 Gompert, Z., Mandeville, E. G., & Buerkle, C. A. (2017). Analysis of Population Genomic
791 Data from Hybrid Zones. *Annual Review of Ecology, Evolution, and Systematics*, *48*(1),
792 207–229.

793 *Heliconius* Genome Consortium. (2012). Butterfly genome reveals promiscuous exchange of
794 mimicry adaptations among species. *Nature*, *487*(7405), 94–98.

795 Jay, P., Whibley, A., Frézal, L., Rodríguez de Cara, M. Á., Nowell, R. W., Mallet, J., …
796 Joron, M. (2018). Supergene Evolution Triggered by the Introgression of a
797 Chromosomal Inversion. *Current Biology: CB*, *28*(11), 1839–1845.e3.

798 Jiggins, C. D., Naisbit, R. E., Coe, R. L., & Mallet, J. (2001). Reproductive isolation caused
799 by colour pattern mimicry. *Nature*, *411*(6835), 302–305.

800 Jiggins, C.D., & Mallet, J. (2000). Bimodal hybrid zones and speciation. *Trends in Ecology
801 and Evolution* 15:250-255.

802 Jombart, T., & Ahmed, I. (2011). adegenet 1.3-1: new tools for the analysis of genome-wide
803 SNP data. *Bioinformatics* , *27*(21), 3070–3071.

804 Jones, F. C., Grabherr, M. G., Chan, Y. F., Russell, P., Mauceli, E., Johnson, J., … Kingsley,
805 D. M. (2012). The genomic basis of adaptive evolution in threespine sticklebacks.
806 *Nature*, *484*(7392), 55–61.

807 Joron, M., Papa, R., Beltrán, M., Chamberlain, N., Mavárez, J., Baxter, S., … Jiggins, C. D.
808 (2006). A conserved supergene locus controls colour pattern diversity in *Heliconius*
809 butterflies. *PLoS Biology*, *4*(10), e303.

810 Kapan, D. D. (2001). Three-butterfly system provides a field test of müllerian mimicry.
811 *Nature*, *409*(6818), 338–340.

812 Kozak, K. M., Wahlberg, N., Neild, A. F. E., Dasmahapatra, K. K., Mallet, J., & Jiggins, C.
813 D. (2015). Multilocus species trees show the recent adaptive radiation of the mimetic
814 H*eliconius* butterflies. *Systematic Biology*, *64*(3), 505–524.

815 Kronforst, M. R., Hansen, M. E. B., Crawford, N. G., Gallant, J. R., Zhang, W., Kulathinal, R.
816 J., … Mullen, S. P. (2013). Hybridization reveals the evolving genomic architecture of
817 speciation. *Cell Reports*, *5*(3), 666–677.

818 Kronforst, M. R., Young, L. G., & Gilbert, L. E. (2007). Reinforcement of mate preference
819 among hybridizing *Heliconius* butterflies. *Journal of Evolutionary Biology*, *20*(1), 278–
820 285.

821 Larson, E. L., Andrés, J. A., Bogdanowicz, S. M., & Harrison, R. G. (2013). Differential
822 introgression in a mosaic hybrid zone reveals candidate barrier genes. *Evolution*, *67*(12),
823 3653–3661.

824 Le Poul, Y., Whibley, A., Chouteau, M., Prunier, F., Llaurens, V., & Joron, M. (2014).
825 Evolution of dominance mechanisms at a butterfly mimicry supergene. *Nature*
826 *Communications*, *5*, 5644.

827 Mallet, J. (2005). Hybridization as an invasion of the genome. *Trends in Ecology &*
828 *Evolution*, *20*(5), 229–237.

829 Mallet, J., & Barton, N. H. (1989). Strong Natural Selection in a Warning-Color Hybrid Zone.
830 *Evolution*, *43*(2), 421–431.

831 Martin, S. H., Dasmahapatra, K. K., Nadeau, N. J., Salazar, C., Walters, J. R., Simpson, F., ...
832 Jiggins, C. D. (2013). Genome-wide evidence for speciation with gene flow in
833 *Heliconius* butterflies. *Genome Research* 23:1817-1828.

834 Martin, S. H., Davey, J. W., Salazar, C., & Jiggins, C. D. (2019). Recombination rate
835 variation shapes barriers to introgression across butterfly genomes. *PLoS Biology*, *17*(2),
836 e2006288.

837 Martin, A., Papa, R., Nadeau, N. J., Hill, R. I., Counterman, B. A., Halder, G., … Reed, R. D.
838 (2012). Diversification of complex butterfly wing patterns by repeated regulatory
839 evolution of a Wnt ligand. *Proceedings of the National Academy of Sciences of the*
840 *United States of America*, *109*(31), 12632–12637.

841 Martin, A., & Reed, R. D. (2014). Wnt signaling underlies evolution and development of the
842 butterfly wing pattern symmetry systems. *Developmental Biology*, *395*(2), 367–378.

843 Mazo-Vargas, A., Concha, C., Livraghi, L., Massardo, D., Wallbank, R. W. R., Zhang, L., …
844 Martin, A. (2017). Macroevolutionary shifts of WntA function potentiate butterfly wing-
845 pattern diversity. *Proceedings of the National Academy of Sciences of the United States*
846 *of America*, *114*(40), 10701–10706.

847 McBride, C. S., & Singer, M. C. (2010). Field studies reveal strong postmating isolation
848 between ecologically divergent butterfly populations. *PLoS Biology*, *8*(10), e1000529.

849 McClure, M., & Elias, M. (2016). Unravelling the role of host plant expansion in the
850 diversification of a Neotropical butterfly genus. *BMC Evolutionary Biology*, *16*(1), 128.

851 McClure, M., Mahrouche, L., Houssin, C., Monllor, M., Le Poul, Y., Frérot, B., … Elias, M.
852 (2019). Does divergent selection predict the evolution of mate preference and
853 reproductive isolation in the tropical butterfly genus *Melinaea* (Nymphalidae:
854 Ithomiini)? *The Journal of Animal Ecology*. doi: 10.1111/1365-2656.12975

855 Merrill R. M., Wallbank R. W. R., Bull V., Salazar P. C. A., Mallet J., Stevens M., & Jiggins
856 C. D. (2012). Disruptive ecological selection on a mating cue. *Proceedings of the Royal*
857 *Society B: Biological Sciences*, *279*(1749), 4907–4913.

858 Merrill, R. M., Gompert, Z., Dembeck, L. M., Kronforst, M. R., McMillan, W. O., & Jiggins,
859 C. D. (2011). Mate preference across the speciation continuum in a clade of mimetic
860 butterflies. *Evolution; International Journal of Organic Evolution*, *65*(5), 1489–1500.

861 Moritz, C., Hoskin, C. J., MacKenzie, J. B., Phillips, B. L., Tonione, M., Silva, N., …
862 Graham, C. H. (2009). Identification and dynamics of a cryptic suture zone in tropical
863 rainforest. *Proceedings of the Royal Society B: Biological Sciences*, 276(1660), 1235–
864 1244.

865 Muller, F. (1879). *Ituna* and *Thyridia*; a remarkable case of mimicry in butterflies.
866 *Proceedings of the Entomological Society of London.*

867 Nadeau, N. J. (2016). Genes controlling mimetic colour pattern variation in butterflies.

Current Opinion in Insect Science, *17*, 24–31.

Nadeau, N. J., Pardo-Diaz, C., Whibley, A., Supple, M. A., Saenko, S. V., Wallbank, R. W. R., … Jiggins, C. D. (2016). The gene *cortex* controls mimicry and crypsis in butterflies and moths. *Nature*, *534*(7605), 106–110.

Nadeau, N. J., Ruiz, M., Salazar, P., Counterman, B., Medina, J. A., Ortiz-Zuazaga, H., … Papa, R. (2014). Population genomics of parallel hybrid zones in the mimetic butterflies, *H. melpomene* and *H. erato*. *Genome Research*, *24*(8), 1316–1333.

Naisbit, R. E., Jiggins, C. D., Linares, M., Salazar, C., & Mallet, J. (2002). Hybrid sterility, Haldane's rule and speciation in *Heliconius cydno* and *H. melpomene*. *Genetics*, *161*(4), 1517–1526.

Nosil, P., Funk, D. J., & Ortiz-Barrientos, D. (2009). Divergent selection and heterogeneous genomic divergence. *Molecular Ecology*, *18*(3), 375–402.

Pallares, L. F., Harr, B., Turner, L. M., & Tautz, D. (2014). Use of a natural hybrid zone for genomewide association mapping of craniofacial traits in the house mouse. *Molecular Ecology*, *23*(23), 5756–5770.

Parchman, T. L., Gompert, Z., Mudge, J., Schilkey, F. D., Benkman, C. W., & Buerkle, C. A. (2012). Genome-wide association genetics of an adaptive trait in lodgepole pine. *Molecular Ecology*, *21*(12), 2991–3005.

Price, A. L., Patterson, N. J., Plenge, R. M., Weinblatt, M. E., Shadick, N. A., & Reich, D. (2006). Principal components analysis corrects for stratification in genome-wide association studies. *Nature Genetics*, *38*(8), 904–909.

Pritchard, J. K., Stephens, M., & Donnelly, P. (2000). Inference of population structure using multilocus genotype data. *Genetics*, *155*(2), 945–959.

Priyam, A., Woodcroft, B. J., Rai, V., Munagala, A., Moghul, I., Ter, F., … Wurm, Y. (2019). Sequenceserver: a modern graphical user interface for custom BLAST databases, *Molecular Biology and Evolution*, msz185.

Ravinet, M., Faria, R., Butlin, R. K., Galindo, J., Bierne, N., Rafajlović, M., … Westram, A. M. (2017). Interpreting the genomic landscape of speciation: a road map for finding barriers to gene flow. *Journal of Evolutionary Biology*, *30*(8), 1450–1477.

Reed, R. D., Papa, R., Martin, A., Hines, H. M., Counterman, B. A., Pardo-Diaz, C., … McMillan, W. O. (2011). *optix* drives the repeated convergent evolution of butterfly wing pattern mimicry. *Science*, *333*(6046), 1137–1141.

Remington, C. L. (1968). Suture-zones of hybrid interaction between recently joined biotas. *Evolutionary Biology* (pp. 321–428).

Rieseberg, L. H., Whitton, J., & Gardner, K. (1999). Hybrid zones and the genetic architecture of a barrier to gene flow between two sunflower species. *Genetics*, *152*(2), 713–727.

Rissler, L. J., & Smith, W. H. (2010). Mapping amphibian contact zones and phylogeographical break hotspots across the United States. *Molecular Ecology*, *19*(24), 5404–5416.

Roberts, J. L., Brown, J. L., May, R. von, Arizabal, W., Schulte, R., & Summers, K. (2006). Genetic divergence and speciation in lowland and montane peruvian poison frogs. *Molecular Phylogenetics and Evolution*, *41*(1), 149–164.

Safran, R. J., & Nosil, P. (2012). Speciation: The origin of new species. *Nature Education Knowledge*, *3*(10), 17.

Schulz, S., Beccaloni, G., Brown, K. S., Jr., Boppre, M., Freitas, A. V. L., Ockenfels, P., & Trigo, J. R. (2004). Semiochemicals derived from pyrrolizidine alkaloids in male ithomiine butterflies (Lepidoptera: Nymphalidae: Ithomiinae). *Biochemical Systematics and Ecology*, *32*.

Simon, J.-C., d'Alençon, E., Guy, E., Jacquin-Joly, E., Jaquiéry, J., Nouhaud, P., … Streiff, R. (2015). Genomics of adaptation to host-plants in herbivorous insects. *Briefings in Functional Genomics*, *14*(6), 413–423.

Smith, B. T., McCormack, J. E., Cuervo, A. M., Hickerson, M. J., Aleixo, A., Cadena, C. D., … Brumfield, R. T. (2014). The drivers of tropical speciation. *Nature*, *515*(7527), 406–409.

Soria-Carrasco, V., Gompert, Z., Comeault, A. A., Farkas, T. E., Parchman, T. L., Johnston, J. S., … Nosil, P. (2014). Stick insect genomes reveal natural selection's role in parallel speciation. *Science*, *344*(6185), 738–742.

Stamm, P., Mann, F., McClure, M., Elias, M., & Schulz, S. (2019). Chemistry of the Androconial Secretion of the Ithomiine Butterfly *Oleria onega*. *Journal of Chemical Ecology*, *45*(9), 768–778.

Teeter, K. C., Payseur, B. A., Harris, L. W., Bakewell, M. A., Thibodeau, L. M., O'Brien, J. E., … Tucker, P. K. (2008). Genome-wide patterns of gene flow across a house mouse hybrid zone. *Genome Research*, *18*(1), 67–76.

Teeter, K. C., Thibodeau, L. M., Gompert, Z., Buerkle, C. A., Nachman, M. W., & Tucker, P. K. (2010). The variable genomic architecture of isolation between hybridizing species of house mice. *Evolution; International Journal of Organic Evolution*, *64*(2), 472–485.

Timmermans Martijn J. T. N., Baxter Simon W., Clark Rebecca, Heckel David G., Vogel Heiko, Collins Steve, … Vogler Alfried P. (2014). Comparative genomics of the mimicry switch in *Papilio dardanus*. *Proceedings of the Royal Society B: Biological Sciences*, *281*(1787), 20140465.

Uricaru, R., Rizk, G., Lacroix, V., Quillery, E., Plantard, O., Chikhi, R., … Peterlongo, P. (2015). Reference-free detection of isolated SNPs. *Nucleic Acids Research*, *43*(2), e11.

Van Belleghem, S. M., Baquero, M., Papa, R., Salazar, C., McMillan, W. O., Counterman, B. A., … Martin, S. H. (2018). Patterns of Z chromosome divergence among *Heliconius* species highlight the importance of historical demography. *Molecular Ecology*, *27*(19), 3852–3872.

Van Belleghem, S. M., Rastas, P., Papanicolaou, A., Martin, S. H., Arias, C. F., Supple, M. A., … Papa, R. (2017). Complex modular architecture around a simple toolkit of wing pattern genes. *Nature Ecology & Evolution*, *1*(3), 52.

Via, S., & Hawthorne, D. J. (2002). The genetic architecture of ecological specialization: correlated gene effects on host use and habitat choice in pea aphids. *The American Naturalist*, *159 Suppl 3*, S76–S88.

Weir, B. S., & Cockerham, C. C. (1984). Estimating *F*-Statistics for the analysis of population structure. *Evolution*, *38*(6), 1358–1370.

Weir, J. T. (2006). Divergent timing and patterns of species accumulation in lowland and highland neotropical birds. *Evolution*, *60*(4), 842–855.

Westerman, E. L., VanKuren, N. W., Massardo, D., Tenger-Trolander, A., Zhang, W., Hill, R. I., … Kronforst, M. R. (2018). Aristaless controls butterfly wing color variation used in mimicry and mate choice. *Current Biology: CB*, *28*(21), 3469–3474.e4.

Whinnett, A., Zimmermann, M., Willmott, K. R., Herrera, N., Mallarino, R., Simpson, F., … Mallet, J. (2005). Strikingly variable divergence times inferred across an Amazonian butterfly "suture zone." *Proceedings of the Royal Society B: Biological Sciences*, *272*(1580), 2525–2533.

Zhang, L., Martin, A., Perry, M. W., van der Burg, K. R. L., Matsuoka, Y., Monteiro, A., & Reed, R. D. (2017). Genetic basis of melanin pigmentation in butterfly wings. *Genetics*, *205*(4), 1537–1550.

Zhou, X., & Stephens, M. (2012). Genome-wide efficient mixed-model analysis for association studies. *Nature Genetics*, *44*(7), 821–824.

Zhou, X., & Stephens, M. (2014). Efficient multivariate linear mixed model algorithms for genome-wide association studies. *Nature Methods*, *11*(4), 407–409.

Figure captions :

Figure 1. The study organisms and sites studied in N.E. Peru. a. Photos of representative specimens from each population of the two studied species (dorsal side shown against a dark background to highlight transparency and ventral side shown against a white background to highlight colour pattern). b. Sampling sites for *I. salapia* populations (top) with Amazonian sites in red (1)Km-26 Yurimaguas-Tarapoto and (2) San Miguel de Achinamiza, the Andean sites in blue (5) Puente Aguas Verdes and sites within the hybrid zone in purple (i3) Km-42 Tarapoto-Yurimaguas and (i4) La Florida. For *O. onega* populations (bottom), Amazonian sites are in green (1)Km-26 Yurimaguas-Tarapoto and (2) San Miguel de Achinamiza, Andean sites are in yellow (5) Puente Serranoyacu and the sites in the hybrid zone are in apple green (o3) Shapaja-Chazuta (o4) from Quebrada Yanayacu to Laguna del Mundo Perdido. Color codes are conserved for all other figures. c. Photos of putative hybrid specimens with intermediate color patterns (ventral side). Photo credits: Céline Houssin

Figure 2. Population structure of pure and hybrid populations of *Ithomia salapia* (top) and *Oleria onega* (bottom). a. Principal component Analysis (PC1: horizontal axis, PC2: vertical axis), the percentage of total inertia explained by each axis is indicated in parentheses and the histograms in the top corners represent the inertia percentages of the first principal components. b. Structure plot for K = 2 and K = 3. The number of individuals that were used is indicated for each site. c. Plot of the hybrid index of each sample from the hybrid populations. The points represent the mean hybrid index value estimated from the posterior distribution and black lines indicate 95% credible intervals. d. Plot of intertaxon ancestry and hybrid index. Population color codes are the same as those in Figure 1b.

Figure 3. Scatterplots representing the relationships between the genomic cline center parameter (α), representing SNP ancestry; the genomic cline rate parameter (β), representing the steepness of the cline; and the differentiation level, F_{ST}, estimated for each SNP. Plots for *I. salapia* and *O. onega* are on theft and right, respectively. Each data point is colored in grey, and darkness increases with point density (i. e., darker areas contain more points). Blue lines frame sets of SNPs for which the genomic cline center parameters (α) significantly deviates from the genome-wide pattern. Green lines frame sets of SNPs for which the genomic cline rate parameters (β) significantly deviates from the genome-wide pattern. Note that for *I. salapia*, no SNPs have genomic cline rate parameters (β) that deviate from the genome-wide pattern. SNPs on the right hand side of the orange lines harbour a significantly higher differentiation (high F_{ST}) than the genome average.

Figure 4. Phenotypic position of 90 *I. salapia* (top) and 94 *O. onega* (bottom) in the wing color space consisting of the two main principal components from the colour pattern modeling approach. Color indicates sample populations as in Figure 1b. Females and males are depicted by circles and triangles, respectively. Representative images of the average phenotypes for population and sex are shown on each side of the figure.

Figure 5. The relationship between the significance of association with color pattern (represented as $-\log_{10}$(p-Wald)) and F_{ST} for *I. salapia* (left) and *O. onega* (right). Yellow points indicate SNPs significantly associated with wing patterns (after both Bonferroni and

FDR corrections). Orange points highlight SNPs with high FST values and red points highlight SNPs with significant association both to wing pattern and to high FST.

Figure 6. Venn diagram combining number of SNPs identified as supported by each approach (differentiation, introgression and admixture mapping) and shared between them. Note that for introgression patterns, no SNP showed deviant genomic cline rate parameters (β) in *I. salapia*. This parameter is therefore not represented in the diagram.

Supplementary material :

Supplementary Figure 1. Mimicry ring example for each studied species and lineages, in black frameworks, including various other butterfly species.

Supplementary Figure 2. Barplots with error bars of the Phenotypic Variation Explained (PVE) by genetic for each variable (PC) explaining more than 1% of the wing pattern variation.

Supplementary Table 1. Sampling information including species, population, sex, location, region, GPS positions, sampling date. For each sample, the number of reads sequenced and SNPs called has been given.

Supplementary Table 2. BLAST results of locus with outlier SNPs identified as potentially involved in local adaptation, adaptive introgression and reproductive isolation, i.e. differential genomic cline center (α), high differentiation level (FST) and differential positive genomic cline rate (β).

Supplementary Table 3. BLAST results of loci with SNPs significantly associated with wing pattern variation.

a.

Ithomia salapia aquinia (Amazon)

Ithomia salapia derasa (Andes)

b.

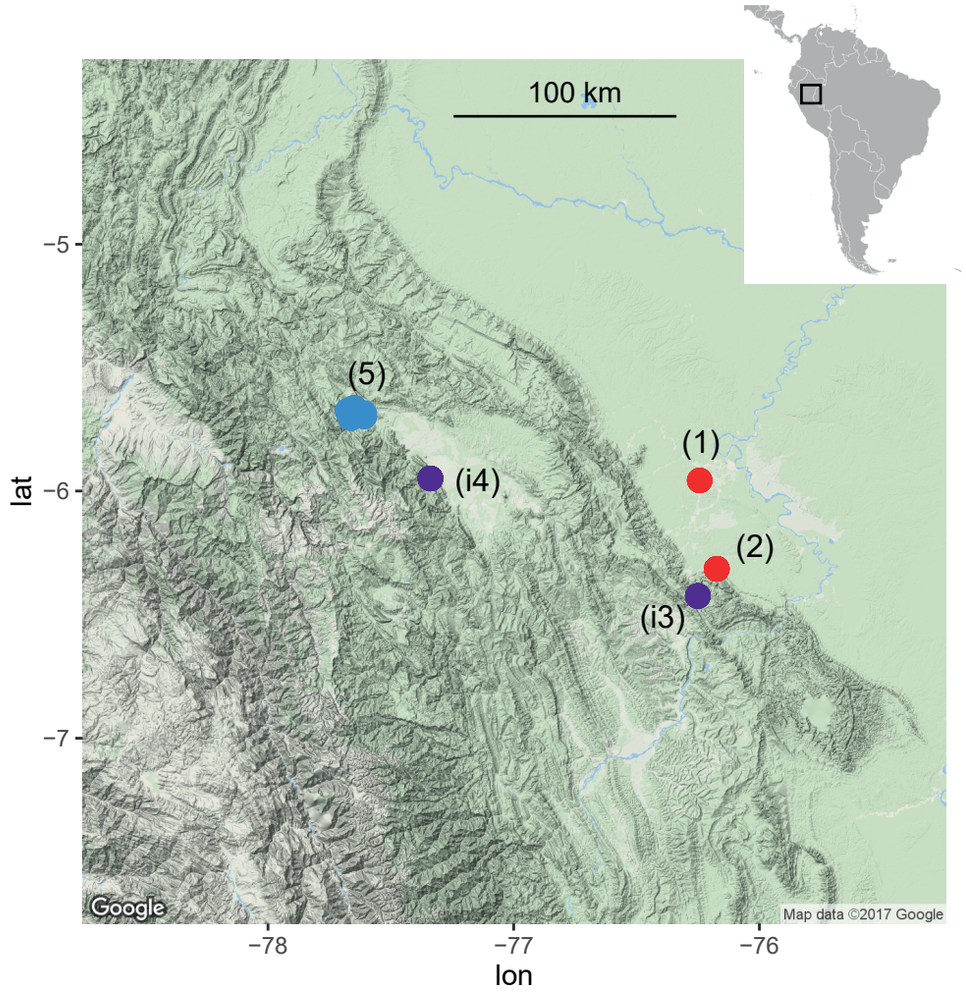

c.

Ithomia salapia hybrid

Oleria onega janarilla (Amazon)

Oleria onega ssp nov 2 (Andes)

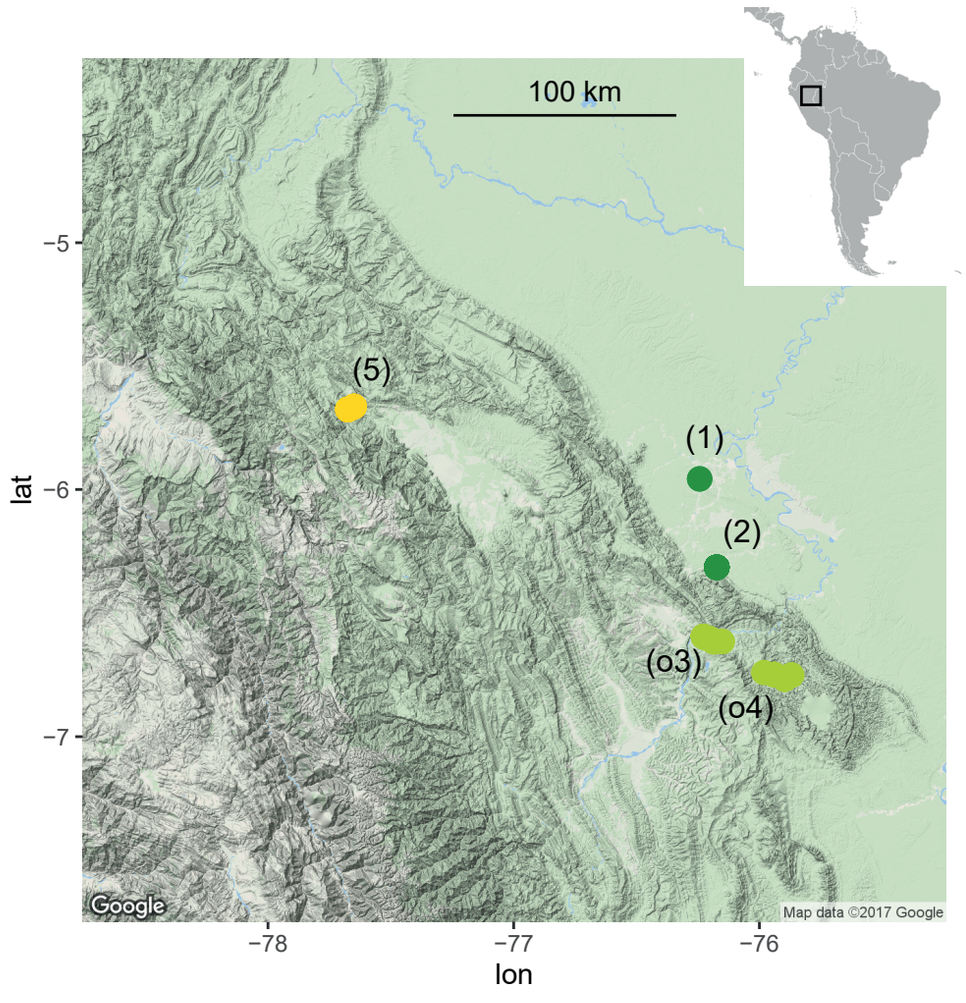

Oleria onega hybrid

a.

Ithomia salapia

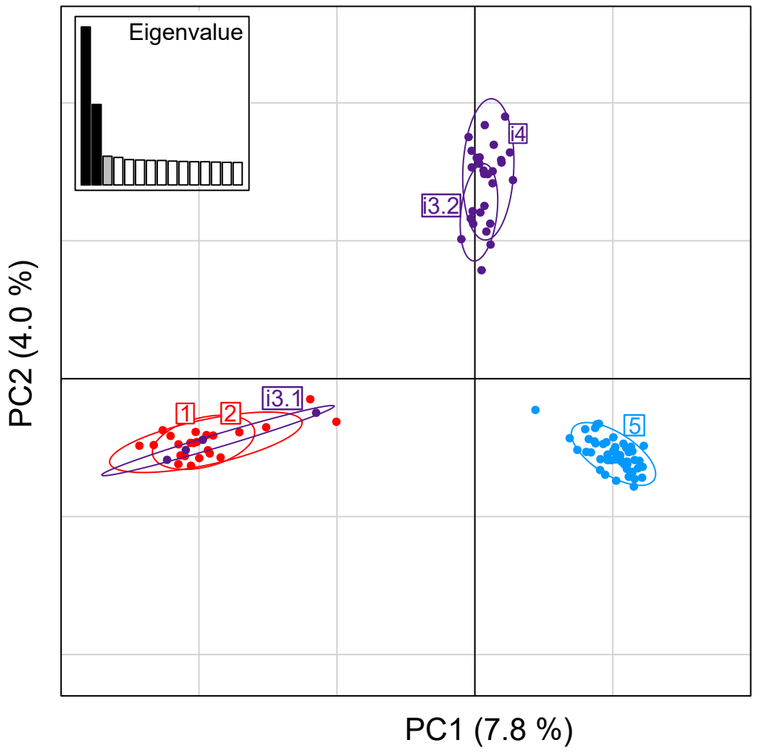

Oleria onega

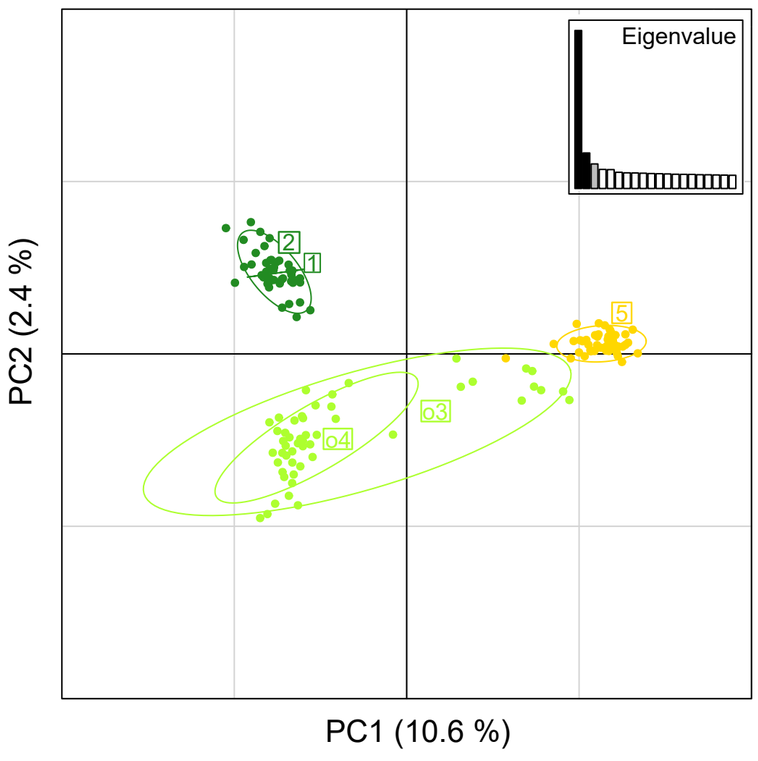

b.

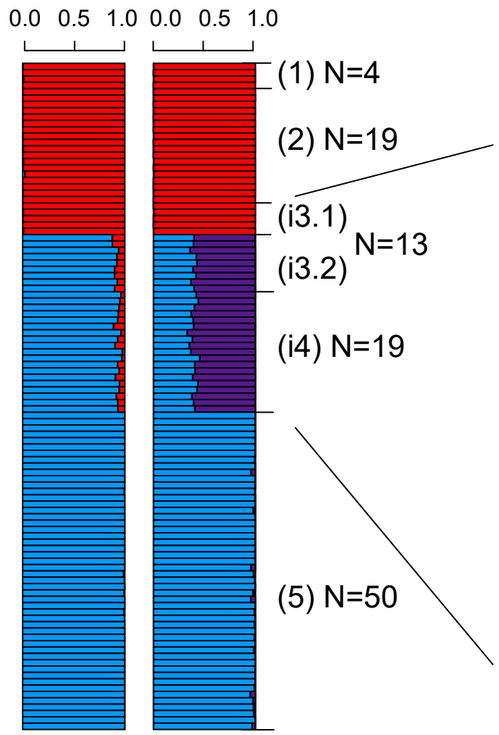

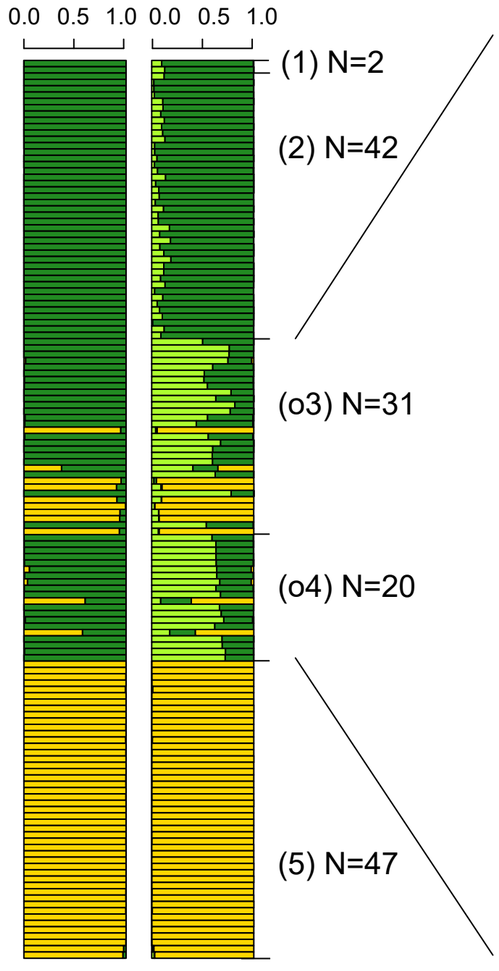

c.

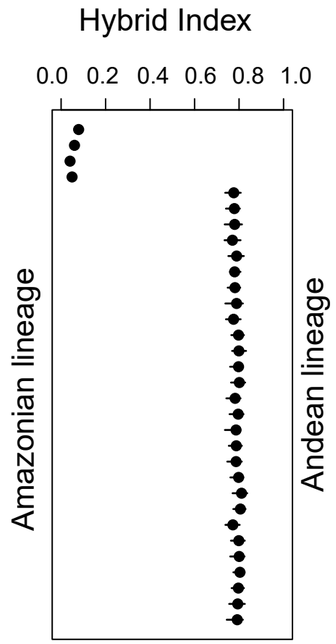

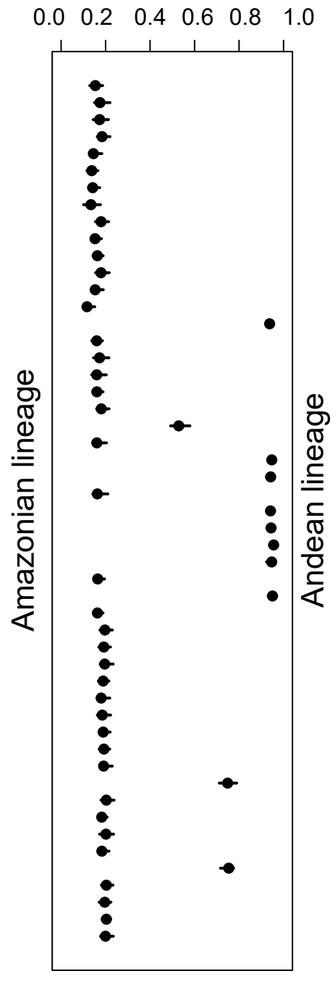

d.

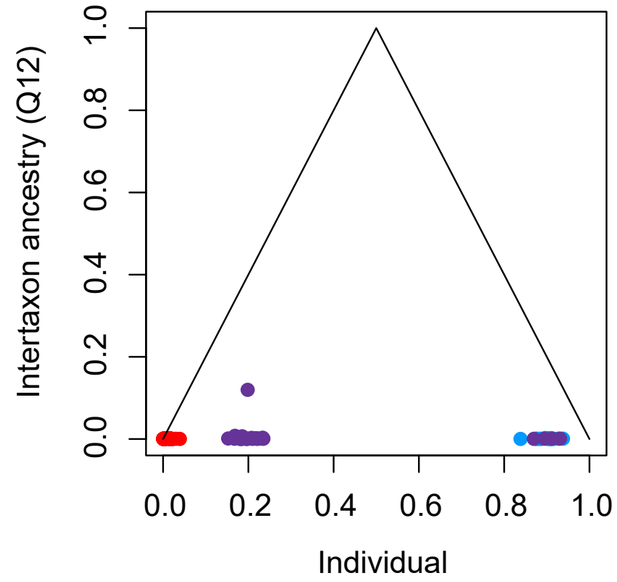

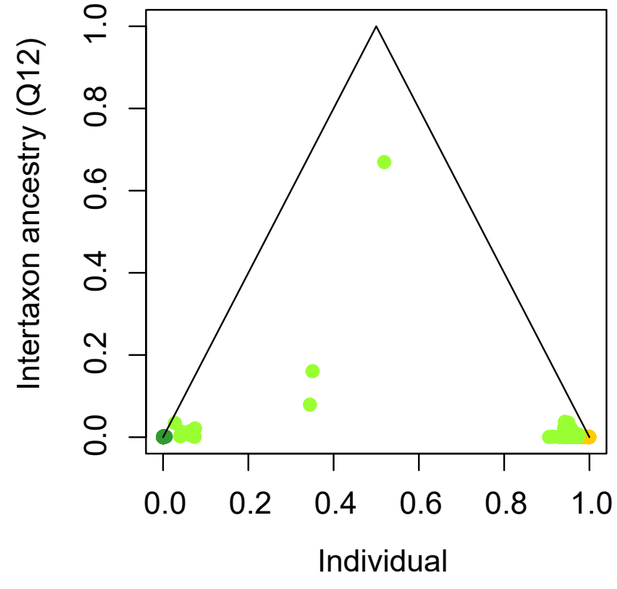

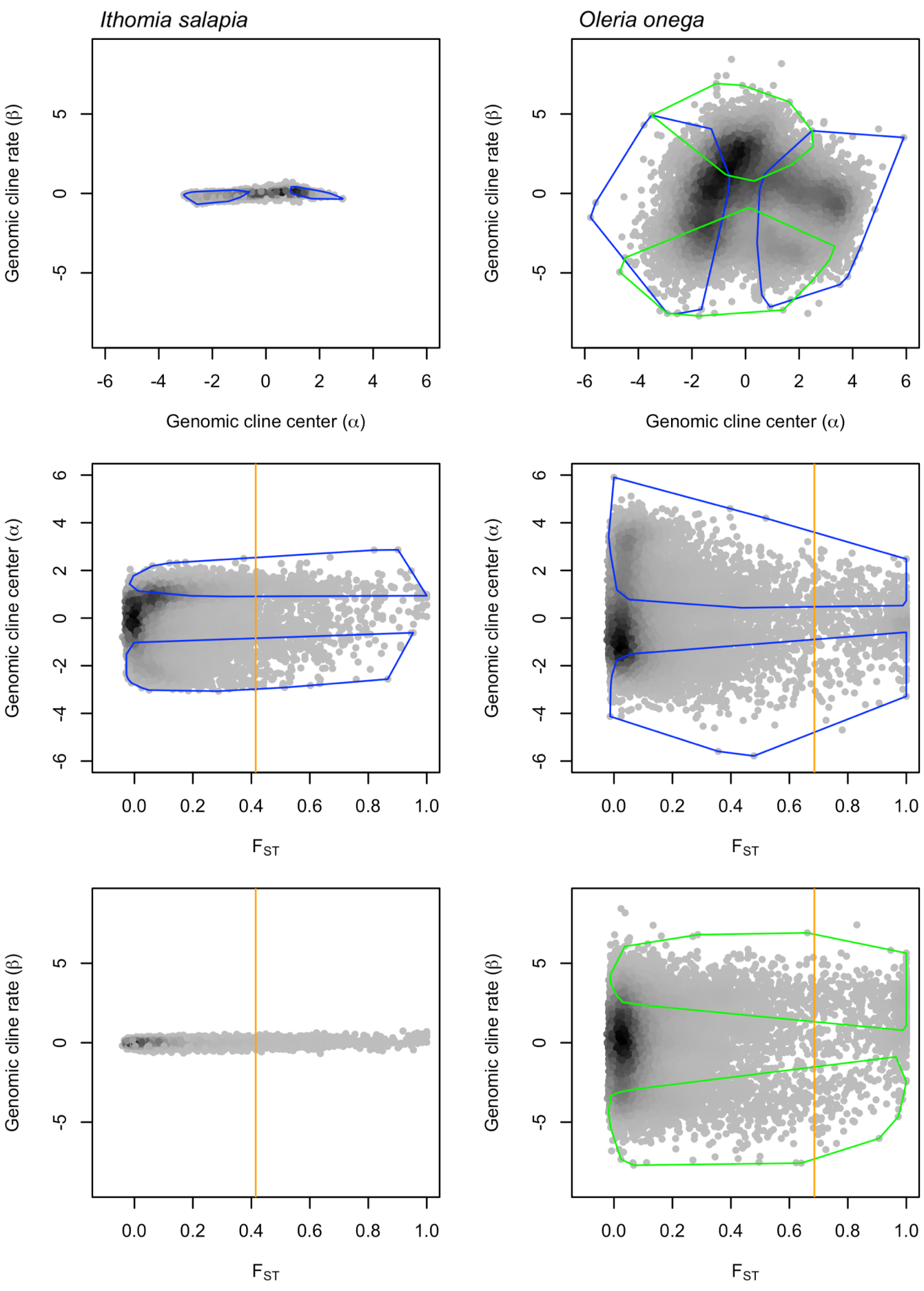
Ithomia salapia
Oleria onega
Genomic cline rate (β)
Genomic cline center (α)
F_ST
-6
-4
-2
0
2
4
6
-5
0
5
0.0
0.2
0.4
0.6
0.8
1.0

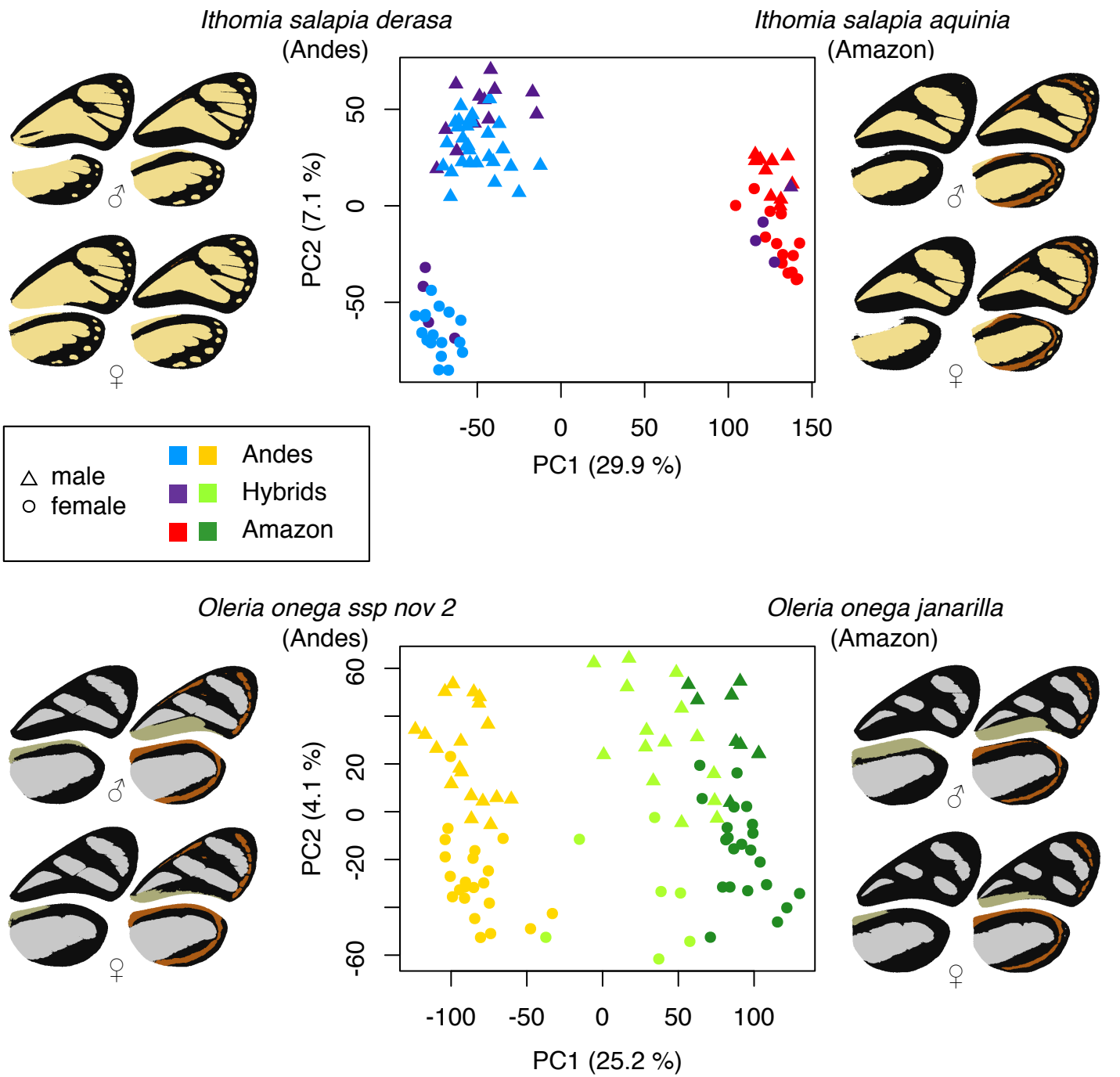
Ithomia salapia derasa
(Andes)
Ithomia salapia aquinia
(Amazon)
PC2 (7.1 %)
PC1 (29.9 %)
△ male
○ female
Andes
Hybrids
Amazon
Oleria onega ssp nov 2
(Andes)
Oleria onega janarilla
(Amazon)
PC2 (4.1 %)
PC1 (25.2 %)

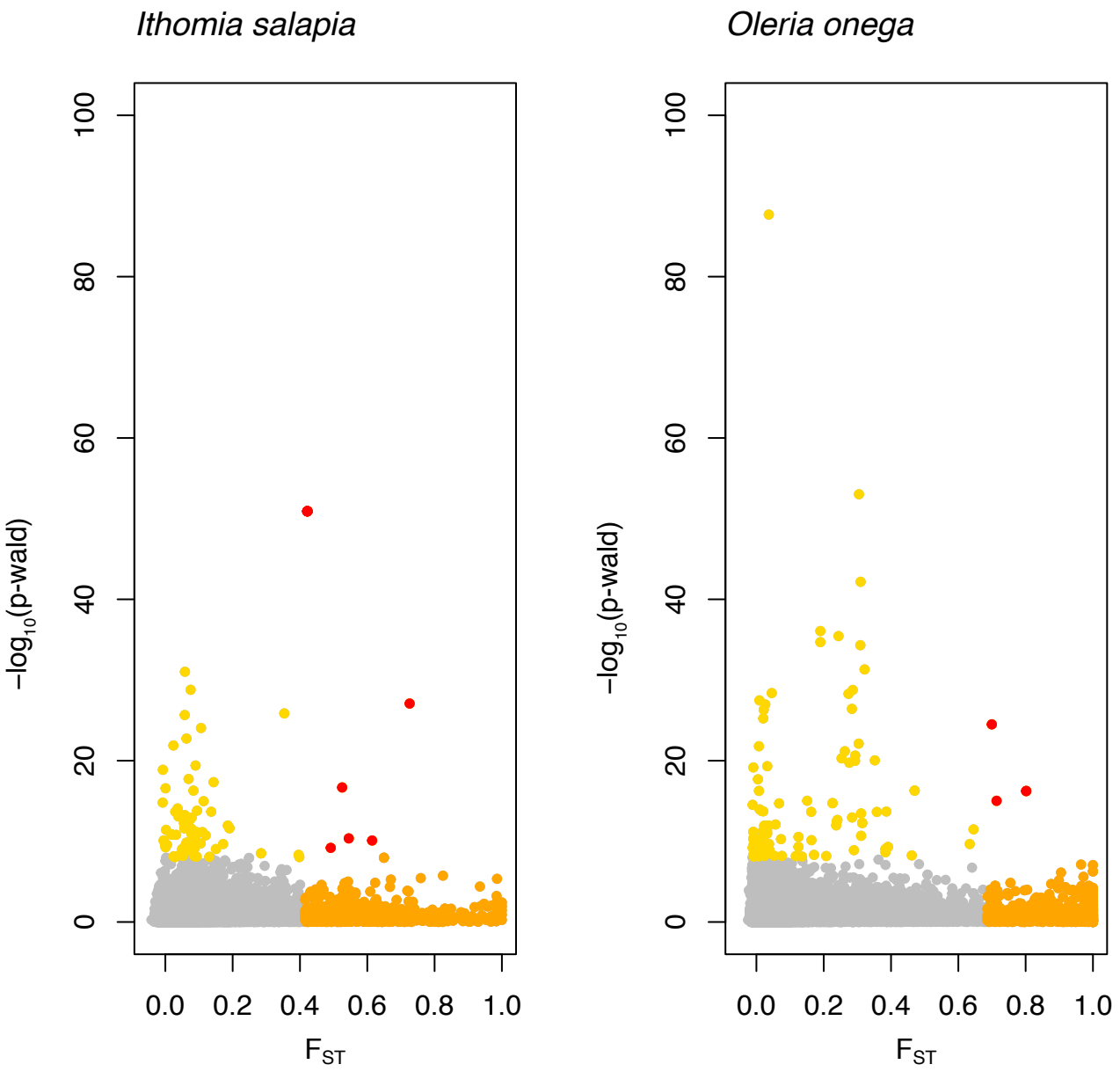
Ithomia salapia
Oleria onega
−log10(p-wald)
FST
0
20
40
60
80
100
0.0
0.2
0.4
0.6
0.8
1.0

Ithomia salapia

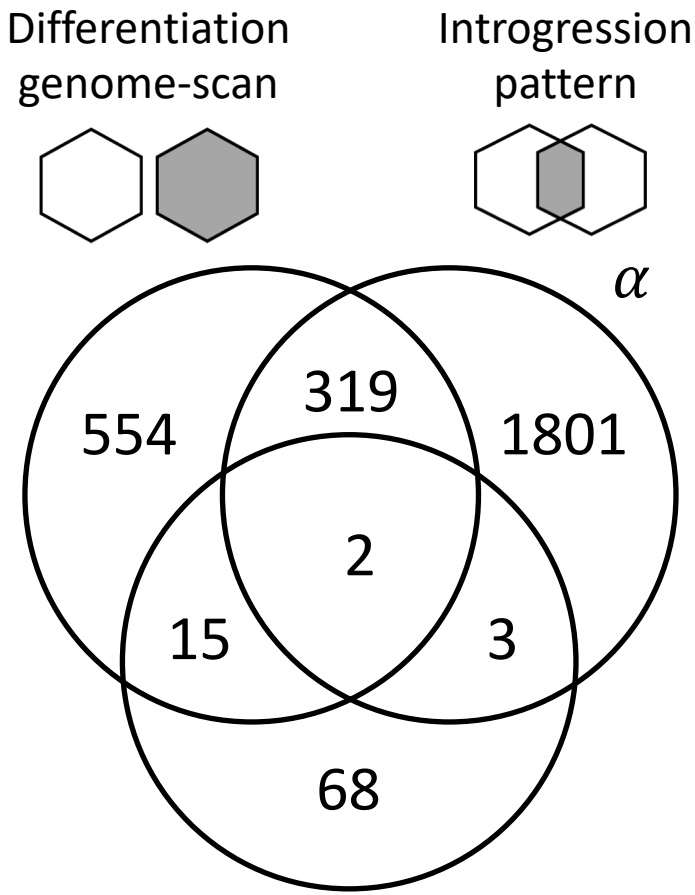

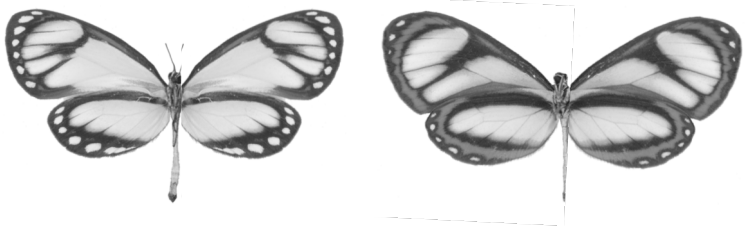

Oleria onega

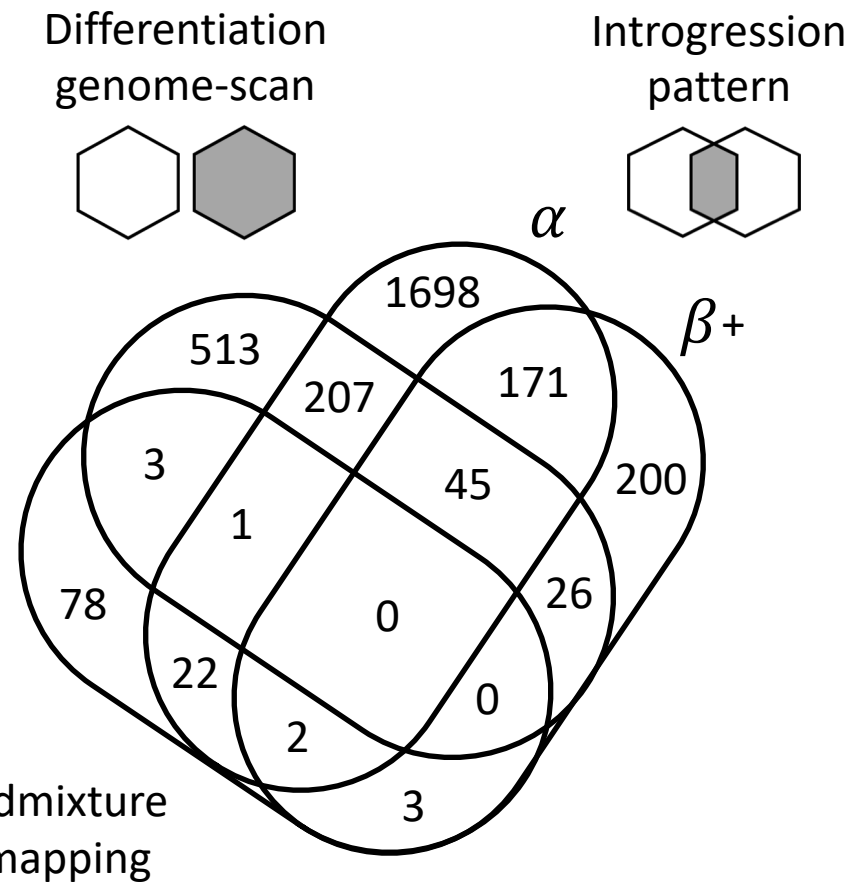

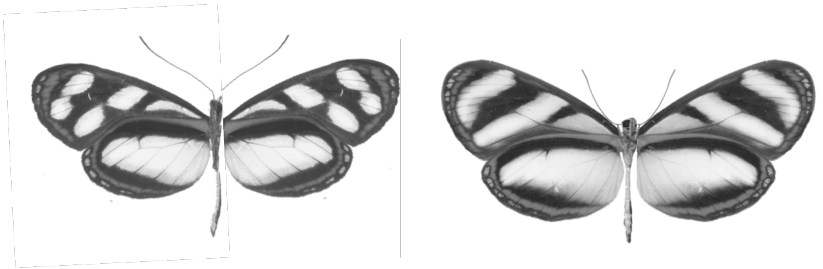

Contrasting genomic and phenotypic outcomes of hybridization between pairs of mimetic butterfly taxa across a suture zone

SUPPLEMENTARY MATERIAL

Supplementary Figure 1. Mimicry ring example for each studied species and lineages, in black frameworks, including various other butterfly species.

Supplementary Figure 2. Barplots with error bars of the Phenotypic Variation Explained (PVE) by genetic for each variable (PC) explaining more than 1% of the wing pattern variation.

Supplementary Table 1. Sampling information including species, population, sex, location, region, GPS positions, sampling date. For each sample, the number of reads sequenced and SNPs called has been given.

Supplementary Table 2. `BLAST` results of locus with outlier SNPs identified as potentially involved in local adaptation, adaptive introgression and reproductive isolation, i.e. differential genomic cline center (α), high differentiation level (F_{ST}) and differential positive genomic cline rate (β).

Supplementary Table 3. `BLAST` results of loci with SNPs significantly associated with wing pattern variation.

	Sample description				Sampling information										Sequencing statistics	SNP calling statistics
Sample	Genus	Species	Phenotype	Sex	Population	Population Code	Location	Region	Country	Latitude	Longitude	Altitude (m)	ID by	Date	#_reads	#_SNP
Isa_Az_02_992	*Ithomia*	*salapia*	aquinia	F	Amazon	1	Km-26, Yurimaguas-Tarapoto (now Km-24)	San Martín	Peru	5° 58' 489" S	76° 13' 856" W	1066	Alaine Whinnet	9/3/2002	454952	116822
Isa_Az_02_991	*Ithomia*	*salapia*	aquinia	M	Amazon	1	Km-26, Yurimaguas-Tarapoto (now Km-24)	San Martín	Peru	5° 58' 489" S	76° 13' 856" W	1066	Alaine Whinnet	9/3/2002	230236	116707
Isa_Az_02_015	*Ithomia*	*salapia*	aquinia	F	Amazon	1	Km-26, Yurimaguas-Tarapoto (now Km-24)	San Martín	Peru	5° 58' 489" S	76° 13' 856" W	1066	Alaine Whinnet	10/1/2002	274811	99365
Isa_Az_02_014	*Ithomia*	*salapia*	aquinia	F	Amazon	1	Km-26, Yurimaguas-Tarapoto (now Km-24)	San Martín	Peru	5° 58' 489" S	76° 13' 856" W	1066	Alaine Whinnet	10/1/2002	181385	77018
Isa_Az_05_1605	*Ithomia*	*salapia*	aquinia	M	Middle1	2	San Miguel de Achinamiza	San Martín	Peru	6° 18' 540" S	76° 09' 843" W	197	Lisa de Silva	3/2/2006	381230	146396
Isa_Az_05_1551	*Ithomia*	*salapia*	aquinia	F	Middle1	2	San Miguel de Achinamiza	San Martín	Peru	6° 18' 540" S	76° 09' 843" W	197	Lisa de Silva	3/1/2006	377803	145858
Isa_Az_05_1560	*Ithomia*	*salapia*	aquinia	M	Middle1	2	San Miguel de Achinamiza	San Martín	Peru	6° 18' 540" S	76° 09' 843" W	197	Lisa de Silva	3/1/2006	336857	138789
Isa_Az_05_1557	*Ithomia*	*salapia*	aquinia	F	Middle1	2	San Miguel de Achinamiza	San Martín	Peru	6° 18' 540" S	76° 09' 843" W	197	Lisa de Silva	3/1/2006	284147	131087
Isa_Az_05_1545	*Ithomia*	*salapia*	aquinia	F	Middle1	2	San Miguel de Achinamiza	San Martín	Peru	6° 18' 540" S	76° 09' 843" W	1066	Lisa de Silva	3/1/2006	563602	118981
Isa_Az_05_1604	*Ithomia*	*salapia*	aquinia	M	Middle1	2	San Miguel de Achinamiza	San Martín	Peru	6° 18' 540" S	76° 09' 843" W	197	Lisa de Silva	3/2/2006	412881	111760
Isa_Az_05_1558	*Ithomia*	*salapia*	aquinia	F	Middle1	2	San Miguel de Achinamiza	San Martín	Peru	6° 18' 540" S	76° 09' 843" W	197	Lisa de Silva	3/1/2006	381997	110760
Isa_Az_05_1603	*Ithomia*	*salapia*	aquinia	F	Middle1	2	San Miguel de Achinamiza	San Martín	Peru	6° 18' 540" S	76° 09' 843" W	197	Lisa de Silva	3/2/2006	351247	106268
Isa_Az_05_1549	*Ithomia*	*salapia*	aquinia	F	Middle1	2	San Miguel de Achinamiza	San Martín	Peru	6° 18' 540" S	76° 09' 843" W	1066	Lisa de Silva	3/1/2006	306833	105299
Isa_Az_05_1554	*Ithomia*	*salapia*	aquinia	F	Middle1	2	San Miguel de Achinamiza	San Martín	Peru	6° 18' 540" S	76° 09' 843" W	197	Lisa de Silva	3/1/2006	337562	104342
Isa_Az_05_1553	*Ithomia*	*salapia*	aquinia	F	Middle1	2	San Miguel de Achinamiza	San Martín	Peru	6° 18' 540" S	76° 09' 843" W	197	Lisa de Silva	3/1/2006	259997	94223
Isa_Az_05_1547	*Ithomia*	*salapia*	aquinia	M	Middle1	2	San Miguel de Achinamiza	San Martín	Peru	6° 18' 540" S	76° 09' 843" W	1066	Lisa de Silva	3/1/2006	272700	94141
Isa_Az_05_1546	*Ithomia*	*salapia*	aquinia	F	Middle1	2	San Miguel de Achinamiza	San Martín	Peru	6° 18' 540" S	76° 09' 843" W	1066	Lisa de Silva	3/1/2006	248524	93416
Isa_Az_05_1555	*Ithomia*	*salapia*	aquinia	F	Middle1	2	San Miguel de Achinamiza	San Martín	Peru	6° 18' 540" S	76° 09' 843" W	197	Lisa de Silva	3/1/2006	234330	90613
Isa_Az_05_1550	*Ithomia*	*salapia*	aquinia	M	Middle1	2	San Miguel de Achinamiza	San Martín	Peru	6° 18' 540" S	76° 09' 843" W	1066	Lisa de Silva	3/1/2006	241126	89967
Isa_Az_05_1548	*Ithomia*	*salapia*	aquinia	F	Middle1	2	San Miguel de Achinamiza	San Martín	Peru	6° 18' 540" S	76° 09' 843" W	1066	Lisa de Silva	3/1/2006	138224	87483
Isa_Az_05_1563	*Ithomia*	*salapia*	aquinia	F	Middle1	2	San Miguel de Achinamiza	San Martín	Peru	6° 18' 540" S	76° 09' 843" W	197	Lisa de Silva	3/1/2006	208816	84834
Isa_Az_05_1601	*Ithomia*	*salapia*	aquinia	M	Middle1	2	San Miguel de Achinamiza	San Martín	Peru	6° 18' 540" S	76° 09' 843" W	197	Lisa de Silva	3/2/2006	141893	60244
Isa_Az_05_1552	*Ithomia*	*salapia*	aquinia	M	Middle1	2	San Miguel de Achinamiza	San Martín	Peru	6° 18' 540" S	76° 09' 843" W	197	Lisa de Silva	3/1/2006	99268	51065
Isa_Mi_02_1371	*Ithomia*	*salapia*	aquinia	F	Middle2	3.1	Km-42, Tarapoto-Yurimaguas	San Martín	Peru	6° 25' 29.4" S	76° 15' 1.6" W	172	Alaine Whinnet	9/9/2002	348506	128985
Isa_Mi_02_1372	*Ithomia*	*salapia*	aquinia	M	Middle2	3.1	Km-42, Tarapoto-Yurimaguas	San Martín	Peru	6° 25' 29.4" S	76° 15' 1.6" W	172	Alaine Whinnet	9/9/2002	591079	122518
Isa_Mi_02_1373	*Ithomia*	*salapia*	aquinia	F	Middle2	3.1	Km-42, Tarapoto-Yurimaguas	San Martín	Peru	6° 25' 29.4" S	76° 15' 1.6" W	197	Alaine Whinnet	9/9/2002	558863	117084
Isa_Mi_02_1370	*Ithomia*	*salapia*	aquinia	F	Middle2	3.1	Km-42, Tarapoto-Yurimaguas	San Martín	Peru	6° 25' 29.4" S	76° 15' 1.6" W	346	Alaine Whinnet	9/9/2002	114518	55353
Isd_Mi_02_1381	*Ithomia*	*salapia*	derasa	F	Middle2	3.2	Km-42, Tarapoto-Yurimaguas	San Martín	Peru	6° 25' 29.4" S	76° 15' 1.6" W	1066	Alaine Whinnet	9/9/2002	370237	140489
Isd_Mi_02_1376	*Ithomia*	*salapia*	derasa	M	Middle2	3.2	Km-42, Tarapoto-Yurimaguas	San Martín	Peru	6° 25' 29.4" S	76° 15' 1.6" W	197	Alaine Whinnet	9/9/2002	211612	112016
Isd_Mi_02_1380	*Ithomia*	*salapia*	derasa	M	Middle2	3.2	Km-42, Tarapoto-Yurimaguas	San Martín	Peru	6° 25' 29.4" S	76° 15' 1.6" W	197	Alaine Whinnet	9/9/2002	187985	107720
Isd_Mi_02_1374	*Ithomia*	*salapia*	derasa	M	Middle2	3.2	Km-42, Tarapoto-Yurimaguas	San Martín	Peru	6° 25' 29.4" S	76° 15' 1.6" W	197	Alaine Whinnet	9/9/2002	209060	82902
Isd_Mi_02_1375	*Ithomia*	*salapia*	derasa	M	Middle2	3.2	Km-42, Tarapoto-Yurimaguas	San Martín	Peru	6° 25' 29.4" S	76° 15' 1.6" W	197	Alaine Whinnet	9/9/2002	183092	75095
Isd_Mi_02_1970	*Ithomia*	*salapia*	derasa	M	Middle2	3.2	Km-42, Tarapoto-Yurimaguas	San Martín	Peru	6° 25' 29.4" S	76° 15' 1.6" W	1066	Alaine Whinnet	10/1/2002	193070	73885
Isd_Mi_02_1378	*Ithomia*	*salapia*	derasa	M	Middle2	3.2	Km-42, Tarapoto-Yurimaguas	San Martín	Peru	6° 25' 29.4" S	76° 15' 1.6" W	197	Alaine Whinnet	9/9/2002	156393	72524
Isd_Mi_02_1379	*Ithomia*	*salapia*	derasa	M	Middle2	3.2	Km-42, Tarapoto-Yurimaguas	San Martín	Peru	6° 25' 29.4" S	76° 15' 1.6" W	197	Alaine Whinnet	9/9/2002	170783	72014
Isd_Mi_02_1971	*Ithomia*	*salapia*	derasa	M	Middle2	3.2	Km-42, Tarapoto-Yurimaguas	San Martín	Peru	6° 25' 29.4" S	76° 15' 1.6" W	1066	Alaine Whinnet	10/1/2002	225970	70000
Isd_Mi_06_952	*Ithomia*	*salapia*	derasa	M	Andes_F	4	La Florida	San Martín	Peru	5° 56' 57.33" S	77° 20' 20.19" W	1014	Fraser Simpson	12/16/2006	490526	144122
Isd_Mi_06_931	*Ithomia*	*salapia*	derasa	M	Andes_F	4	La Florida	San Martín	Peru	5° 56' 57.33" S	77° 20' 20.19" W	1014	Fraser Simpson	12/14/2006	507490	141484
Isd_Mi_06_925	*Ithomia*	*salapia*	derasa	F	Andes_F	4	La Florida	San Martín	Peru	5° 56' 57.33" S	77° 20' 20.19" W	1014	Fraser Simpson	12/14/2006	367821	129525
Isd_Mi_06_930	*Ithomia*	*salapia*	derasa	F	Andes_F	4	La Florida	San Martín	Peru	5° 56' 57.33" S	77° 20' 20.19" W	1014	Fraser Simpson	12/14/2006	368515	125334
Isd_Mi_06_960	*Ithomia*	*salapia*	derasa	M	Andes_F	4	La Florida	San Martín	Peru	5° 56' 57.33" S	77° 20' 20.19" W	1014	Fraser Simpson	12/16/2006	331577	124740
Isd_Mi_06_961	*Ithomia*	*salapia*	derasa	F	Andes_F	4	La Florida	San Martín	Peru	5° 56' 57.33" S	77° 20' 20.19" W	1014	Fraser Simpson	12/16/2006	330313	123957
Isd_Mi_06_953	*Ithomia*	*salapia*	derasa	M	Andes_F	4	La Florida	San Martín	Peru	5° 56' 57.33" S	77° 20' 20.19" W	1014	Fraser Simpson	12/16/2006	657199	121184
Isd_Mi_06_954	*Ithomia*	*salapia*	derasa	F	Andes_F	4	La Florida	San Martín	Peru	5° 56' 57.33" S	77° 20' 20.19" W	1014	Fraser Simpson	12/16/2006	507080	111595
Isd_Mi_06_932	*Ithomia*	*salapia*	derasa	M	Andes_F	4	La Florida	San Martín	Peru	5° 56' 57.33" S	77° 20' 20.19" W	1014	Fraser Simpson	12/14/2006	568199	111517
Isd_Mi_06_959	*Ithomia*	*salapia*	derasa	M	Andes_F	4	La Florida	San Martín	Peru	5° 56' 57.33" S	77° 20' 20.19" W	1014	Fraser Simpson	12/16/2006	503967	110317
Isd_Mi_06_962	*Ithomia*	*salapia*	derasa	F	Andes_F	4	La Florida	San Martín	Peru	5° 56' 57.33" S	77° 20' 20.19" W	1014	Fraser Simpson	12/16/2006	501325	110309
Isd_Mi_06_958	*Ithomia*	*salapia*	derasa	M	Andes_F	4	La Florida	San Martín	Peru	5° 56' 57.33" S	77° 20' 20.19" W	1014	Fraser Simpson	12/16/2006	455718	108748
Isd_Mi_06_928	*Ithomia*	*salapia*	derasa	M	Andes_F	4	La Florida	San Martín	Peru	5° 56' 57.33" S	77° 20' 20.19" W	1014	Fraser Simpson	12/14/2006	448953	104193
Isd_Mi_06_924	*Ithomia*	*salapia*	derasa	F	Andes_F	4	La Florida	San Martín	Peru	5° 56' 57.33" S	77° 20' 20.19" W	1014	Fraser Simpson	12/14/2006	403484	101895
Isd_Mi_06_956	*Ithomia*	*salapia*	derasa	M	Andes_F	4	La Florida	San Martín	Peru	5° 56' 57.33" S	77° 20' 20.19" W	1014	Fraser Simpson	12/16/2006	356353	94711
Isd_Mi_06_926	*Ithomia*	*salapia*	derasa	M	Andes_F	4	La Florida	San Martín	Peru	5° 56' 57.33" S	77° 20' 20.19" W	1014	Fraser Simpson	12/14/2006	354030	93484
Isd_Mi_06_927	*Ithomia*	*salapia*	derasa	M	Andes_F	4	La Florida	San Martín	Peru	5° 56' 57.33" S	77° 20' 20.19" W	1014	Fraser Simpson	12/14/2006	156253	81048
Isd_Mi_06_929	*Ithomia*	*salapia*	derasa	M	Andes_F	4	La Florida	San Martín	Peru	5° 56' 57.33" S	77° 20' 20.19" W	1014	Fraser Simpson	12/14/2006	190255	72132
Isd_Mi_06_955	*Ithomia*	*salapia*	derasa	M	Andes_F	4	La Florida	San Martín	Peru	5° 56' 57.33" S	77° 20' 20.19" W	1014	Fraser Simpson	12/16/2006	135224	56150
Isd_An_06_853	*Ithomia*	*salapia*	derasa	M	Andes	5	Aguas Claras	San Martín	Peru	5° 41' 50.9" S	77° 36' 30.7'' W	1201	Fraser Simpson	12/12/2006	606382	150944
Isd_An_06_852	*Ithomia*	*salapia*	derasa	F	Andes	5	Aguas Claras	San Martín	Peru	5° 41' 50.9" S	77° 36' 30.7'' W	1201	Fraser Simpson	12/12/2006	569526	110756
Isd_An_06_855	*Ithomia*	*salapia*	derasa	F	Andes	5	Aguas Claras	San Martín	Peru	5° 41' 50.9" S	77° 36' 30.7'' W	1201	Fraser Simpson	12/12/2006	597492	110614
Isd_An_06_854	*Ithomia*	*salapia*	derasa	M	Andes	5	Aguas Claras	San Martín	Peru	5° 41' 50.9" S	77° 36' 30.7'' W	1201	Fraser Simpson	12/12/2006	456598	105811
Isd_An_06_849	*Ithomia*	*salapia*	derasa	F	Andes	5	Aguas Claras	San Martín	Peru	5° 41' 50.9" S	77° 36' 30.7'' W	1201	Fraser Simpson	12/12/2006	418672	103556
Isd_An_06_848	*Ithomia*	*salapia*	derasa	M	Andes	5	Aguas Claras	San Martín	Peru	5° 41' 50.9" S	77° 36' 30.7'' W	1201	Fraser Simpson	12/12/2006	211662	101375

Isd_An_06_851	*Ithomia*	*salapia*	derasa	F	Andes	5	Aguas Claras	San Martín	Peru	5° 41' 50.9" S	77° 36' 30.7'' W	1201	Fraser Simpson	12/12/2006	214917	98884
Isd_An_06_850	*Ithomia*	*salapia*	derasa	F	Andes	5	Aguas Claras	San Martín	Peru	5° 41' 50.9" S	77° 36' 30.7'' W	1201	Fraser Simpson	12/12/2006	266876	81990
Isd_An_06_836	*Ithomia*	*salapia*	derasa	F	Andes	5	Puente Aguas Verdes	San Martín	Peru	5° 41' 3.3" S	77° 39' 30.5'' W	1201	Fraser Simpson	12/11/2006	704542	162179
Isd_An_05_1052	*Ithomia*	*salapia*	derasa	F	Andes	5	Puente Aguas Verdes	San Martín	Peru	5° 41' 77" S	77° 39' 487" W	976	Mathieu Joron	11/24/2005	342677	132539
Isd_An_05_1098	*Ithomia*	*salapia*	derasa	M	Andes	5	Puente Aguas Verdes	San Martín	Peru	5° 41' 77" S	77° 39' 487" W	976	Mathieu Joron	11/24/2005	347770	129502
Isd_An_05_1101	*Ithomia*	*salapia*	derasa	M	Andes	5	Puente Aguas Verdes	San Martín	Peru	5° 41' 77" S	77° 39' 487" W	1201	Mathieu Joron	11/24/2005	650088	119736
Isd_An_05_1100	*Ithomia*	*salapia*	derasa	M	Andes	5	Puente Aguas Verdes	San Martín	Peru	5° 41' 77" S	77° 39' 487" W	976	Mathieu Joron	11/24/2005	567976	118704
Isd_An_05_1094	*Ithomia*	*salapia*	derasa	M	Andes	5	Puente Aguas Verdes	San Martín	Peru	5° 41' 77" S	77° 39' 487" W	976	Mathieu Joron	11/24/2005	441325	107140
Isd_An_06_840	*Ithomia*	*salapia*	derasa	M	Andes	5	Puente Aguas Verdes	San Martín	Peru	5° 41' 3.3" S	77° 39' 30.5'' W	1201	Fraser Simpson	12/11/2006	379681	99587
Isd_An_02_901	*Ithomia*	*salapia*	derasa	M	Andes	5	Puente Aguas Verdes trail	San Martín	Peru	5° 39' 50" S	77° 38' 58" W	1066	Alaine Whinnet	8/29/2002	565740	160319
Isd_An_02_896	*Ithomia*	*salapia*	derasa	M	Andes	5	Puente Aguas Verdes trail	San Martín	Peru	5° 39' 50" S	77° 38' 58" W	1066	Alaine Whinnet	8/29/2002	470065	151613
Isd_An_02_1721	*Ithomia*	*salapia*	derasa	M	Andes	5	Puente Aguas Verdes trail	San Martín	Peru	5° 39' 50" S	77° 38' 58" W	1090	Alaine Whinnet	9/19/2002	459893	151363
Isd_An_02_898	*Ithomia*	*salapia*	derasa	M	Andes	5	Puente Aguas Verdes trail	San Martín	Peru	5° 39' 50" S	77° 38' 58" W	1201	Alaine Whinnet	8/29/2002	413394	142849
Isd_An_02_899	*Ithomia*	*salapia*	derasa	M	Andes	5	Puente Aguas Verdes trail	San Martín	Peru	5° 39' 50" S	77° 38' 58" W	1201	Alaine Whinnet	8/29/2002	690905	124531
Isd_An_02_1722	*Ithomia*	*salapia*	derasa	M	Andes	5	Puente Aguas Verdes trail	San Martín	Peru	5° 39' 50" S	77° 38' 58" W	1090	Alaine Whinnet	9/19/2002	271322	122205
Isd_An_02_902	*Ithomia*	*salapia*	derasa	M	Andes	5	Puente Aguas Verdes trail	San Martín	Peru	5° 39' 50" S	77° 38' 58" W	1066	Alaine Whinnet	8/29/2002	257394	121014
Isd_An_02_906	*Ithomia*	*salapia*	derasa	M	Andes	5	Puente Aguas Verdes trail	San Martín	Peru	5° 39' 50" S	77° 38' 58" W	1066	Alaine Whinnet	8/29/2002	400639	108240
Isd_An_02_897	*Ithomia*	*salapia*	derasa	F	Andes	5	Puente Aguas Verdes trail	San Martín	Peru	5° 39' 50" S	77° 38' 58" W	1201	Alaine Whinnet	8/29/2002	422771	105606
Isd_An_02_908	*Ithomia*	*salapia*	derasa	M	Andes	5	Puente Aguas Verdes trail	San Martín	Peru	5° 39' 50" S	77° 38' 58" W	1100	Alaine Whinnet	8/29/2002	371034	103783
Isd_An_02_905	*Ithomia*	*salapia*	derasa	F	Andes	5	Puente Aguas Verdes trail	San Martín	Peru	5° 39' 50" S	77° 38' 58" W	1066	Alaine Whinnet	8/29/2002	180808	101321
Isd_An_02_1724	*Ithomia*	*salapia*	derasa	M	Andes	5	Puente Aguas Verdes trail	San Martín	Peru	5° 39' 50" S	77° 38' 58" W	976	Alaine Whinnet	9/19/2002	364472	100935
Isd_An_02_1729	*Ithomia*	*salapia*	derasa	F	Andes	5	Puente Aguas Verdes trail	San Martín	Peru	5° 39' 50" S	77° 38' 58" W	976	Alaine Whinnet	9/19/2002	257248	87472
Isd_An_02_1723	*Ithomia*	*salapia*	derasa	M	Andes	5	Puente Aguas Verdes trail	San Martín	Peru	5° 39' 50" S	77° 38' 58" W	1090	Alaine Whinnet	9/19/2002	231591	79106
Isd_An_02_900	*Ithomia*	*salapia*	derasa	M	Andes	5	Puente Aguas Verdes trail	San Martín	Peru	5° 39' 50" S	77° 38' 58" W	1201	Alaine Whinnet	8/29/2002	577042	77838
Isd_An_02_904	*Ithomia*	*salapia*	derasa	M	Andes	5	Puente Aguas Verdes trail	San Martín	Peru	5° 39' 50" S	77° 38' 58" W	1066	Alaine Whinnet	8/29/2002	307487	77225
Isd_An_02_907	*Ithomia*	*salapia*	derasa	M	Andes	5	Puente Aguas Verdes trail	San Martín	Peru	5° 39' 50" S	77° 38' 58" W	1100	Alaine Whinnet	8/29/2002	313912	74194
Isd_An_02_1726	*Ithomia*	*salapia*	derasa	M	Andes	5	Puente Aguas Verdes trail	San Martín	Peru	5° 39' 50" S	77° 38' 58" W	976	Alaine Whinnet	9/19/2002	220199	51733
Isd_An_02_735	*Ithomia*	*salapia*	derasa	M	Andes	5	Puente Serranoyacu	San Martín	Peru	5° 40' 31.6" S	77° 40' 28.7" W	1201	Alaine Whinnet	8/28/2002	524492	158048
Isd_An_02_1711	*Ithomia*	*salapia*	derasa	F	Andes	5	Puente Serranoyacu	San Martín	Peru	5° 40' 31.6" S	77° 40' 28.7" W	1100	Alaine Whinnet	9/19/2002	403720	143738
Isd_An_02_1713	*Ithomia*	*salapia*	derasa	F	Andes	5	Puente Serranoyacu	San Martín	Peru	5° 40' 31.6" S	77° 40' 28.7" W	1100	Alaine Whinnet	9/19/2002	659923	122440
Isd_An_02_949	*Ithomia*	*salapia*	derasa	M	Andes	5	Puente Serranoyacu	San Martín	Peru	5° 40' 31.6" S	77° 40' 28.7" W	1100	Alaine Whinnet	8/30/2002	481296	115849
Isd_An_02_739	*Ithomia*	*salapia*	derasa	M	Andes	5	Puente Serranoyacu	San Martín	Peru	5° 40' 31.6" S	77° 40' 28.7" W	1100	Alaine Whinnet	8/28/2002	192516	112003
Isd_An_02_948	*Ithomia*	*salapia*	derasa	M	Andes	5	Puente Serranoyacu	San Martín	Peru	5° 40' 31.6" S	77° 40' 28.7" W	1100	Alaine Whinnet	8/30/2002	255224	110614
Isd_An_02_741	*Ithomia*	*salapia*	derasa	M	Andes	5	Puente Serranoyacu	San Martín	Peru	5° 40' 31.6" S	77° 40' 28.7" W	1100	Alaine Whinnet	8/28/2002	211526	110333
Isd_An_02_1620	*Ithomia*	*salapia*	derasa	M	Andes	5	Puente Serranoyacu	San Martín	Peru	5° 40' 31.6" S	77° 40' 28.7" W	1100	Alaine Whinnet	9/17/2002	463807	109222
Isd_An_02_945	*Ithomia*	*salapia*	derasa	M	Andes	5	Puente Serranoyacu	San Martín	Peru	5° 40' 31.6" S	77° 40' 28.7" W	1100	Alaine Whinnet	8/30/2002	215777	109173
Isd_An_02_1712	*Ithomia*	*salapia*	derasa	F	Andes	5	Puente Serranoyacu	San Martín	Peru	5° 40' 31.6" S	77° 40' 28.7" W	1100	Alaine Whinnet	9/19/2002	370949	103796
Isd_An_02_736	*Ithomia*	*salapia*	derasa	M	Andes	5	Puente Serranoyacu	San Martín	Peru	5° 40' 31.6" S	77° 40' 28.7" W	1100	Alaine Whinnet	8/28/2002	265938	96506
Isd_An_02_946	*Ithomia*	*salapia*	derasa	F	Andes	5	Puente Serranoyacu	San Martín	Peru	5° 40' 31.6" S	77° 40' 28.7" W	1100	Alaine Whinnet	8/30/2002	251901	89526
Isd_An_02_947	*Ithomia*	*salapia*	derasa	F	Andes	5	Puente Serranoyacu	San Martín	Peru	5° 40' 31.6" S	77° 40' 28.7" W	1100	Alaine Whinnet	8/30/2002	257666	87816
Isd_An_02_743	*Ithomia*	*salapia*	derasa	F	Andes	5	Puente Serranoyacu	San Martín	Peru	5° 40' 31.6" S	77° 40' 28.7" W	1100	Alaine Whinnet	8/28/2002	213690	82570
Isd_An_02_740	*Ithomia*	*salapia*	derasa	F	Andes	5	Puente Serranoyacu	San Martín	Peru	5° 40' 31.6" S	77° 40' 28.7" W	1100	Alaine Whinnet	8/28/2002	193002	77998
Isd_An_02_737	*Ithomia*	*salapia*	derasa	F	Andes	5	Puente Serranoyacu	San Martín	Peru	5° 40' 31.6" S	77° 40' 28.7" W	1100	Alaine Whinnet	8/28/2002	191013	77741
Isd_An_02_742	*Ithomia*	*salapia*	derasa	F	Andes	5	Puente Serranoyacu	San Martín	Peru	5° 40' 31.6" S	77° 40' 28.7" W	1100	Alaine Whinnet	8/28/2002	147837	67703
Ooj_Az_02_2021	*Oleria*	*onega*	janarilla	M	Amazon	1	Km-26, Yurimaguas-Tarapoto (now Km-24)	San Martín	Peru	5° 58' 489" S	76° 13' 856" W		Keith Willmott	10/1/2002	199801	170257
Ooj_Az_02_2092	*Oleria*	*onega*	janarilla	F	Amazon	1	Km-26, Yurimaguas-Tarapoto (now Km-24)	San Martín	Peru	5° 58' 489" S	76° 13' 856" W		Keith Willmott	10/1/2002	313305	175701
Ooj_Az_05_1505	*Oleria*	*onega*	janarilla	F	Middle1	2	San Miguel de Achinamiza	San Martín	Peru	6° 18' 540" S	76° 09' 843" W	197	Lisa de Silva	3/1/2006	241071	150741
Ooj_Az_05_1506	*Oleria*	*onega*	janarilla	F	Middle1	2	San Miguel de Achinamiza	San Martín	Peru	6° 18' 540" S	76° 09' 843" W	197	Lisa de Silva	3/1/2006	172694	127069
Ooj_Az_05_1507	*Oleria*	*onega*	janarilla	F	Middle1	2	San Miguel de Achinamiza	San Martín	Peru	6° 18' 540" S	76° 09' 843" W	197	Lisa de Silva	3/1/2006	133191	101790
Ooj_Az_05_1508	*Oleria*	*onega*	janarilla	F	Middle1	2	San Miguel de Achinamiza	San Martín	Peru	6° 18' 540" S	76° 09' 843" W	197	Lisa de Silva	3/1/2006	195976	139490
Ooj_Az_05_1510	*Oleria*	*onega*	janarilla	M	Middle1	2	San Miguel de Achinamiza	San Martín	Peru	6° 18' 540" S	76° 09' 843" W	197	Lisa de Silva	3/1/2006	210931	143424
Ooj_Az_05_1511	*Oleria*	*onega*	janarilla	F	Middle1	2	San Miguel de Achinamiza	San Martín	Peru	6° 18' 540" S	76° 09' 843" W	197	Lisa de Silva	3/1/2006	190543	130808
Ooj_Az_05_1512	*Oleria*	*onega*	janarilla	F	Middle1	2	San Miguel de Achinamiza	San Martín	Peru	6° 18' 540" S	76° 09' 843" W	197	Lisa de Silva	3/1/2006	179412	155490
Ooj_Az_05_1513	*Oleria*	*onega*	janarilla	F	Middle1	2	San Miguel de Achinamiza	San Martín	Peru	6° 18' 540" S	76° 09' 843" W	197	Lisa de Silva	3/1/2006	317877	180661
Ooj_Az_05_1514	*Oleria*	*onega*	janarilla	M	Middle1	2	San Miguel de Achinamiza	San Martín	Peru	6° 18' 540" S	76° 09' 843" W	197	Lisa de Silva	3/1/2006	382887	191352
Ooj_Az_05_1515	*Oleria*	*onega*	janarilla	F	Middle1	2	San Miguel de Achinamiza	San Martín	Peru	6° 18' 540" S	76° 09' 843" W	197	Lisa de Silva	3/1/2006	154363	142230
Ooj_Az_05_1516	*Oleria*	*onega*	janarilla	F	Middle1	2	San Miguel de Achinamiza	San Martín	Peru	6° 18' 540" S	76° 09' 843" W	197	Lisa de Silva	3/1/2006	274775	165335
Ooj_Az_05_1517	*Oleria*	*onega*	janarilla	F	Middle1	2	San Miguel de Achinamiza	San Martín	Peru	6° 18' 540" S	76° 09' 843" W	197	Lisa de Silva	3/1/2006	458906	206777
Ooj_Az_05_1518	*Oleria*	*onega*	janarilla	F	Middle1	2	San Miguel de Achinamiza	San Martín	Peru	6° 18' 540" S	76° 09' 843" W	197	Lisa de Silva	3/1/2006	153756	116095
Ooj_Az_05_1519	*Oleria*	*onega*	janarilla	F	Middle1	2	San Miguel de Achinamiza	San Martín	Peru	6° 18' 540" S	76° 09' 843" W	197	Lisa de Silva	3/1/2006	154909	112635
Ooj_Az_05_1520	*Oleria*	*onega*	janarilla	M	Middle1	2	San Miguel de Achinamiza	San Martín	Peru	6° 18' 540" S	76° 09' 843" W	197	Lisa de Silva	3/1/2006	303033	171790
Ooj_Az_05_1521	*Oleria*	*onega*	janarilla	F	Middle1	2	San Miguel de Achinamiza	San Martín	Peru	6° 18' 540" S	76° 09' 843" W	197	Lisa de Silva	3/1/2006	171865	120698
Ooj_Az_05_1522	*Oleria*	*onega*	janarilla	F	Middle1	2	San Miguel de Achinamiza	San Martín	Peru	6° 18' 540" S	76° 09' 843" W	197	Lisa de Silva	3/1/2006	292691	171716
Ooj_Az_05_1523	*Oleria*	*onega*	janarilla	F	Middle1	2	San Miguel de Achinamiza	San Martín	Peru	6° 18' 540" S	76° 09' 843" W	197	Lisa de Silva	3/1/2006	201178	133155

Ooj_Az_05_1524	*Oleria*	*onega*	janarilla	F	Middle1	2	San Miguel de Achinamiza	San Martín	Peru	6° 18' 540" S	76° 09' 843" W	197	Lisa de Silva	3/1/2006	295560	206342
Ooj_Az_05_1527	*Oleria*	*onega*	janarilla	F	Middle1	2	San Miguel de Achinamiza	San Martín	Peru	6° 18' 540" S	76° 09' 843" W	197	Lisa de Silva	3/1/2006	192823	164123
Ooj_Az_05_1528	*Oleria*	*onega*	janarilla	F	Middle1	2	San Miguel de Achinamiza	San Martín	Peru	6° 18' 540" S	76° 09' 843" W	197	Lisa de Silva	3/1/2006	169102	122461
Ooj_Az_05_1529	*Oleria*	*onega*	janarilla	F	Middle1	2	San Miguel de Achinamiza	San Martín	Peru	6° 18' 540" S	76° 09' 843" W	197	Lisa de Silva	3/1/2006	289337	165440
Ooj_Az_05_1530	*Oleria*	*onega*	janarilla	F	Middle1	2	San Miguel de Achinamiza	San Martín	Peru	6° 18' 540" S	76° 09' 843" W	197	Lisa de Silva	3/1/2006	232265	153226
Ooj_Az_05_1531	*Oleria*	*onega*	janarilla	F	Middle1	2	San Miguel de Achinamiza	San Martín	Peru	6° 18' 540" S	76° 09' 843" W	197	Lisa de Silva	3/1/2006	388445	186992
Ooj_Az_05_1532	*Oleria*	*onega*	janarilla	F	Middle1	2	San Miguel de Achinamiza	San Martín	Peru	6° 18' 540" S	76° 09' 843" W	197	Lisa de Silva	3/1/2006	121406	96990
Ooj_Az_05_1533	*Oleria*	*onega*	janarilla	F	Middle1	2	San Miguel de Achinamiza	San Martín	Peru	6° 18' 540" S	76° 09' 843" W	197	Lisa de Silva	3/1/2006	321705	172391
Ooj_Az_05_1534	*Oleria*	*onega*	janarilla	M	Middle1	2	San Miguel de Achinamiza	San Martín	Peru	6° 18' 540" S	76° 09' 843" W	197	Lisa de Silva	3/1/2006	193003	135341
Ooj_Az_05_1535	*Oleria*	*onega*	janarilla	M	Middle1	2	San Miguel de Achinamiza	San Martín	Peru	6° 18' 540" S	76° 09' 843" W	197	Lisa de Silva	3/1/2006	277285	162771
Ooj_Az_05_1536	*Oleria*	*onega*	janarilla	F	Middle1	2	San Miguel de Achinamiza	San Martín	Peru	6° 18' 540" S	76° 09' 843" W	197	Lisa de Silva	3/1/2006	232091	184205
Ooj_Az_05_1564	*Oleria*	*onega*	janarilla	M	Middle1	2	San Miguel de Achinamiza	San Martín	Peru	6° 18' 540" S	76° 09' 843" W	197	Lisa de Silva	3/2/2006	147037	112252
Ooj_Az_05_1565	*Oleria*	*onega*	janarilla	F	Middle1	2	San Miguel de Achinamiza	San Martín	Peru	6° 18' 540" S	76° 09' 843" W	197	Lisa de Silva	3/2/2006	392422	137005
Ooj_Az_05_1566	*Oleria*	*onega*	janarilla	F	Middle1	2	San Miguel de Achinamiza	San Martín	Peru	6° 18' 540" S	76° 09' 843" W	197	Lisa de Silva	3/2/2006	141350	107904
Ooj_Az_05_1567	*Oleria*	*onega*	janarilla	M	Middle1	2	San Miguel de Achinamiza	San Martín	Peru	6° 18' 540" S	76° 09' 843" W	197	Lisa de Silva	3/2/2006	381558	186296
Ooj_Az_05_1568	*Oleria*	*onega*	janarilla	M	Middle1	2	San Miguel de Achinamiza	San Martín	Peru	6° 18' 540" S	76° 09' 843" W	197	Lisa de Silva	3/2/2006	462862	247693
Ooj_Az_05_1569	*Oleria*	*onega*	janarilla	M	Middle1	2	San Miguel de Achinamiza	San Martín	Peru	6° 18' 540" S	76° 09' 843" W	197	Lisa de Silva	3/2/2006	216592	146638
Ooj_Az_05_1570	*Oleria*	*onega*	janarilla	M	Middle1	2	San Miguel de Achinamiza	San Martín	Peru	6° 18' 540" S	76° 09' 843" W	197	Lisa de Silva	3/2/2006	200001	135074
Ooj_Az_05_1571	*Oleria*	*onega*	janarilla	M	Middle1	2	San Miguel de Achinamiza	San Martín	Peru	6° 18' 540" S	76° 09' 843" W	197	Lisa de Silva	3/2/2006	173924	122910
Ooj_Az_05_1572	*Oleria*	*onega*	janarilla	M	Middle1	2	San Miguel de Achinamiza	San Martín	Peru	6° 18' 540" S	76° 09' 843" W	197	Lisa de Silva	3/2/2006	369526	192198
Ooj_Az_05_1573	*Oleria*	*onega*	janarilla	M	Middle1	2	San Miguel de Achinamiza	San Martín	Peru	6° 18' 540" S	76° 09' 843" W	197	Lisa de Silva	3/2/2006	237176	149081
Ooj_Az_05_1574	*Oleria*	*onega*	janarilla	M	Middle1	2	San Miguel de Achinamiza	San Martín	Peru	6° 18' 540" S	76° 09' 843" W	197	Lisa de Silva	3/2/2006	123924	99098
Ooj_Az_05_1575	*Oleria*	*onega*	janarilla	M	Middle1	2	San Miguel de Achinamiza	San Martín	Peru	6° 18' 540" S	76° 09' 843" W	197	Lisa de Silva	3/2/2006	203682	138558
Ooj_Az_05_1576	*Oleria*	*onega*	janarilla	M	Middle1	2	San Miguel de Achinamiza	San Martín	Peru	6° 18' 540" S	76° 09' 843" W	197	Lisa de Silva	3/2/2006	340248	181641
Oos_Mi_02_1482	*Oleria*	*onega*	janarilla - hybrid	M	Middle3	3	Chumia, Km-14, Shapaja-Chazuta	San Martín	Peru	6° 36' 57" S	76° 11' 10" W	262	Alaine Whinnet	9/9/2002	378329	191328
Ooj_Mi_02_1479	*Oleria*	*onega*	janarilla - hybrid	M	Middle3	3	Chumia, Km-14, Shapaja-Chazuta	San Martín	Peru	6° 36' 57" S	76° 11' 10" W	262	Keith Willmott	9/9/2002	268063	167629
Ooj_Mi_02_1480	*Oleria*	*onega*	janarilla - hybrid	M	Middle3	3	Chumia, Km-14, Shapaja-Chazuta	San Martín	Peru	6° 36' 57" S	76° 11' 10" W	262	Keith Willmott	9/9/2002	273438	158741
Oos_Mi_02_1481	*Oleria*	*onega*	janarilla - hybrid	M	Middle3	3	Chumia, Km-14, Shapaja-Chazuta	San Martín	Peru	6° 36' 57" S	76° 11' 10" W	262	Keith Willmott	9/9/2002	225757	148679
Oos_Mi_06_330	*Oleria*	*onega*	ssp. nov. 2	M	Middle3	3	Km-11, Shapaja-Chazuta	San Martín	Peru	6° 36' 979" S	76° 12' 136" W	180	Lisa de Silva	10/19/2006	187840	136185
Oos_Mi_06_332	*Oleria*	*onega*	ssp. nov. 2	F	Middle3	3	Km-11, Shapaja-Chazuta	San Martín	Peru	6° 36' 979" S	76° 12' 136" W	180	Lisa de Silva	10/19/2006	72091	63426
Oos_Mi_06_333	*Oleria*	*onega*	ssp. nov. 2	M	Middle3	3	Km-11, Shapaja-Chazuta	San Martín	Peru	6° 36' 979" S	76° 12' 136" W	180	Lisa de Silva	10/19/2006	336381	184874
Ooj_Mi_06_347	*Oleria*	*onega*	janarilla	M	Middle3	3	Km-19, Shapaja-Chazuta	San Martín	Peru	6° 36' 554" S	76° 09' 612" W	195	Lisa de Silva	11/17/2006	181897	132834
Oos_Mi_06_345	*Oleria*	*onega*	ssp. nov. 2	M	Middle3	3	Km-19, Shapaja-Chazuta	San Martín	Peru	6° 36' 554" S	76° 09' 612" W	195	Lisa de Silva	11/17/2006	183887	132973
Oos_Mi_06_346	*Oleria*	*onega*	ssp. nov. 2	M	Middle3	3	Km-19, Shapaja-Chazuta	San Martín	Peru	6° 36' 554" S	76° 09' 612" W	195	Lisa de Silva	11/17/2006	130376	99334
Ooj_Mi_02_1166	*Oleria*	*onega*	janarilla	M	Middle3	3	Km5 Shapaja-Chazuta	San Martín	Peru	6° 35' 56.33" S	76° 13' 10.86" W	390	Keith Willmott	9/4/2002	346096	228682
Ooj_Mi_02_1172	*Oleria*	*onega*	janarilla	M	Middle3	3	Km5 Shapaja-Chazuta	San Martín	Peru	6° 35' 56.33" S	76° 13' 10.86" W	390	Keith Willmott	9/4/2002	230260	148931
Ooj_Mi_02_1175	*Oleria*	*onega*	janarilla	M	Middle3	3	Km5 Shapaja-Chazuta	San Martín	Peru	6° 35' 56.33" S	76° 13' 10.86" W	390	Keith Willmott	9/4/2002	196596	134495
Ooj_Mi_02_1176	*Oleria*	*onega*	janarilla	F	Middle3	3	Km5 Shapaja-Chazuta	San Martín	Peru	6° 35' 56.33" S	76° 13' 10.86" W	390	Keith Willmott	9/4/2002	151164	106813
Ooj_Mi_02_1583	*Oleria*	*onega*	janarilla	F	Middle3	3	Km5 Shapaja-Chazuta	San Martín	Peru	6° 35' 56.33" S	76° 13' 10.86" W	390	Keith Willmott	9/14/2002	510317	207543
Ooj_Mi_02_1584	*Oleria*	*onega*	janarilla	M	Middle3	3	Km5 Shapaja-Chazuta	San Martín	Peru	6° 35' 56.33" S	76° 13' 10.86" W	390	Keith Willmott	9/14/2002	390247	239099
Ooj_Mi_02_1587	*Oleria*	*onega*	janarilla	F	Middle3	3	Km5 Shapaja-Chazuta	San Martín	Peru	6° 35' 56.33" S	76° 13' 10.86" W	390	Keith Willmott	9/14/2002	362310	190647
Ooj_Mi_02_1588	*Oleria*	*onega*	janarilla	F	Middle3	3	Km5 Shapaja-Chazuta	San Martín	Peru	6° 35' 56.33" S	76° 13' 10.86" W	390	Keith Willmott	9/14/2002	225911	140931
Ooj_Mi_02_1959	*Oleria*	*onega*	janarilla	M	Middle3	3	Km5 Shapaja-Chazuta	San Martín	Peru	6° 35' 56.33" S	76° 13' 10.86" W	390	Keith Willmott	10/7/2002	297137	169368
Ooj_Mi_02_1961	*Oleria*	*onega*	janarilla	M	Middle3	3	Km5 Shapaja-Chazuta	San Martín	Peru	6° 35' 56.33" S	76° 13' 10.86" W	390	Keith Willmott	10/7/2002	375111	188144
Ooj_Mi_02_1962	*Oleria*	*onega*	janarilla	F	Middle3	3	Km5 Shapaja-Chazuta	San Martín	Peru	6° 35' 56.33" S	76° 13' 10.86" W	390	Keith Willmott	10/7/2002	183451	126185
Ooj_Mi_07_151	*Oleria*	*onega*	hybrid	M	Middle3	3	Km5 Shapaja-Chazuta	San Martín	Peru	6° 35' 424" S	76° 13' 394" W	1201		7/31/2007	398209	232534
Ooj_Mi_07_153	*Oleria*	*onega*	hybrid	M	Middle3	3	Km5 Shapaja-Chazuta	San Martín	Peru	6° 35' 424" S	76° 13' 394" W	1201		7/31/2007	261216	127959
Ooj_Mi_07_155	*Oleria*	*onega*	hybrid	M	Middle3	3	Km5 Shapaja-Chazuta	San Martín	Peru	6° 35' 424" S	76° 13' 394" W	1201		7/31/2007	367726	186259
Ooj_Mi_07_158	*Oleria*	*onega*	hybrid	M	Middle3	3	Km5 Shapaja-Chazuta	San Martín	Peru	6° 35' 424" S	76° 13' 394" W	1201		7/31/2007	456383	197003
Ooj_Mi_07_159	*Oleria*	*onega*	hybrid	M	Middle3	3	Km5 Shapaja-Chazuta	San Martín	Peru	6° 35' 424" S	76° 13' 394" W	1201		7/31/2007	239122	182966
Ooj_Mi_07_160	*Oleria*	*onega*	ssp. nov. 2	M	Middle3	3	Km5 Shapaja-Chazuta	San Martín	Peru	6° 35' 424" S	76° 13' 394" W	1201		7/31/2007	339588	192395
Oos_Mi_02_1585	*Oleria*	*onega*	ssp. nov. 2	F	Middle3	3	Km5 Shapaja-Chazuta	San Martín	Peru	6° 35' 56.33" S	76° 13' 10.86" W	390	Keith Willmott	9/14/2002	148046	121259
Oos_Mi_02_1589	*Oleria*	*onega*	ssp. nov. 2	F	Middle3	3	Km5 Shapaja-Chazuta	San Martín	Peru	6° 35' 56.33" S	76° 13' 10.86" W	390	Keith Willmott	9/14/2002	201653	145045
Oos_Mi_02_1958	*Oleria*	*onega*	janarilla	F	Middle3	3	Km5 Shapaja-Chazuta	San Martín	Peru	6° 35' 56.33" S	76° 13' 10.86" W	390		10/7/2002	318151	178419
Oos_Mi_07_157	*Oleria*	*onega*	ssp. nov. 2	M	Middle3	3	Km5 Shapaja-Chazuta	San Martín	Peru	6° 35' 424" S	76° 13' 394" W	1201		7/31/2007	300656	174133
Ooj_Mi_05_829	*Oleria*	*onega*	janarilla - hybrid	M	Middle4	4	Camp 2 on trail from Quebrada Yanayacu to Laguna del Mundo Perdido , PNCAZ	San Martín	Peru	6° 46' 42.06" S	75° 53' 49.44" W	517		9/10/2005	406986	188518
Ooj_Mi_05_830	*Oleria*	*onega*	janarilla - hybrid	M	Middle4	4	Camp 2 on trail from Quebrada Yanayacu to Laguna del Mundo Perdido , PNCAZ	San Martín	Peru	6° 46' 42.06" S	75° 53' 49.44" W	517		9/10/2005	389112	229671
Ooj_Mi_05_831	*Oleria*	*onega*	janarilla - hybrid	F	Middle4	4	Camp 2 on trail from Quebrada Yanayacu to Laguna del Mundo Perdido , PNCAZ	San Martín	Peru	6° 46' 42.06" S	75° 53' 49.44" W	517		9/10/2005	169286	120139
Ooj_Mi_05_832	*Oleria*	*onega*	janarilla	M	Middle4	4	Camp 2 on trail from Quebrada Yanayacu to Laguna del Mundo Perdido , PNCAZ	San Martín	Peru	6° 46' 42.06" S	75° 53' 49.44" W	517		9/10/2005	406041	184406
Ooj_Mi_05_833	*Oleria*	*onega*	janarilla - hybrid	F	Middle4	4	Camp 2 on trail from Quebrada Yanayacu to Laguna del Mundo Perdido , PNCAZ	San Martín	Peru	6° 46' 42.06" S	75° 53' 49.44" W	517		9/10/2005	286051	89215
Ooj_Mi_05_834	*Oleria*	*onega*	janarilla - hybrid	M	Middle4	4	Camp 2 on trail from Quebrada Yanayacu to Laguna del Mundo Perdido , PNCAZ	San Martín	Peru	6° 46' 42.06" S	75° 53' 49.44" W	517		9/10/2005	390592	174811
Ooj_Mi_05_835	*Oleria*	*onega*	janarilla	M	Middle4	4	Camp 2 on trail from Quebrada Yanayacu to Laguna del Mundo Perdido , PNCAZ	San Martín	Peru	6° 46' 42.06" S	75° 53' 49.44" W	517		9/10/2005	303849	171845
Ooj_Mi_05_836	*Oleria*	*onega*	janarilla	F	Middle4	4	Camp 2 on trail from Quebrada Yanayacu to Laguna del Mundo Perdido , PNCAZ	San Martín	Peru	6° 46' 42.06" S	75° 53' 49.44" W	517		9/10/2005	385890	224777
Ooj_Mi_05_837	*Oleria*	*onega*	janarilla	F	Middle4	4	Camp 2 on trail from Quebrada Yanayacu to Laguna del Mundo Perdido , PNCAZ	San Martín	Peru	6° 46' 42.06" S	75° 53' 49.44" W	517		9/10/2005	275970	157117
Ooj_Mi_05_863	*Oleria*	*onega*	janarilla - hybrid	F	Middle4	4	Laguna del Mundo Perdido, PNCAZ	San Martín	Peru	6° 45' 4.54" S	75° 52' 8.29" W	498		9/11/2005	402310	184638

Ooj_Mi_05_864	*Oleria*	*onega*	janarilla - hybrid	M	Middle4	4	Laguna del Mundo Perdido, PNCAZ	San Martín	Peru	6° 45' 4.54" S	75° 52' 8.29" W	498		9/11/2005	357668	224635
Ooj_Mi_05_865	*Oleria*	*onega*	janarilla - hybrid	F	Middle4	4	Laguna del Mundo Perdido, PNCAZ	San Martín	Peru	6° 45' 4.54" S	75° 52' 8.29" W	498		9/11/2005	412047	189457
Ooj_Mi_05_866	*Oleria*	*onega*	janarilla - hybrid	M	Middle4	4	Laguna del Mundo Perdido, PNCAZ	San Martín	Peru	6° 45' 4.54" S	75° 52' 8.29" W	498		9/11/2005	347567	174853
Ooj_Mi_05_810	*Oleria*	*onega*	janarilla - hybrid	M	Middle4	4	Quebrada Yanayacu (Camp 1) to Camp 2 on trail to Laguna del Mundo Perdido, PNCAZ	San Martín	Peru	6° 44' 55.55" S	75° 56' 23.44" W	640		9/10/2005	386582	231181
Ooj_Mi_05_811	*Oleria*	*onega*	janarilla - hybrid	M	Middle4	4	Quebrada Yanayacu (Camp 1) to Camp 2 on trail to Laguna del Mundo Perdido, PNCAZ	San Martín	Peru	6° 44' 55.55" S	75° 56' 23.44" W	640		9/10/2005	425980	200211
Ooj_Mi_05_812	*Oleria*	*onega*	janarilla - hybrid	F	Middle4	4	Quebrada Yanayacu (Camp 1) to Camp 2 on trail to Laguna del Mundo Perdido, PNCAZ	San Martín	Peru	6° 44' 55.55" S	75° 56' 23.44" W	640		9/10/2005	330543	165178
Ooj_Mi_05_813	*Oleria*	*onega*	janarilla - hybrid	M	Middle4	4	Quebrada Yanayacu (Camp 1) to Camp 2 on trail to Laguna del Mundo Perdido, PNCAZ	San Martín	Peru	6° 44' 55.55" S	75° 56' 23.44" W	640		9/10/2005	192508	160657
Ooj_Mi_05_815	*Oleria*	*onega*	janarilla	F	Middle4	4	Quebrada Yanayacu (Camp 1) to Camp 2 on trail to Laguna del Mundo Perdido, PNCAZ	San Martín	Peru	6° 44' 55.55" S	75° 56' 23.44" W	640		9/10/2005	307948	168829
Ooj_Mi_05_816	*Oleria*	*onega*	janarilla - hybrid	M	Middle4	4	Quebrada Yanayacu (Camp 1) to Camp 2 on trail to Laguna del Mundo Perdido, PNCAZ	San Martín	Peru	6° 44' 55.55" S	75° 56' 23.44" W	640		9/10/2005	304297	130274
Ooj_Mi_05_730	*Oleria*	*onega*	janarilla - hybrid	M	Middle4	4	Robashca to Quebrada Yanayacu, Camp 1, PNCAZ	San Martín	Peru	6° 44' 26.62" S	75° 58' 54.31" W	616		9/9/2005	301524	166249
Oos_An_02_1718	*Oleria*	*onega*	ssp. nov. 2	F	Andes	5	Puente Aguas Verdes trail	San Martín	Peru	5° 39' 50" S	77° 38' 58" W	1066	Keith Willmott	9/19/2002	286321	169554
Oos_An_02_1719	*Oleria*	*onega*	ssp. nov. 2	M	Andes	5	Puente Aguas Verdes trail	San Martín	Peru	5° 39' 50" S	77° 38' 58" W	1066	Keith Willmott	9/19/2002	462742	190396
Oos_An_02_918	*Oleria*	*onega*	ssp. nov. 2	M	Andes	5	Puente Aguas Verdes trail	San Martín	Peru	5° 39' 50" S	77° 38' 58" W	1066	Keith Willmott	8/29/2002	392028	184165
Oos_An_02_919	*Oleria*	*onega*	ssp. nov. 2	M	Andes	5	Puente Aguas Verdes trail	San Martín	Peru	5° 39' 50" S	77° 38' 58" W	1066	Keith Willmott	8/29/2002	342214	170008
Oos_An_02_920	*Oleria*	*onega*	ssp. nov. 2	M	Andes	5	Puente Aguas Verdes trail	San Martín	Peru	5° 39' 50" S	77° 38' 58" W	1066	Keith Willmott	8/29/2002	349081	225905
Oos_An_02_921	*Oleria*	*onega*	ssp. nov. 2	M	Andes	5	Puente Aguas Verdes trail	San Martín	Peru	5° 39' 50" S	77° 38' 58" W	1066	Keith Willmott	8/29/2002	350903	179186
Oos_An_02_922	*Oleria*	*onega*	ssp. nov. 2	M	Andes	5	Puente Aguas Verdes trail	San Martín	Peru	5° 39' 50" S	77° 38' 58" W	1066	Keith Willmott	8/29/2002	348830	182579
Oos_An_02_923	*Oleria*	*onega*	ssp. nov. 2	M	Andes	5	Puente Aguas Verdes trail	San Martín	Peru	5° 39' 50" S	77° 38' 58" W	1066	Keith Willmott	8/29/2002	254360	151347
Oos_An_02_924	*Oleria*	*onega*	ssp. nov. 2	M	Andes	5	Puente Aguas Verdes trail	San Martín	Peru	5° 39' 50" S	77° 38' 58" W	1066	Keith Willmott	8/29/2002	142643	140786
Oos_An_02_1672	*Oleria*	*onega*	ssp. nov. 2	M	Andes	5	Puente Serranoyacu	San Martín	Peru	5°40' 31.6" S	77° 40' 28.7'' W	1201	Keith Willmott	9/17/2002	344175	181222
Oos_An_02_1673	*Oleria*	*onega*	ssp. nov. 2	M	Andes	5	Puente Serranoyacu	San Martín	Peru	5°40' 31.6" S	77° 40' 28.7'' W	1201	Keith Willmott	9/17/2002	215651	187862
Oos_An_02_1675	*Oleria*	*onega*	ssp. nov. 2	M	Andes	5	Puente Serranoyacu	San Martín	Peru	5°40' 31.6" S	77° 40' 28.7'' W	1201	Keith Willmott	9/17/2002	215663	147556
Oos_An_02_1676	*Oleria*	*onega*	ssp. nov. 2	F	Andes	5	Puente Serranoyacu	San Martín	Peru	5°40' 31.6" S	77° 40' 28.7'' W	1201	Keith Willmott	9/17/2002	326070	219112
Oos_An_02_1677	*Oleria*	*onega*	ssp. nov. 2	F	Andes	5	Puente Serranoyacu	San Martín	Peru	5°40' 31.6" S	77° 40' 28.7'' W	1201	Keith Willmott	9/17/2002	333937	175629
Oos_An_02_1678	*Oleria*	*onega*	ssp. nov. 2	F	Andes	5	Puente Serranoyacu	San Martín	Peru	5°40' 31.6" S	77° 40' 28.7'' W	1201	Keith Willmott	9/17/2002	199812	140256
Oos_An_02_1679	*Oleria*	*onega*	ssp. nov. 2	F	Andes	5	Puente Serranoyacu	San Martín	Peru	5°40' 31.6" S	77° 40' 28.7'' W	1201	Keith Willmott	9/17/2002	263049	202843
Oos_An_02_1680	*Oleria*	*onega*	ssp. nov. 2	F	Andes	5	Puente Serranoyacu	San Martín	Peru	5°40' 31.6" S	77° 40' 28.7'' W	1201	Keith Willmott	9/17/2002	205875	141804
Oos_An_02_1682	*Oleria*	*onega*	ssp. nov. 2	F	Andes	5	Puente Serranoyacu	San Martín	Peru	5°40' 31.6" S	77° 40' 28.7'' W	1201	Keith Willmott	9/17/2002	222098	142853
Oos_An_02_1683	*Oleria*	*onega*	ssp. nov. 2	F	Andes	5	Puente Serranoyacu	San Martín	Peru	5°40' 31.6" S	77° 40' 28.7'' W	1201	Keith Willmott	9/17/2002	371159	229211
Oos_An_02_1684	*Oleria*	*onega*	ssp. nov. 2	F	Andes	5	Puente Serranoyacu	San Martín	Peru	5°40' 31.6" S	77° 40' 28.7'' W	1201	Keith Willmott	9/17/2002	319998	173505
Oos_An_02_1685	*Oleria*	*onega*	ssp. nov. 2	F	Andes	5	Puente Serranoyacu	San Martín	Peru	5°40' 31.6" S	77° 40' 28.7'' W	1201	Keith Willmott	9/17/2002	280730	161994
Oos_An_02_1708	*Oleria*	*onega*	ssp. nov. 2	M	Andes	5	Puente Serranoyacu	San Martín	Peru	5°40' 31.6" S	77° 40' 28.7'' W	1201	Keith Willmott	9/19/2002	113182	93455
Oos_An_02_1710	*Oleria*	*onega*	ssp. nov. 2	M	Andes	5	Puente Serranoyacu	San Martín	Peru	5°40' 31.6" S	77° 40' 28.7'' W	1201	Keith Willmott	9/19/2002	347791	225594
Oos_An_02_825	*Oleria*	*onega*	ssp. nov. 2	F	Andes	5	Puente Serranoyacu	San Martín	Peru	5°40' 31.6" S	77° 40' 28.7'' W	1201	Keith Willmott	8/28/2002	300325	167718
Oos_An_02_826	*Oleria*	*onega*	ssp. nov. 2	M	Andes	5	Puente Serranoyacu	San Martín	Peru	5°40' 31.6" S	77° 40' 28.7'' W	1201	Keith Willmott	8/28/2002	296678	172454
Oos_An_02_827	*Oleria*	*onega*	ssp. nov. 2	F	Andes	5	Puente Serranoyacu	San Martín	Peru	5°40' 31.6" S	77° 40' 28.7'' W	1201	Keith Willmott	8/28/2002	210928	185109
Oos_An_02_828	*Oleria*	*onega*	ssp. nov. 2	M	Andes	5	Puente Serranoyacu	San Martín	Peru	5°40' 31.6" S	77° 40' 28.7'' W	1201	Keith Willmott	8/28/2002	279793	167466
Oos_An_02_830	*Oleria*	*onega*	ssp. nov. 2	F	Andes	5	Puente Serranoyacu	San Martín	Peru	5°40' 31.6" S	77° 40' 28.7'' W	1201	Keith Willmott	8/28/2002	432194	238041
Oos_An_02_831	*Oleria*	*onega*	ssp. nov. 2	F	Andes	5	Puente Serranoyacu	San Martín	Peru	5°40' 31.6" S	77° 40' 28.7'' W	1201	Keith Willmott	8/28/2002	366723	179649
Oos_An_02_832	*Oleria*	*onega*	ssp. nov. 2	F	Andes	5	Puente Serranoyacu	San Martín	Peru	5°40' 31.6" S	77° 40' 28.7'' W	1201	Keith Willmott	8/28/2002	329948	178568
Oos_An_02_833	*Oleria*	*onega*	ssp. nov. 2	F	Andes	5	Puente Serranoyacu	San Martín	Peru	5°40' 31.6" S	77° 40' 28.7'' W	1201	Keith Willmott	8/28/2002	273206	158486
Oos_An_02_834	*Oleria*	*onega*	ssp. nov. 2	M	Andes	5	Puente Serranoyacu	San Martín	Peru	5°40' 31.6" S	77° 40' 28.7'' W	1201	Keith Willmott	8/28/2002	252864	202717
Oos_An_02_835	*Oleria*	*onega*	ssp. nov. 2	F	Andes	5	Puente Serranoyacu	San Martín	Peru	5°40' 31.6" S	77° 40' 28.7'' W	1201	Keith Willmott	8/28/2002	321872	178120
Oos_An_02_836	*Oleria*	*onega*	ssp. nov. 2	F	Andes	5	Puente Serranoyacu	San Martín	Peru	5°40' 31.6" S	77° 40' 28.7'' W	1201	Keith Willmott	8/28/2002	451875	187767
Oos_An_02_837	*Oleria*	*onega*	ssp. nov. 2	F	Andes	5	Puente Serranoyacu	San Martín	Peru	5°40' 31.6" S	77° 40' 28.7'' W	1201	Keith Willmott	8/28/2002	310434	218288
Oos_An_02_838	*Oleria*	*onega*	ssp. nov. 2	M	Andes	5	Puente Serranoyacu	San Martín	Peru	5°40' 31.6" S	77° 40' 28.7'' W	1201	Keith Willmott	8/28/2002	205329	140802
Oos_An_02_839	*Oleria*	*onega*	ssp. nov. 2	M	Andes	5	Puente Serranoyacu	San Martín	Peru	5°40' 31.6" S	77° 40' 28.7'' W	1201	Keith Willmott	8/28/2002	300789	212359
Oos_An_02_840	*Oleria*	*onega*	ssp. nov. 2	F	Andes	5	Puente Serranoyacu	San Martín	Peru	5°40' 31.6" S	77° 40' 28.7'' W	1201	Keith Willmott	8/28/2002	212864	146524
Oos_An_02_841	*Oleria*	*onega*	ssp. nov. 2	F	Andes	5	Puente Serranoyacu	San Martín	Peru	5°40' 31.6" S	77° 40' 28.7'' W	1201	Keith Willmott	8/28/2002	382792	184449
Oos_An_02_842	*Oleria*	*onega*	ssp. nov. 2	F	Andes	5	Puente Serranoyacu	San Martín	Peru	5°40' 31.6" S	77° 40' 28.7'' W	1201	Keith Willmott	8/28/2002	358039	226681
Oos_An_02_844	*Oleria*	*onega*	ssp. nov. 2	F	Andes	5	Puente Serranoyacu	San Martín	Peru	5°40' 31.6" S	77° 40' 28.7'' W	1201	Keith Willmott	8/28/2002	192903	118397
Oos_An_02_845	*Oleria*	*onega*	ssp. nov. 2	M	Andes	5	Puente Serranoyacu	San Martín	Peru	5°40' 31.6" S	77° 40' 28.7'' W	1201	Keith Willmott	8/28/2002	297813	165335
Oos_An_02_847	*Oleria*	*onega*	ssp. nov. 2	M	Andes	5	Puente Serranoyacu	San Martín	Peru	5°40' 31.6" S	77° 40' 28.7'' W	1201	Keith Willmott	8/28/2002	329074	179614
Oos_An_02_848	*Oleria*	*onega*	ssp. nov. 2	F	Andes	5	Puente Serranoyacu	San Martín	Peru	5°40' 31.6" S	77° 40' 28.7'' W	1201	Keith Willmott	8/28/2002	219898	137874
Oos_An_02_849	*Oleria*	*onega*	ssp. nov. 2	M	Andes	5	Puente Serranoyacu	San Martín	Peru	5°40' 31.6" S	77° 40' 28.7'' W	1201	Keith Willmott	8/28/2002	351661	224683
Oos_An_02_850	*Oleria*	*onega*	ssp. nov. 2	M	Andes	5	Puente Serranoyacu	San Martín	Peru	5°40' 31.6" S	77° 40' 28.7'' W	1201	Keith Willmott	8/28/2002	328030	175067
Oos_An_02_851	*Oleria*	*onega*	ssp. nov. 2	M	Andes	5	Puente Serranoyacu	San Martín	Peru	5°40' 31.6" S	77° 40' 28.7'' W	1201	Keith Willmott	8/28/2002	238640	197139

Locus_ID	BLASTn Best-Hit Danaus plexippus scaffold	start	stop	%_id	alignment length	e-value	Score	Danaus plexippus cds	Protein homology
Ithomia salapia									
Adaptive introgression loci (diverging genomic cline center (α) + high differentiation level (FST))									
locus_20794	DPSCF300001	2255382	2255463	85.37	82	4,00E-19	95.1	DPOGS207061-TA	
locus_49453	DPSCF300003	1757941	1758023	80.72	83	3,00E-14	78.8	DPOGS203415-TA	
locus_19916	DPSCF300006	780102	780018	83.53	85	4,00E-18	91.5		
locus_20816	DPSCF300008	93324	93266	87.30	63	9,00E-14	77.0		
locus_14403	DPSCF300008	1238880	1238796	96.47	85	1,00E-32	140		
locus_28434	DPSCF300009	1937088	1937006	79.52	83	1,00E-12	73.4	DPOGS208993-TA	
locus_28611	DPSCF300010	1978358	1978428	81.69	71	1,00E-11	69.8		
locus_32677	DPSCF300012	1198547	1198467	81.71	82	1,00E-11	69.8		
locus_91	DPSCF300014	846573	846515	89.83	59	8,00E-15	80.6		
locus_17576	DPSCF300015	681524	681610	86.36	88	3,00E-20	98.7		
locus_24148	DPSCF300017	331577	331503	85.33	75	2,00E-16	86.0		
locus_1838	DPSCF300017	764025	763943	89.16	83	2,00E-23	109		
locus_13643	DPSCF300028	1192556	1192640	77.65	85	5,00E-11	68.0	DPOGS206136-TA	
locus_7322	DPSCF300064	159016	158934	83.13	83	5,00E-17	87.8	DPOGS208522-TA	
locus_22050	DPSCF300073	640050	639972	86.08	79	1,00E-18	93.3		
locus_15377	DPSCF300081	548500	548415	84.88	86	1,00E-19	96.9	DPOGS205859-TA	Down syndrome critical region protein 3 homolog
locus_18829	DPSCF300091	307474	307391	85.71	84	3,00E-20	98.7		
locus_16344	DPSCF300114	46930	46851	81.25	80	1,00E-13	77.0	DPOGS213191-TA	
locus_15693	DPSCF300121	264102	264039	84.38	64	4,00E-12	71.6		
locus_12790	DPSCF300127	454398	454316	83.13	83	5,00E-17	87.8	DPOGS209486-TA	
locus_11228	DPSCF300127	454413	454480	83.82	68	1,00E-12	73.4	DPOGS209486-TA	
locus_11261	DPSCF300131	603666	603750	80.00	85	1,00E-13	77.0	DPOGS202495-TA	
locus_15366	DPSCF300153	187359	187435	81.82	77	1,00E-13	77.0	DPOGS214916-TA	
locus_14723	DPSCF300154	292667	292598	85.71	70	3,00E-14	78.8		
locus_874	DPSCF300176	896628	896547	84.15	82	2,00E-17	89.7		
locus_11740	DPSCF300177	83862	83792	85.92	71	6,00E-16	84.2	DPOGS207516-TA	
locus_21620	DPSCF300200	112178	112250	82.19	73	1,00E-12	73.4	DPOGS204071-TA	Lactase-phlorizin hydrolase
locus_5119	DPSCF300211	597	508	76.67	90	3,00E-13	75.2		
locus_11544	DPSCF300211	279599	279549	90.20	51	1,00E-11	69.8		
locus_21834	DPSCF300219	461394	461479	88.37	86	5,00E-24	111	DPOGS213665-TA	
locus_2581	DPSCF300232	508892	508818	82.67	75	1,00E-13	77.0		
locus_21052	DPSCF300268	80273	80342	84.29	70	1,00E-13	77.0		
locus_36372	DPSCF300307	138643	138561	86.75	83	3,00E-20	98.7		
locus_24886	DPSCF300324	76126	76041	86.05	86	2,00E-21	102	DPOGS202701-TA	
locus_63	DPSCF300338	140335	140254	89.02	82	6,00E-23	107	DPOGS207656-TA	
locus_29426	DPSCF300391	9101	9025	87.01	77	4,00E-19	95.1	DPOGS201653-TA	
locus_47081	DPSCF300391	179887	179804	80.95	84	8,00E-15	80.6	DPOGS203107-TA	
Oleria onega									
Adaptive introgression loci (diverging genomic cline center (α) + high differentiation level (FST))									

locus_39916	DPSCF300001	1760764	1760847	83.33	84	2,00E-17	89.7	DPOGS206900-TA	
locus_6600	DPSCF300001	2445655	2445571	77.65	85	5,00E-11	68.0	DPOGS207070-TA	Bleomycin hydrolase
locus_18737	DPSCF300001	2898435	2898352	84.52	84	1,00E-18	93.3	DPOGS206854-TA	
locus_291	DPSCF300001	4348908	4348825	79.07	86	1,00E-11	69.8		
locus_24405	DPSCF300004	1289625	1289544	84.15	82	2,00E-17	89.7	DPOGS211019-TA	
locus_18889	DPSCF300004	1527412	1527329	88.10	84	6,00E-23	107		
locus_11213	DPSCF300006	94744	94826	81.93	83	2,00E-15	82.4	DPOGS201471-TA	
locus_30280	DPSCF300006	804531	804587	87.72	57	4,00E-12	71.6	DPOGS201447-TA	
locus_6020	DPSCF300009	179886	179969	90.48	84	1,00E-25	116	DPOGS208940-TA	Contactin
locus_63224	DPSCF300009	765102	765185	89.29	84	5,00E-24	111	DPOGS208957-TA	
locus_41437	DPSCF300009	1494818	1494900	95.18	83	1,00E-30	132		
locus_5544	DPSCF300014	973146	973230	87.06	85	7,00E-22	104		
locus_53694	DPSCF300019	1083985	1084069	78.82	85	1,00E-12	73.4	DPOGS212316-TA	
locus_6837	DPSCF300024	24576	24661	83.72	86	4,00E-18	91.5		
locus_939	DPSCF300027	157690	157608	89.16	83	2,00E-23	109		
locus_36129	DPSCF300038	1105994	1106051	91.38	58	2,00E-15	82.4		
locus_28726	DPSCF300041	1563919	1563853	92.54	67	3,00E-20	98.7		
locus_7639	DPSCF300042	1148866	1148782	85.88	85	8,00E-21	100	DPOGS207841-TA	
locus_20657	DPSCF300048	132467	132383	96.47	85	1,00E-31	136		
locus_5259	DPSCF300049	818458	818521	87.50	64	3,00E-14	78.8		
locus_39337	DPSCF300050	197880	197799	87.80	82	7,00E-22	104	DPOGS214621-TA	
locus_5676	DPSCF300051	459989	460071	85.54	83	1,00E-19	96.9	DPOGS207483-TA	
locus_40167	DPSCF300051	482393	482477	88.24	85	2,00E-23	109	DPOGS207445-TA	
locus_51320	DPSCF300052	511744	511813	90.00	70	4,00E-18	91.5		
locus_9796	DPSCF300053	1109584	1109645	83.87	62	5,00E-11	68.0		
locus_30776	DPSCF300056	274712	274639	81.08	74	4,00E-12	71.6	DPOGS205507-TA	
locus_4041	DPSCF300057	52461	52377	77.65	85	5,00E-11	68.0		
locus_11635	DPSCF300058	44474	44542	86.96	69	5,00E-16	84.2	DPOGS208156-TA	
locus_16883	DPSCF300064	259762	259678	84.71	85	4,00E-19	95.1	DPOGS208524-TA	
locus_14881	DPSCF300064	1707322	1707239	89.29	84	5,00E-24	111	DPOGS208460-TA	Cadherin-related tumor suppressor
locus_40108	DPSCF300066	454834	454751	84.52	84	4,00E-18	91.5		
locus_14418	DPSCF300073	565519	565435	92.94	85	6,00E-29	127		
locus_16119	DPSCF300082	1222334	1222416	86.75	83	8,00E-21	100	DPOGS206300-TA	
locus_36677	DPSCF300089	376974	376890	84.71	85	4,00E-19	95.1	DPOGS205916-TA	Serine/threonine-protein kinase N3
locus_35425	DPSCF300094	144496	144424	82.89	76	1,00E-13	77.0		
locus_25295	DPSCF300095	151289	151371	91.76	85	9,00E-27	120		
locus_17924	DPSCF300095	220263	220183	81.48	81	3,00E-14	78.8		
locus_19646	DPSCF300098	588403	588320	94.05	84	2,00E-29	129		
locus_31990	DPSCF300122	617164	617245	82.93	82	2,00E-16	86.0	DPOGS214469-TA	Potassium voltage-gated channel subfamily D member 2
locus_30027	DPSCF300125	447801	447882	84.34	83	5,00E-17	87.8		
locus_23486	DPSCF300128	685283	685351	82.61	69	4,00E-12	71.6	DPOGS200181-TA	Chromodomain-helicase-DNA-binding protein 4
locus_8696	DPSCF300131	292633	292709	79.22	77	5,00E-11	68.0	DPOGS202524-TA	Dynein heavy chain, cytoplasmic
locus_17973	DPSCF300133	205697	205773	80.52	77	4,00E-12	71.6		
locus_9927	DPSCF300145	423602	423519	90.48	84	1,00E-25	116	DPOGS206960-TA	
locus_17455	DPSCF300154	359812	359895	78.57	84	4,00E-12	71.6	DPOGS208109-TA	
locus_38972	DPSCF300162	224765	224849	84.71	85	4,00E-19	95.1	DPOGS202151-TA	
locus_40071	DPSCF300168	21644	21726	81.93	83	2,00E-15	82.4	DPOGS210608-TA	
locus_3709	DPSCF300168	103826	103878	88.68	53	1,00E-11	69.8		
locus_21454	DPSCF300170	429546	429467	86.25	80	4,00E-19	95.1		

locus_14350	DPSCF300171	455112	455200	88.76	89	4,00E-25	114		
locus_38803	DPSCF300182	11272	11350	87.34	79	3,00E-20	98.7	DPOGS216113-TA	
locus_13278	DPSCF300184	311089	310999	81.32	91	2,00E-17	89.7	DPOGS204141-TA	
locus_21125	DPSCF300188	254025	253943	80.72	83	3,00E-14	78.8	DPOGS207347-TA	
locus_27398	DPSCF300206	88373	88457	88.24	85	2,00E-23	109		
locus_14969	DPSCF300210	32672	32755	83.33	84	2,00E-17	89.7	DPOGS203241-TA	E3 ubiquitin-protein ligase Smurf1
locus_12981	DPSCF300212	876257	876175	84.34	83	4,00E-18	91.5	DPOGS213742-TA	
locus_38548	DPSCF300219	579537	579452	84.88	86	1,00E-19	96.9	DPOGS213705-TA	
locus_23097	DPSCF300231	390393	390313	92.59	81	9,00E-27	120	DPOGS204749-TA	
locus_38495	DPSCF300242	161615	161690	82.89	76	3,00E-14	78.8	DPOGS203439-TA	
locus_16210	DPSCF300258	210889	210825	83.08	65	5,00E-11	68.0		
locus_20793	DPSCF300270	226701	226777	81.82	77	1,00E-13	77.0	DPOGS208007-TA	
locus_6434	DPSCF300271	119860	119810	94.12	51	3,00E-14	78.8		
locus_42203	DPSCF300296	235411	235349	87.30	63	3,00E-13	75.2		
locus_3798	DPSCF300325	4824	4749	84.21	76	6,00E-16	84.2	DPOGS211639-TA	
locus_52767	DPSCF300382	158605	158685	90.12	81	5,00E-24	111	DPOGS206254-TA	
locus_21333	DPSCF300547	1509	1588	92.50	80	4,00E-25	114		

Oleria onega

Reproductive isolation loci (high diverging positive genomic cline rate (β))

locus_56496	DPSCF300002	448758	448841	83.33	84	2,00E-17	89.7	DPOGS204463-TA	
locus_23233	DPSCF300002	1313553	1313619	85.07	67	1,00E-13	77.0		
locus_14217	DPSCF300009	1484490	1484408	97.59	83	3,00E-32	138		
locus_41437	DPSCF300009	1494818	1494900	95.18	83	1,00E-30	132		
locus_6715	DPSCF300010	503894	503822	83.56	73	3,00E-14	78.8		
locus_13325	DPSCF300010	1174123	1174177	96.36	55	3,00E-18	91.5		
locus_7285	DPSCF300010	2856044	2856110	97.01	67	1,00E-24	113		
locus_16456	DPSCF300011	910922	910840	81.93	83	2,00E-15	82.4	DPOGS211875-TA	
locus_2045	DPSCF300012	17595	17663	88.57	70	6,00E-16	84.2		
locus_5796	DPSCF300013	724317	724236	85.37	82	4,00E-19	95.1	DPOGS210690-TA	
locus_5544	DPSCF300014	973146	973230	88.24	85	2,00E-23	109		
locus_13402	DPSCF300014	2159403	2159488	95.35	86	3,00E-32	138		
locus_5347	DPSCF300018	791599	791676	83.33	78	2,00E-15	82.4	DPOGS202792-TA	
locus_635	DPSCF300019	386290	386224	91.04	67	4,00E-19	95.1		
locus_6133	DPSCF300021	679108	679192	94.12	85	5,00E-30	131		
locus_17850	DPSCF300021	1255675	1255754	82.50	80	2,00E-15	82.4		
locus_3400	DPSCF300022	1406128	1406086	100.00	43	3,00E-14	78.8		
locus_2334	DPSCF300025	217171	217087	89.41	85	1,00E-24	113	DPOGS210344-TA	Low-density lipoprotein receptor-related protein 2
locus_53	DPSCF300028	1715782	1715719	87.50	64	8,00E-15	80.6		
locus_7065	DPSCF300030	1210754	1210819	89.39	66	4,00E-16	84.2		
locus_56182	DPSCF300032	800216	800170	95.83	48	3,00E-13	75.2		
locus_9208	DPSCF300033	37338	37255	83.33	84	1,00E-17	89.7	DPOGS213564-TA	Protein disulfide-isomerase
locus_39358	DPSCF300034	225066	225150	85.88	85	8,00E-21	100	DPOGS204184-TA	
locus_36129	DPSCF300038	1105994	1106051	91.38	58	2,00E-15	82.4		
locus_9061	DPSCF300041	1435324	1435406	87.95	83	2,00E-22	105	DPOGS215762-TA	
locus_18124	DPSCF300041	1632655	1632739	84.71	85	4,00E-19	95.1	DPOGS215771-TA	Uncharacterized helicase C17H9.02
locus_7639	DPSCF300042	1148866	1148782	85.88	85	8,00E-21	100	DPOGS207841-TA	
locus_15855	DPSCF300044	922991	923073	83.53	85	2,00E-15	82.4		

locus_9976	DPSCF300047	27674	27596	83.54	79	7,00E-16	84.2	DPOGS215265-TA	
locus_13421	DPSCF300048	729948	730032	87.06	85	7,00E-22	104	DPOGS206628-TA	
locus_16663	DPSCF300048	860848	860929	92.68	82	3,00E-27	122		
locus_11355	DPSCF300052	339442	339358	80.00	85	1,00E-13	77.0	DPOGS208609-TA	
locus_51320	DPSCF300052	511744	511813	90.00	70	4,00E-18	91.5		
locus_16883	DPSCF300064	259762	259678	84.71	85	4,00E-19	95.1	DPOGS208524-TA	
locus_1104	DPSCF300066	72184	72264	82.72	81	8,00E-15	80.6		
locus_14418	DPSCF300073	565519	565435	92.94	85	6,00E-29	127		
locus_26323	DPSCF300074	116559	116475	84.71	85	4,00E-19	95.1	DPOGS205078-TA	
locus_3251	DPSCF300082	579057	579142	83.72	86	1,00E-18	93.3	DPOGS206318-TA	DNA-directed RNA polymerase I subunit rpa1
locus_6613	DPSCF300092	467872	467788	89.41	85	2,00E-23	109		
locus_17924	DPSCF300095	220263	220183	81.48	81	3,00E-14	78.8		
locus_17571	DPSCF300099	149029	149094	93.94	66	2,00E-21	102		
locus_6969	DPSCF300112	257821	257733	87.64	89	1,00E-24	113		
locus_42925	DPSCF300117	317371	317306	83.58	67	5,00E-11	68.0		
locus_80	DPSCF300119	307017	306933	98.82	85	2,00E-35	149		
locus_8829	DPSCF300128	685276	685191	77.91	86	1,00E-11	69.8	DPOGS200181-TA	Chromodomain-helicase-DNA-binding protein 4
locus_23486	DPSCF300128	685283	685351	82.61	69	4,00E-12	71.6	DPOGS200181-TA	Chromodomain-helicase-DNA-binding protein 4
locus_10447	DPSCF300129	295733	295816	91.67	84	9,00E-27	120	DPOGS215550-TA	
locus_8696	DPSCF300131	292633	292709	79.22	77	5,00E-11	68.0	DPOGS202524-TA	Dynein heavy chain, cytoplasmic
locus_24658	DPSCF300153	302796	302868	80.82	73	1,00E-11	69.8	DPOGS214919-TA	Structural maintenance of chromosomes protein 4 (Fragment)
locus_50550	DPSCF300160	254056	254135	81.25	80	3,00E-14	78.8		
locus_4637	DPSCF300160	502195	502271	89.61	77	7,00E-22	104		
locus_1279	DPSCF300160	533929	534011	96.39	83	1,00E-31	136		
locus_25495	DPSCF300170	555014	554930	92.94	85	6,00E-29	127	DPOGS204700-TA	Inhibitor of growth protein 4
locus_760	DPSCF300171	509326	509246	91.36	81	4,00E-25	114		
locus_15055	DPSCF300172	330603	330522	81.71	82	8,00E-15	80.6	DPOGS205104-TA	ATP-binding cassette sub-family G member 4
locus_44871	DPSCF300176	877906	877987	81.71	82	8,00E-15	80.6	DPOGS201276-TA	
locus_13278	DPSCF300184	311089	310999	81.32	91	2,00E-17	89.7	DPOGS204141-TA	
locus_10628	DPSCF300189	257	334	82.05	78	3,00E-14	78.8	DPOGS212552-TA	
locus_45809	DPSCF300192	328851	328931	90.12	81	5,00E-24	111		
locus_50	DPSCF300196	630167	630237	92.96	71	2,00E-22	105	DPOGS207656-TA	
locus_36202	DPSCF300224	20899	20974	89.47	76	2,00E-21	102		
locus_3993	DPSCF300235	508167	508086	84.34	83	5,00E-17	87.8		
locus_4021	DPSCF300250	293523	293607	95.29	85	1,00E-31	136		
locus_19317	DPSCF300258	53527	53451	80.52	77	4,00E-12	71.6	DPOGS212418-TA	
locus_16210	DPSCF300258	210889	210825	83.08	65	5,00E-11	68.0		
locus_11201	DPSCF300283	220103	220179	84.42	77	2,00E-16	86.0	DPOGS210186-TA	
locus_21486	DPSCF300298	103299	103230	82.19	73	4,00E-12	71.6	DPOGS215444-TA	
locus_13053	DPSCF300300	50254	50175	91.25	80	1,00E-24	113		
locus_14218	DPSCF300304	184614	184531	79.76	84	3,00E-13	75.2	DPOGS210561-TA	Cyclin-dependent kinase 2
locus_9530	DPSCF300407	236218	236141	84.62	78	6,00E-16	84.2	DPOGS205394-TA	Fructose-1,6-bisphosphatase isozyme 2
locus_878	DPSCF300424	30626	30707	89.02	82	6,00E-23	107		
locus_8293	DPSCF300446	77824	77901	92.31	78	5,00E-24	111		
locus_17	DPSCF300575	2185	2124	90.32	62	2,00E-16	86.0		

Locus_ID	BLASTn Best-Hit Danaus plexippus scaffold	start	stop	%_id	alignment length	e-value	Score	Danaus plexippus cds	Protein homology
Ithomia salapia									
locus_575	DPSCF300006	929124	929055	85.71	70	2E-15	82.4		
locus_10434	DPSCF300037	729941	730017	81.82	77	1E-12	73.4		
locus_6641	DPSCF300038	1144841	1144764	86.42	81	4E-19	95.1	DPOGS212179-TA	Serine/threonine kinase
locus_5230	DPSCF300046	93689	93772	96.43	84	3E-32	138		
locus_11053	DPSCF300054	645838	645902	89.23	65	3E-14	78.8		
locus_3841	DPSCF300071	431640	431701	88.71	62	8E-15	80.6		
locus_15377	DPSCF300081	548500	548415	84.88	86	1E-19	96.9	DPOGS205859-TA	Down syndrome critical region protein 3 homolog
locus_10724	DPSCF300164	45882	45969	85.23	88	3E-20	98.7		
locus_16002	DPSCF300171	38821	38903	80.72	83	3E-14	78.8	DPOGS214065-TA	Carnitine O-palmitoyltransferase 2
locus_2581	DPSCF300232	508892	508818	82.67	75	1E-13	77.0		
locus_9663	DPSCF300395	68400	68317	89.29	84	5E-24	111		
locus_4352	DPSCF300598	15776	15694	80.72	83	3E-14	78.8	DPOGS200524-TA	
Oleria onega									
locus_6600	DPSCF300001	2445655	2445571	80.00	85	1,00E-13	77.0	DPOGS207070-TA	Bleomycin hydrolase
locus_54320	DPSCF300001	2487997	2488051	89.09	55	1,00E-12	73.4	DPOGS207073-TA	
locus_2138	DPSCF300001	5999940	5999893	91.67	48	1,00E-11	69.8		
locus_5821	DPSCF300002	991352	991435	78.57	84	4,00E-12	71.6	DPOGS204406-TA	
locus_18347	DPSCF300012	275034	274963	86.11	72	2,00E-16	86.0		
locus_50	DPSCF300013	1476318	1476235	90.48	84	1,00E-25	116	DPOGS207656-TA	
locus_2696	DPSCF300016	1060706	1060623	83.33	84	2,00E-17	89.7	DPOGS213145-TA	Thioredoxin-like protein 1
locus_291	DPSCF300046	701709	701774	92.42	66	1,00E-19	96.9	DPOGS204311-TA	
locus_4636	DPSCF300051	713048	712964	87.06	85	7,00E-22	104	DPOGS207490-TA	Teneurin-a
locus_302	DPSCF300063	548496	548419	81.18	85	3,00E-14	78.8		
locus_14881	DPSCF300064	1707322	1707239	91.67	84	9,00E-27	120	DPOGS208460-TA	Cadherin-related tumor suppressor
locus_2602	DPSCF300073	701149	701226	88.46	78	1,00E-19	96.9		
locus_8241	DPSCF300086	693323	693404	86.59	82	3,00E-20	98.7		
locus_24045	DPSCF300115	366338	366397	95.00	60	3,00E-19	95.1		
locus_6523	DPSCF300120	68784	68700	83.53	85	4,00E-18	91.5	DPOGS215317-TA	Innexin inx1
locus_12311	DPSCF300162	175614	175527	81.82	88	2,00E-16	86.0		
locus_6481	DPSCF300196	262147	262068	82.50	80	2,00E-15	82.4		
locus_1830	DPSCF300209	256021	255940	86.59	82	3,00E-19	95.1		
locus_47502	DPSCF300221	281710	281775	82.86	70	5,00E-11	68.0		
locus_878	DPSCF300424	30618	30696	92.50	80	5,00E-24	111		
locus_14178	DPSCF300431	40916	41000	77.65	85	5,00E-11	68.0		

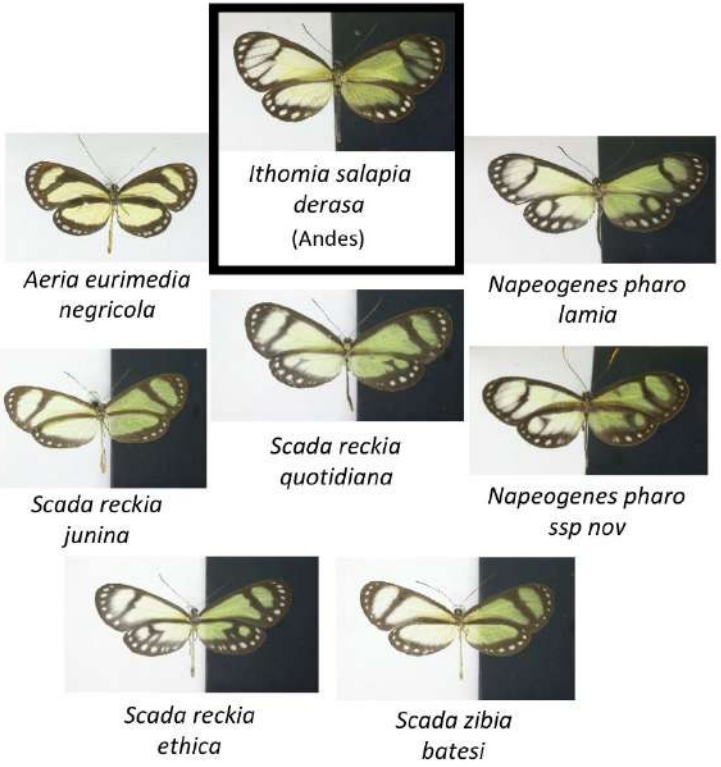
Ithomia salapia derasa
(Andes)
Aeria eurimedia negricola
Napeogenes pharo lamia
Scada reckia quotidiana
Scada reckia junina
Napeogenes pharo ssp nov
Scada reckia ethica
Scada zibia batesi

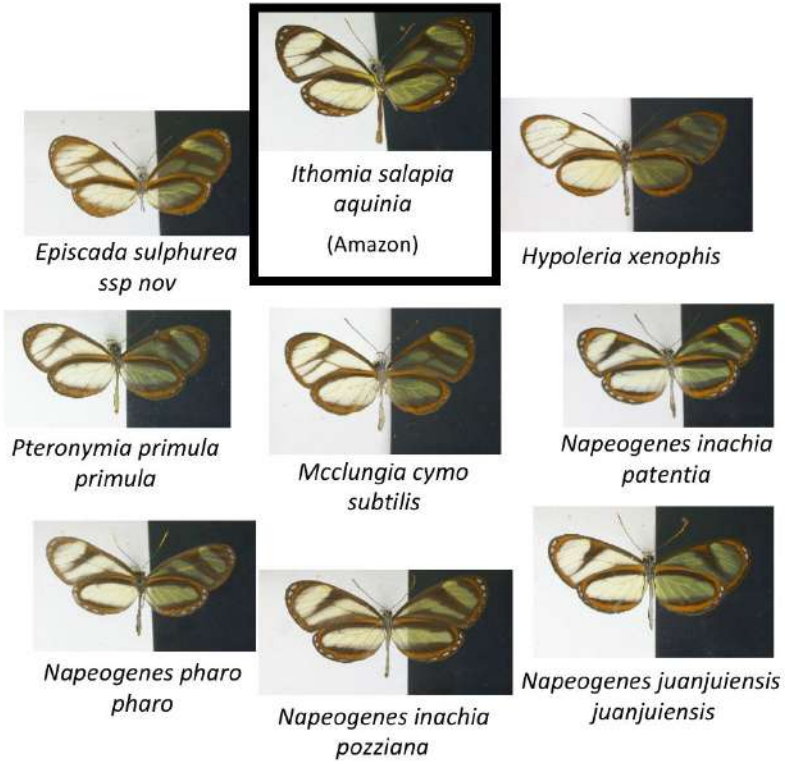
Ithomia salapia aquinia
(Amazon)
Episcada sulphurea ssp nov
Hypoleria xenophis
Pteronymia primula primula
Mcclungia cymo subtilis
Napeogenes inachia patentia
Napeogenes pharo pharo
Napeogenes inachia pozziana
Napeogenes juanjuiensis juanjuiensis

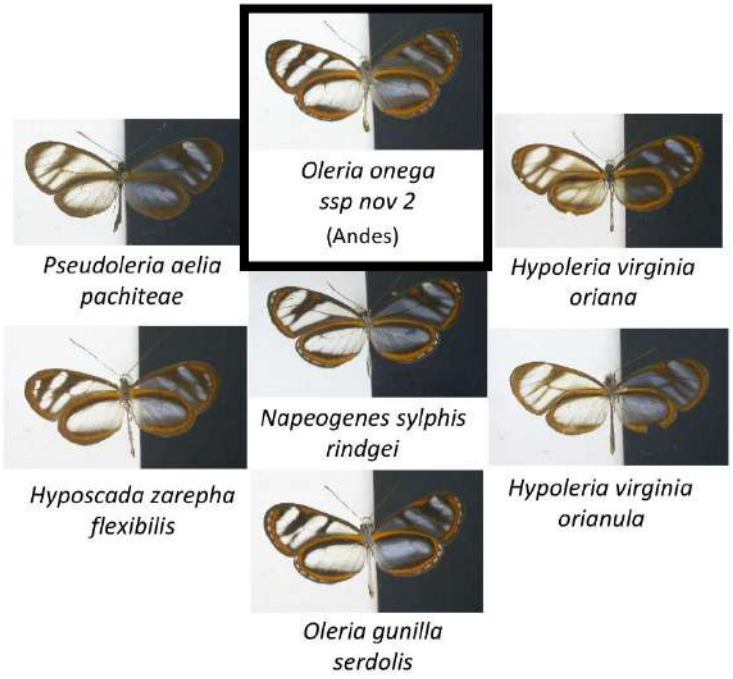
Oleria onega ssp nov 2
(Andes)
Pseudoleria aelia pachiteae
Hypoleria virginia oriana
Napeogenes sylphis rindgei
Hyposcada zarepha flexibilis
Hypoleria virginia orianula
Oleria gunilla serdolis

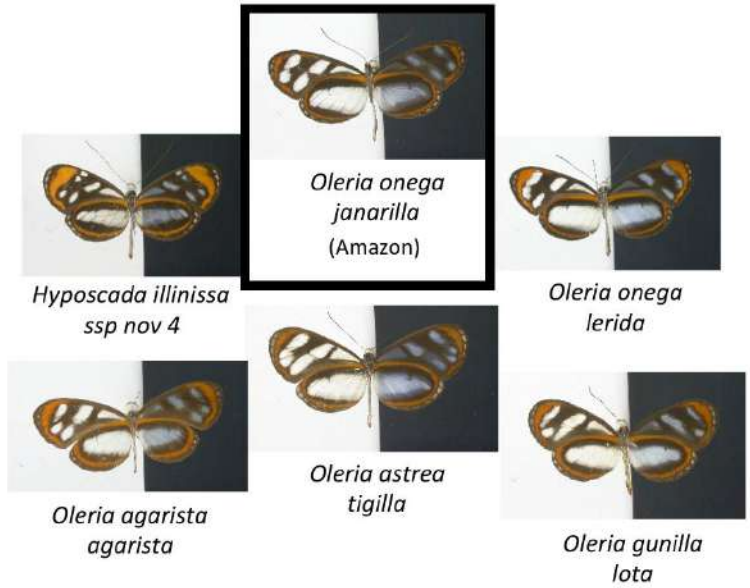
Oleria onega janarilla
(Amazon)
Hyposcada illinissa ssp nov 4
Oleria onega lerida
Oleria agarista agarista
Oleria astrea tigilla
Oleria gunilla lota

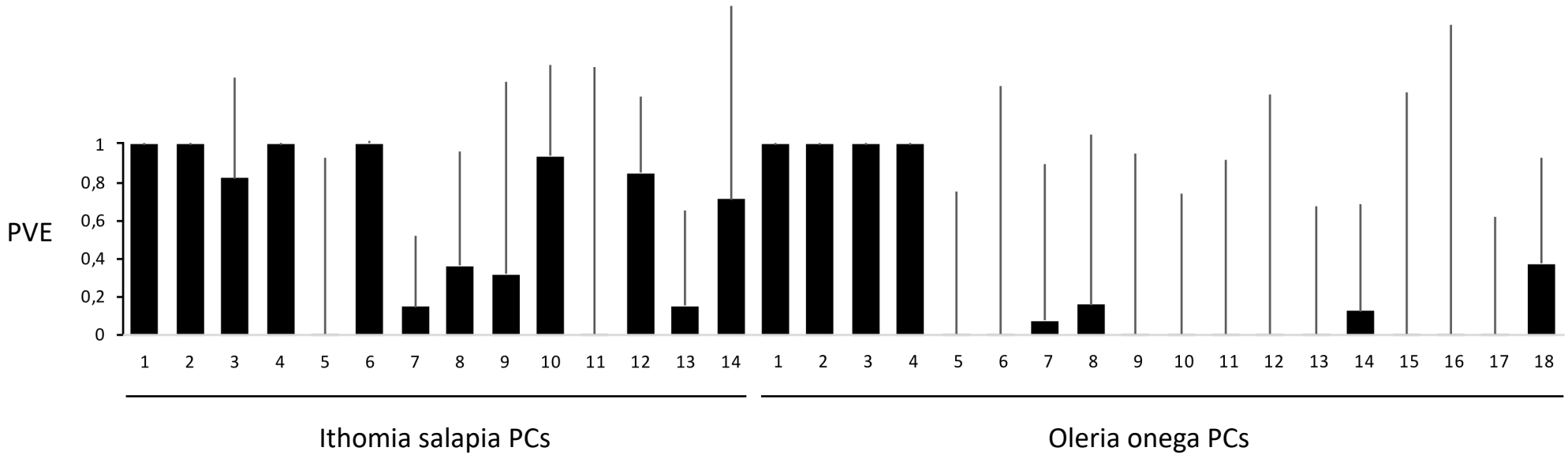
PVE
1
0,8
0,6
0,4
0,2
0
1 2 3 4 5 6 7 8 9 10 11 12 13 14
1 2 3 4 5 6 7 8 9 10 11 12 13 14 15 16 17 18
Ithomia salapia PCs
Oleria onega PCs